PART II
CORROSION INHIBITION STUDIES

Vinod P Raphael "Physicochemical, corrosion inhibition and biological studies on schiff bases derived from heterocyclic carbonyl compounds and their metal complexes" Thesis. Department of Chemistry, St. Thomas College Thrissur, University of Calicut, 2014

PART II

CORROSION INHIBITION STUDIES

CHAPTER 1

INTRODUCTION AND REVIEW

The slow destruction of metal under environmental conditions such as acidic gases, humidity etc is termed as metallic corrosion. Metallic corrosion takes place naturally and usually the metals will be converted into their most stable oxides. Some metals such as silver, copper etc slowly changes into their sulphides and basic carbonates respectively. The slow rusting of the iron that takes place naturally is a well known example for the corrosion in the world. In the chemical point of view, corrosion is an electrochemical phenomenon. The rate of corrosion enhances rapidly in the presence of acidic environment and electrolytes.

Metallic corrosion has got a great attention among scientists and technologists, primarily due to its economic impact and secondly due to its safety consequences. Corrosion will lead to the lowering of the efficiency of plants, increasing the maintenance cost, contamination or loss of the products and may lead to the catastrophic damages. India has been losing around 1.52 lakh crore annually due to corrosion in various sectors such as infrastructure, production and manufacturing, defense, petrochemicals, railway, metal industries and nuclear power plants. In developed countries such as U.S. and Japan, the estimated loss due to corrosion is approximately 3% of their respective gross domestic product (GDP) which is about half of the loss estimated in India.[1]

It is estimated that about 10-15% of the globally extracted iron from its ores will turn back to the nature per annum in the form of rust as a result of natural as well as accelerated corrosion. Apart from the natural and unavoidable

corrosions, manmade activities such as acid pickling, de-scaling, oil-well acidizing will escalate the rate of corrosion considerably and these activities are considered as the major reasons for the corrosion problems in the metal industries and oil industries.

De-scaling and Acid Pickling

De-scaling and pickling are the metal surface cleaning techniques which consumes enormous quantities of hydrochloric acid and sulphuric acid. The thin oxide film (e.g., hydrated ferric oxide or rust), organic and inorganic stains and other impurities on the metal surfaces can be eliminated by treating the metal specimens for a stipulated time in acidic solutions and thus the original metallic appearance can be reinstated. Similarly the basic carbonate formed on the surface of copper and brass can be easily removed by treating the surface with mild acids. Treating aluminium with mild acids regains its original metallic luster. To minimize the corrosion during surface cleaning process, it is customary to add certain inhibitors into the aggressive solutions [2-5].

Petrochemical Industry and Corrosion

The economic losses in oil industry due to corrosion mainly occur by the direct contact between the metallic oil pipelines and equipment with the aggressive media. The prolonged interaction between the aggressive media and pipelines is unavoidable during the production of oil, refining and transportation. The addition of corrosion inhibitors during these processes will help to decrease the corrosion rate considerably [6].

The acidic environment in the oil industry arises mainly due to two major reasons. a) Dissolution of the corrosive gases such as H_2S and CO_2 and b) hydrolysis of the acidic salts present in the aqueous phase to produce hydrochloric acid.

Enormous amount of concentrated acids have been used for stimulating the oil wells and to obtain the unrecovered hydrocarbons. The underground rocks which are basic in nature (e.g., limestone) can be destroyed by the treatment with concentrated hydrochloric acid or acetic acid on injection. The hydrocarbons trapped between the rocks will be easily ejected by this treatment. Hydrofluoric acid is commonly employed for silica or sand stone based rocks. These acidizing process will cause to shoot up the corrosion rate of the metallic pipes inside the oil wells. In the presence of hydrogen sulphide, the dissolved metal in acidic medium will cause to precipitate the iron oxide and iron sulphide. These precipitates will negatively affect the quality of crude oil and oil production equipments. The addition of corrosion inhibitors is very essential to reduce the rate of the corrosion considerably.

Prevention of Corrosion

It is a fact that corrosion can't be prevented completely, but the most economical solution is to adopt more practical techniques for controlling the rate of corrosion. There are number of corrosion controlling techniques available depending upon the type and nature of corrosion. Surface coating is the most widely accepted method for controlling natural corrosion. Galvanizing, anodizing etc are used for decreasing the rate of galvanic corrosion. Accelerated corrosions

such as acid pickling, de-scaling, oil well corrosion etc are chiefly controlled by the addition of certain corrosion inhibitors into the acidic solutions.

Corrosion Inhibitors

The use of corrosion inhibitors is the most practical way for decreasing the rate of corrosion especially in acidic media. Since corrosion is an electrochemical phenomenon, oxidation and reduction are the two major processes taking place during the corrosion. Metal atoms which undergo oxidation will act as the anodic regions and the electrons released by the same atoms will be accepted by the protons, which are at the immediate vicinity of the metal surface and will get reduced to hydrogen atoms. This region of the metal is behaving as cathode. Corrosion inhibitors are classified into three according to their inhibitive mechanism. They are a) anodic inhibitors b) cathodic inhibitors and c) mixed type inhibitors. The role of a corrosion inhibitor is to protect the metallic surface by interacting with metal atoms directly or reacting the environment by which the surface is exposed. The inhibitive action of a corrosion inhibitor on the metal surface in a homogeneous liquid corrosive medium may be due to

a) Increasing the anodic or cathodic polarization
b) Reducing the diffusion of H^+ ions from the bulk to the metal surface or
c) Increasing the electrical resistance and thus by reducing the corrosion current density on the metallic surface.

Anodic corrosion inhibitors

The action of these inhibitors is to control the rate of anodic oxidation and thus prevent corrosion [7]. They can make large anodic shift of the corrosion

potential. These types of inhibitors can passivate the steel by making passive oxide layers on the metal surface. They may be oxidizing (e.g., chromates, nitrites and nitrates) or non oxidizing type (e.g., ortho phosphate, tungstate and molybdates). The first type make protective layer in the absence of oxygen, while the second type require oxygen for making the passive layer [8,9].

These inhibitors are sometimes referred as “dangerous inhibitors” since, small pores and defects on the oxide layer of these inhibitors, may lead to the accelerated corrosion of the metals [10].

Cathodic corrosion inhibitors

These inhibitors will decrease the rate of reduction process taking place on the cathodic sites, by shifting the potential more towards negative direction (cathodic side). The localized precipitation of species on cathodic site will enhance the corrosion resistance and thus reduce the migration of ions towards cathodic region considerably. The reduction of oxygen will be difficult in this scenario. Some cathodic inhibitors can act as oxygen scavengers and thus help to control the corrosion by preventing the cathodic depolarization caused by oxygen. Examples for cathodic inhibitors are metal ions (calcium, zinc etc), bicarbonates, polyphosphates, sulphites etc. Organic compounds such as imidazole and benzamide are usually used as cathodic inhibitors in boilers, which will help to prevent the deposition of calcium and magnesium [11].

Generally cathodic corrosion inhibitors are termed as “safe inhibitors” since they can reduce the rate of cathodic process even at low concentrations.

Mixed inhibitors

These inhibitors influence both anodic and cathodic processes of corrosion. Many organic molecules come under this category. Various amines, triazoles, thiourea, quinolines can act as mixed corrosion inhibitors especially for steel and copper in acidic media [12,13].

Organic inhibitors

There are several natural as well as synthetic organic molecules, which act as corrosion inhibitors for different metals such as iron, copper, zinc etc in acidic, basic and neutral media. Majority of the organic inhibitors are acting as mixed type corrosion inhibitor. At sufficient concentrations they can make good protective film via adsorption on the surface of the corroding metal. Adsorption may be physical or chemical depending upon the molecular structure of the compound. In general, inhibition efficiency of the organic inhibitors is found to increase with the concentration. Even though most of the organic molecules are acting as the mixed type inhibitors, some of them may affect more at anodic or cathodic site. It was well established that the organic molecules containing hetero atoms such as O, S, N etc and compounds possess azomethine linkage (>C=N-) i.e., Schiff bases act as good corrosion inhibitors for various grades of steels, zinc and copper in acidic as well as NaCl solution. The efficiency of these compounds depend on the number of active probes on the molecule, charge density, molecular size, concentration, nature of adsorption and ability to form metallic complexes. The unshared pair and π electrons on the molecule can interact well with the empty orbitals of the metal atoms and cause to the firm adsorption of aromatic

Schiff bases on the metal surface. In addition to this processes, the back donation of the electrons from the filled metal orbitals to the unoccupied π^*-orbitals of the Schiff base also come into play during the interaction, which will help the molecule to make good protective layer on the metal surface.

Schiff Bases as Corrosion Inhibitors- A Review

Large numbers of Schiff bases were screened for their corrosion inhibition capacity in acidic media. Many of them were effective against the corrosion of mild or carbon steel in acidic media. Few of them were acted as efficient inhibitor against the corrosion of copper and zinc in aggressive medium. The subsequent paragraphs explore the ability of certain newly synthesized Schiff bases to act as good inhibitors against the metallic corrosion in acidic media, which was reported by the previous researchers.

Two newly synthesised Schiff bases N,N′-*ortho*-phenylene(salicylaldimine-acetylacetone imine) and *N*,*N*′-*ortho*-phenylene(salicylaldimine-2-hydroxy-1-naphthaldimine) were studied as inhibitors for the corrosion of mild steel in 0.5 M sulphuric acid by M. Hosseini et al [14]. They confirmed by weight loss studies, electrochemical impedance and Tafel polarization measurements that both compounds act as good inhibitors, with efficiencies of around 95% at a concentration of 400 ppm. The nature of inhibition in both cases was mixed type (anodic and cathodic). Temkin isotherm is found to provide an accurate description of the adsorption behaviour of the investigated Schiff bases.

N. Saxena et al investigated the corrosion performance of mild steel in nitric acid solution containing various concentrations of Schiff bases derived from anisaldehyde such as N-(4-nitro phenyl) p-anisalidine, as N-(4-chloro phenyl) p-

anisalidine, as N-(4-phenyl) p-anisalidine, as N-(4-methoxy phenyl) p-anisalidine, as N-(4-hydroxy phenyl) p-anisalidine using mass loss, thermometric and potentiostatic polarization studies [15]. All compounds exhibited appreciable corrosion inhibition efficiencies. The inhibition efficiency was found larger than their parent amines and a maximum of 98.32% of efficiency was obtained.

2-alkyl-N-benzylidenehydrazinecarbothioamide of fatty acid hydrazides from nontraditional oils (neem, rice bran and karanja) have been synthesized and evaluated as corrosion inhibitors for mild steel in hydrochloric acid solution using weight loss method by Toliwal et al. Adsorption of all Schiff bases on mild steel surface in acid solution obeyed Temkin adsorption isotherm. Inhibition efficiency of these compounds was increased with the concentration of the compound, and varies with solution temperature, immersion time and concentration of acid solution. Various thermodynamic parameters were also calculated to investigate the mechanism of corrosion inhibition [16].

The inhibiting effect of (NE)-4-phenoxy-N-(3-phenylallylidene) aniline (PAC) on the corrosion of mild steel in 1.0 M HCl has been studied by H. Keles et al, very recently, by electrochemical impedance spectroscopy and Tafel polarization measurements. They determined the corrosion rate theoretically in terms of mm per year, using current density values of mild steel in 1.0 M HCl medium. It was found that PAC has remarkable inhibition efficiency on the corrosion of mild steel especially at high temperatures. By thermometric studies they proved that transformation of physical adsorption into chemical adsorption took place as the temperature of the system increased. The thermodynamic

functions of adsorption processes were also evaluated. Scanning electron microscope observations of the electrode surface confirmed the existence of a protective adsorbed film of the inhibitor on the electrode surface [17].

D. Gopi et al has reported the corrosion inhibition efficiency of of 3,5-diamino-1,2,4-triazole Schiff base derivatives, based on the effect of changing functional groups. An attempt has been done to establish a relationship between inhibitor efficiency and molecular structure using weight loss method, electrochemical and Fourier transform infrared spectral techniques. They found that the molecules containing more electron donating groups have higher inhibition efficiency than the corresponding compounds with low electron donating groups. The results indicated that the order of inhibition efficiency of the triazole and its Schiff bases in solution and the extent of their tendency to adsorb on mild steel surfaces were as follows: vanilidine 3,5-diamino-1,2,4-triazole > furfuraldine 3,5-diamino-1,2,4-triazole > anisalidine 3,5-diamino-1,2,4-triazole > 3,5-diamino-1,2,4-triazole [18].

A novel Schiff base 2,2′-[bis-N(4-choloro benzaldimin)]-1,1′-dithio has been synthesized by S. M. A. Hosseini et al and its inhibiting action on the corrosion of mild steel in 0.5 M sulfuric acid was investigated by various corrosion monitoring techniques, such as weight loss and potentiodynamic polarization techniques. They showed that this compound acted as a good corrosion inhibitor for mild steel and the inhibition efficiency increased with the inhibitor concentration. This organic compound behaved as mixed type inhibitor

in the acid solution, and its adsorption on the mild steel surface was found to obey the Langmuir adsorption isotherm [19].

Recently A. J. A. Nasser et al have investigated the influence of N-[morpholin-4-yl(phenyl)methyl]benzamide (MPB) on corrosion inhibition of mild steel in 1.0 M HCl by weight loss, effect of temperature, potentiodynamic polarization and electrochemical impedance spectroscopic studies. They found that the adsorption of MPB on the mild steel surface obeyed the Temkin adsorption isotherm. Potentiodynamic polarization curves showed that MPB act as a cathodic inhibition predominantly in hydrochloric acid [20].

Schiff base N-[(2-chloroquinolin-3-yl) methylidene]-2-methylaniline (CQM) was synthesized by S. Jauhari et al and its inhibitive effect on mild steel in 1.0 M HCl solution was investigated by weight loss measurement and electrochemical tests. From the studies, they observed that the inhibition efficiency increased with the Schiff base concentration and reached a maximum at the optimum concentration. This was further confirmed by the decrease in corrosion rate of mild steel with the inhibitor concentration. They also proved that the system follows Langmuir adsorption isotherm [21].

A. S. Fouda et al [22] have investigated the corrosion behavior of carbon steel in 0.5 M HCl solution in the absence and presence of new five Schiff bases of indole derivatives by electrochemical impedance spectroscopy (EIS), electrochemical frequency modulation (EFM) and potentiodynamic polarization techniques. All the experimental results showed that these Schiff bases have excellent corrosion inhibition performance. The polarization curves showed that

these compounds act as mixed type inhibitors. The adsorption of these Schiff bases on carbon steel surface is consistent with Langmuir adsorption isotherm. The effect of temperature on the rate of corrosion in the absence and presence of these compounds were also studied.

The inhibiting action of 4-amino-antipyrine (AAP) and its Schiff bases 4-[(benzylidene)-amino]-antipyrine (BAAP), 4-[(4-hydroxy benzylidene)-amino]-antipyrine (SAAP) and 4-[(4-methoxy benzylidene)-amino]-antipyrine (AAAP) which are derived from 4-amino-antipyrine with benzaldehyde, salicylaldehyde and anisaldehyde, towards the corrosion behavior of mild steel in 1.0 M HCl solution was investigated by K. M. Govindaraju et al [23] using weight loss, potentiodynamic polarization, electrochemical impedance and FT-IR spectroscopic techniques. They found that all the synthesized Schiff base compounds were behaved well to retard the corrosion rate very effectively. The inhibitor efficiencies calculated from all the applied methods were in good agreement and were found to be in the order: AAAP > SAAP > BAAP > AAP.

R. K. Upadhyay et al have reported the corrosion inhibition capacity of Schiff bases N-(furfurlidine)-4-methoxy aniline, N-(furfurlidine)-4-methylaniline, N-(salicylidine)-4-methoxy aniline, N-(cinnamalidine)-4-methoxy aniline, and N-(cinnamalidine)-2-methylaniline. They adopted mass loss and thermometric studies to evaluate the inhibition of corrosion of mild steel in hydrochloric acid. Results of inhibition efficiency yielded by the two methods were in good agreement and depend on the inhibitor and acid concentration. Maximum inhibition efficiency of 98% was reported by them [24].

Two series of long chained Schiff base amphiphiles were prepared by condensation of benzaldehyde or anisaldehyde with three different alkyl chain length fatty amines namely: dodecyl, hexadecyl and octadecyl amine by I. A. Aiad et al. The synthesized Schiff bases were evaluated as corrosion inhibitors for low carbon steel in various acidic media (HCl and H_2SO_4) using weight loss technique. The corrosion inhibition measurements of these inhibitors showed high protection against corrosion process in the tested acidic media at different doses. Attempts to correlate the inhibition efficiency of these compounds with their chemical structures have also been done [25].

Recently S. Issaadi et al have reported the corrosion inhibition studies of novel thiophene based Schiff bases. The Schiff bases, 4,4′-bis(3-carboxaldehyde thiophene) diphenyl diimino ether and 4,4′-bis(3-carboxaldehyde thiophene) diphenyl diimino ethane, were obtained by the condensation of 3-carboxaldehydethiophene and its corresponding amine. Polarization curves revealed that both compounds were mixed type (cathodic/anodic) inhibitors and inhibition efficiency (%IE) increases with increasing concentration of compounds. They suggested that corrosion inhibitive response of the compounds depend on their concentrations and the molecular structures. Adsorption of compounds on mild steel surface was spontaneous and obeyed Langmuir isotherm [26].

The behavior of the Schiff base *N*,*N*′-bis(salicylidene)-1,2-ethylenediamine (Salen), and a mixture of its parent molecules, ethylenediamine and salicylaldehyde, as carbon steel corrosion inhibitors in 1.0 M HCl solution was studied by A. B. da Silva et al [27] using corrosion potential measurements,

potentiodynamic polarization curves, electrochemical impedance spectroscopy and spectrophotometry measurements. They reported that results obtained in the presence of Salen were similar to those obtained in the presence of the salicylaldehyde and ethylenediamine mixture, showing that in acid medium the Salen molecule undergoes hydrolysis, regenerating its precursor molecules.

Corrosion inhibition investigations of pyridine based Schiff bases were reported by A. Yurt et al [28] on carbon steel in HCl medium using potentiodynamic and ac impedance studies. The Schiff bases under examination were synthesized by the condensation between pyridine-2-carboxaldehyde and respective amines. All compounds were found to act as good corrosion inhibitors.

Scope and Objectives of the Present Investigation

Vigorous research on corrosion and corrosion prevention techniques are undergoing globally by various scientists and surface engineers to minimize the rate of corrosion, since it is a potential threat which may affect directly or indirectly the economy and safety measures. The need for novel corrosion prevention techniques and corrosion inhibitors are increasing day by day. To reduce rate of corrosion of a metal in an aggressive medium with the aid of corrosion inhibitors is a challenging and interesting area of research. Synthesizing novel molecules and monitoring their corrosion inhibition capacities on various metals, especially mild and carbon steels and to implement these molecules as useful corrosion inhibitors are of keen interest for researchers and corrosion/ surface engineers related to metal and petroleum based industries. Even though a large number of organic molecules especially Schiff bases were screened for their

corrosion inhibition capacity on metals in acidic media, still remains unanswered questions about the corrosion behavior of various heterocyclic Schiff bases. A very few of the articles have been reported by the previous researchers on the corrosion inhibition behavior of pyridine, thiophene and furfural based Schiff bases which was confirmed by thorough literature survey.

In the present course of investigation it is proposed to determine the corrosion inhibition properties of eight different heterocyclic Schiff bases derived from 3-acetyl pyridine, furan-2-aldehyde and thiophene-2-aldehyde on carbon steel in hydrochloric acid and sulphuric acid by the conventional mass loss studies, electrochemical studies such as Tafel polarization and ac impedance measurements. It is also proposed to investigate the mechanism of corrosion inhibition by plotting various adsorption isotherms. Thermodynamic parameters such as adsorption equilibrium constant and free energy of adsorptions are also proposed to evaluate from adsorption isotherms.

Temperature effect on corrosion was investigated in order to determine thermodynamic parameters such as activation energy, enthalpy and entropy. Present investigation also aims to improve the corrosion inhibition capacities of certain organic molecules by utilizing the synergistic properties of iodide ions. In the present study, an attempt was also made to correlate the corrosion inhibition capacity of these molecules with their structural interactions on carbon steel surface.

CHAPTER 2

MATERIALS AND METHODS

It is not a tedious job to create a natural corrosive environment in the experimental settings of a laboratory. At the same time, since natural corrosion is a slow phenomenon and the monitoring of the rate of decay of a metal is very time consuming process, it is customary to adopt accelerated corrosion techniques which will mimic the corrosive environment. Accelerated corrosion tests of various metals are mainly performed in acidic (aggressive) solutions.

To investigate the rate of corrosion and the behavior of corrosion inhibitors, conventionally accepted acceleration tests are mass loss or gravimetric studies and electrochemical studies. Electrochemical studies are mainly subdivided into Tafel polarization studies and electrochemical impedance spectroscopy (EIS). This chapter describes the preparation of metal specimens used for corrosion studies, its composition, aggressive solutions, details of corrosion monitoring techniques employed for the investigation and the electrochemical instrumental set up used for corrosion measurement.

Metal Specimens

Carbon steel (composition: 0.58 %; Mn, 0.07 %; P, 0.02 %; S, 0.015 %; Si, 0.02 % and the rest Fe, determined by EDAX method) were cut in the dimension 1.5x 1.5x 0.114 cm and abraded with various grades of silicon carbide papers (120, 400, 600, 800, 1000 and 1200) to obtain well polished surfaces as per ASTM standards. The total surface area of the metal specimens was accurately determined using vernier calipers and screw gage. Metal specimens were

degreased with acetone, washed with detergent and distilled water, dried and finally weighed. Specimens were immersed in aggressive solutions with and without the inhibitor in different concentrations using hooks and fishing lines.

Aggressive Solutions

HCl and H_2SO_4 (Merck samples) were diluted to 1.0 M and 0.5 M concentrations respectively using distilled water. A stock solution of the inhibitor was first prepared and diluted with respective acidic solutions to obtain inhibitor solutions having concentrations 0.2 mM –1.0 mM for performing the corrosion studies of Schiff bases derived from 3-acetylpyridine and solutions in the concentration 0.1 mM- 0.5 mM for Schiff bases derived from furan-2-aldehyde and thiophene-2-aldehyde. The total volume of the medium was 50ml for gravimetric studies but 100ml was maintained for all electrochemical investigations.

Gravimetric Corrosion Studies

Gravimetric corrosion inhibition studies were performed by immersing the well polished carbon steel (CS) specimens in aggressive solutions having different concentrations of the inhibitor for 24 hours. A blank experiment was also conducted without adding the inhibitor. The weight loss occurred for metal specimens were measured after 24 h. For good reproducibility, all experiments were carried out in duplicate and the average values were reported. The corrosion rates and percentage of inhibition efficiencies were calculated by the following equations. The corrosion rates were expressed in mm/y and the inhibition efficiencies were obtained from corrosion rates.

$$\text{Rate of corrosion } W = \frac{K \times \text{wt.loss in grams}}{\text{Area in sq.cm} \times \text{time in Hrs} \times \text{Density}} \quad (1)$$

where 'K' =87600 (This is a factor used for the conversion of cm/hour into mm/year)

Density of CS specimen= 7.88g/cc

Percentage of inhibition or the inhibition efficiency (η) was calculated by

$$\eta = \frac{W - W'}{W} \times 100 \quad (2)$$

where W & W' are the corrosion rate of the CS specimen in the absence and presence of the inhibitor respectively.

Corrosion Inhibition Studies of Parent Compounds

To compare the corrosion inhibition efficiency of Schiff base and its parent aldehyde/ketone and amine, gravimetric corrosion studies of the parent compounds were performed in aggressive solutions for 24 h. This study has considerable significance in two aspects. At first, one can validate the higher inhibition efficiency of the Schiff base when compared to the corrosion inhibition efficiency of parent compounds. Sometimes Schiff base molecules undergo hydrolysis in the acidic media into their parent compounds and an appreciable change in the inhibition efficiency occur with time. In such cases the corrosion inhibition efficiency of the mixture of parent compounds were performed and compared with the inhibition efficiency of Schiff bases. The information regarding the hydrolysis and inhibition efficiency of the hydrolyzed product is the second aspect of this study.

Synergistic Effect Studies

Synergistic effect study was conducted with aggressive solutions (sulphuric acid) together with 0.2 mM KI solutions. Gravimetric studies and electrochemical studies were performed separately to check the synergistic effect of iodide ions with the Schiff base molecules on carbon steel surface. If synergism plays, the addition of KI (1ml, 0.2 mM KI for gravimetric and 2ml for electrochemical studies) into the aggressive solution will raise the corrosion inhibition efficiency drastically.

Adsorption Isotherms

The mechanism of inhibition of various organic molecules on the surface of a corroding metal can be well explained by adsorption. To verify the nature of interaction between the metal surface and inhibitor molecules, adsorption isotherms were plotted by calculating the surface coverage from the inhibition efficiency. The different models of adsorption isotherms proposed was Langmiur, Freundlich, Temkin and Frumkin and the recently formulated thermodynamic/kinetic model, El-Awady isotherm. Among the isotherms mentioned above, the most suitable one was chosen with the help of correlation coefficient. The important thermodynamic parameters such as adsorption equilibrium constant (K_{ads}) and free energy of adsorption (ΔG^{o}_{ads}) were calculated from the adsorption isotherms. These parameters are of key important in predicting the spontaneity of the process and the nature of adsorption i.e., physisorption or chemisorption or a combination of both. The important models

of adsorption isotherms considered and the equation for the free energy of adsorption isotherm are given as follows [29-32].

Langmiur adsorption isotherm $\frac{C}{\theta} = \frac{1}{K_{ads}} + C$ (3)

Freundlich adsorption isotherm $\theta = K_{ads}$ C (4)

Temkin adsorption isotherm $e^{f\theta} = K_{ads}$ C (5)

Frumkin adsorption isotherm $\frac{\theta}{1-\theta}\exp(f\theta) = K_{ads}$ C (6)

El-Awady adsorption isotherm $log\frac{\theta}{1-\theta} = logK + y\,logC$ (7)

In the above equations C represents the concentration of the inhibitor, θ is the surface coverage and K_{ads} is the adsorption equilibrium constant. In El-Awady isotherm, $K_{ads} = K_{1/y}$, where y= number of active sites. If 1/y is less than 1, it implies multilayer adsorption and if 1/y is greater than 1, suggests that a given inhibitor molecule occupies more than one active site. Free energy of adsorption is related to adsorption equilibrium constant by the following equation.

$\Delta G^0_{ads} = -RTln(55.5\ K_{ads})$ (8)

Surface Analysis Using SEM

Surface morphological studies give insight to the mechanism of inhibition by which an organic molecules decrease the rate of corrosion. This was done by taking the scanning electron micrographs (SEM) of the metal surfaces at different conditions. SEM images of well polished bare metal specimen, metal specimen in acid solution (blank, treated for 48 h) and specimens in the inhibitor solution (treated for 48 h) were taken in the resolution 2.00x and compared. Hitachi

SU6600 model scanning electron microscope was used for performing the surface morphological studies.

Temperature Studies

Gravimetric corrosion inhibition studies were performed in the temperature range 30-60^{0}C for investigating various thermodynamic parameters of corrosion such as enthalpy of corrosion (ΔH*), entropy of corrosion (ΔS*), activation energy (E_a) and Arrhenius parameter (A). The rate of corrosion is related to the energy of activation by the well known Arrhenius equation

$$K = A \exp\left(-\frac{E_a}{RT}\right) \quad (9)$$

where K is the rate constant, A is pre exponential or Arrhenius factor, E_a is the activation energy, R is the universal gas constant and T is the temperature in Kelvin scale. From the above equation it is evident that a plot of logK Vs 1000/T will be a straight line having slope -E_a/2.303R and intercept log A.

The enthalpy and entropy of activation (ΔH*, ΔS*) were calculated from the transition state theory [33]

$$K = \left(\frac{RT}{Nh}\right) \exp\left(\frac{\Delta S*}{R}\right) \exp\left(\frac{-\Delta H*}{RT}\right) \quad (10)$$

Here, N is the Avogadro number and h is the Planks constant. The equation can be rewritten in the form y= mx +c to obtain

$$log\frac{K}{T} = log\frac{R}{Nh} + \frac{\Delta S}{2.303\,R} - \frac{\Delta H}{2.303\,R\,T} \quad (11)$$

The slope of the above equation is -ΔH/2.303R, from which enthalpy of activation can be calculated. Entropy of activation can be calculated from the intercept of the above equation i.e., $log\frac{R}{Nh} + \frac{\Delta S}{2.303\,R}$ (12)

Electrochemical Investigations

It is well known that corrosion is an electrochemical phenomenon. The measurable electrochemical parameters such as corrosion current density, corrosion potential, charge transfer resistance, cathodic and anodic slope values (from current-potential response) etc will quantify the corrosion and help one to predict the rate of corrosion and to determine the mechanism of the corrosion. In the presence of corrosion inhibitors, the electrochemical parameters change considerably and hence affect the rate of corrosion. Exploiting these responses of corroding metals in the presence and absence of the inhibitor with the help of sophisticated electrochemical systems, is the major strategy adopted by the corrosion researchers to predict the inhibitive capacity of the various organic molecules in acidic media. Widely practiced electrochemical corrosion measurement techniques are Electrochemical Impedance Spectroscopy (EIS) and polarization studies. Polarization techniques are further classified into Tafel polarization analysis and linear polarization resistance analysis. Applications of the electrochemical methods are widely accepted for the investigation of corrosion [34-39].

The main advantage of the electrochemical investigation than the conventional gravimetric studies is that the former one require short span of time. All electrochemical measurements are computer assisted, and most modern softwares and electrochemical systems are using for the corrosion analysis. More refined and accurate values for the electrochemical analyses is thus possible than the conventional time consuming gravimetric investigations.

In the present corrosion investigation, Ivium compactstat-e (made in Netherlands) electrochemical system was used. Latest version of the software 'IviumSoft' was powered the electrochemical analysis. Various analytical procedures like selection of proper equivalent circuit, simulation of curves obtained by the analysis, calculation of resistance and current densities etc can be easily performed with the software.

For all electrochemical measurements a cell with three electrode assembly was used. Platinum electrode having area $1cm^2$ was used as the counter or auxiliary electrode and saturated calomel electrode (SCE) was the reference electrode. Well polished metal surface having an exposed area of $1cm^2$ towards the corroding medium acted as the working electrode.

The three electrode system eliminates the limitations of the conventional two electrode system. The conventional two electrode set up consists of a working electrode and a reference electrode only. A desired potential is applied in a controlled way on the working electrode to facilitate the charger transfer process during the electrochemical experiments. A second electrode having a fixed potential must be used in conjunction with the working electrode to gauge the exact potential of working electrode by balancing the charge added or removed by the working electrode. This setup has serious shortcomings since practically it is very difficult to maintain the constant potential of the reference electrode during the passage of current to the working electrode. These limitations can be overcome with the help of three electrode assembly (Figure 2.1)

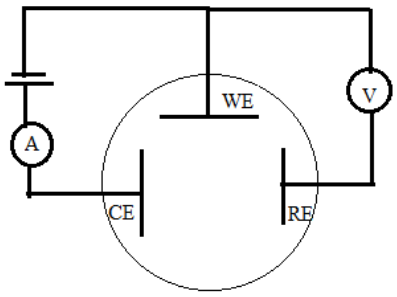

Fig. 2.1 Three electrode circuitry

In the above figure, CE, RE and WE represent counter, reference and working electrodes respectively. Additional electrodes namely counter or auxiliary electrode is inserted into the cell assembly. Now the role of the reference electrode is to control and measure the electrode potential of the working electrode only and practically no current is passed through the it. The auxiliary electrode allows the passage of whole current required for balancing the current of the working electrode.

Polarization studies

Polarization studies are performed by changing the applied potential of the working electrode in a controlled manner and scanned at constant rate (potentiodynamic). Mainly, Polarization studies can be divided into two a) Tafel extrapolation technique (Stern method) and b) Polarization resistance studies (Stern and Geary method) [40-43].

Tafel extrapolation technique

The basis of the polarization techniques is mainly derived from mixed potential theory proposed by Wagner and Traud [44,45]. According to this theory, an overall electrochemical reaction can be algebraically divided into half cell

reactions i.e., oxidation and reduction half cell reactions. In the cases of iron/copper based metal specimens, the reaction usually takes place at anodic areas is $M \rightarrow M^{2+} + 2e^-$, where 'M' represents iron/copper. The main cathodic reaction takes place during corrosion is the reduction of H^+ ions to H_2. Since the cathodic reaction is slower than the anodic process, the rate is usually controlled by the cathodic reaction. If the rate of anodic and cathodic processes is equal, there will be no charge accumulation. The mixed potential at this moment is called the open circuit potential (OCP) and commonly designated as corrosion potential or E_{corr}. This corrosion potential is distinctly different from the reversible potential of the corroding metal or the species in the solution that is reduced at the cathode. The current at this mixed potential is designated as corrosion current density and denoted by i_{corr}.

An electrode can be polarized by the application of external voltage. The magnitude of polarization can be measured in terms of overvoltage i.e., the difference between the equilibrium potential and the external potential. Polarization can be either anodic direction (noble) or cathodic direction (active). To get i_{app} (measured or applied current density) as a function of E (applied potential), applied potential between the reference electrode and the working electrode is controlled and scanned at constant rate. The important types of polarization that occur during electrochemical measurements are activation polarization and concentration. Since the main steps in the electrochemical corrosion are controlled by activation or charge transfer, the effect due to concentration polarization can be neglected. For the reversible electrodes which

are controlled by activation process, the polarization can be best described by the equation similar to Butler-Volmer equation [46]

$$i_{app} = i_{corr}\left\{exp\left[\frac{\alpha_a}{RT}\, zF(E - E_{corr})\right] - exp\left[-\frac{\alpha_c}{RT}\, zF(E - E_{corr})\right]\right\} \quad (13)$$

i_{app} is applied or measured current density; i_{corr} is corrosion current density; α_a and α_c are the charge transfer coefficients for anodic and cathodic reactions, respectively. $E\text{-}E_{corr}$ is the polarization or the over potential obtained by the difference between applied and corrosion potential; z is metal valence; F is Faraday constant; R, the gas constant and T is the absolute temperature.

When the polarization is in the anodic direction (positive), $E >> E_{corr}$ and the second term in the above equation can be neglected. Now equation 13 can more simply expressed as

$$i_{app} = i_{corr}\left\{exp\left[\frac{\alpha_a}{RT}\, zF(E - E_{corr})\right]\right\} \quad (14)$$

The Tafel slope for the anodic process from the above equation is

$$b_a = \frac{2.303\, RT}{\alpha_a\, zF}$$

Similarly, for cathodic process, $E_{corr} >> E$, then the first term in equation 13 can be neglected. The simplified equation for the cathodic reaction can be expressed as

$$i_{app} = i_{corr}\left\{exp\left[-\frac{\alpha_c}{RT}\, zF(E - E_{corr})\right]\right\} \quad (15)$$

Tafel slope for cathodic reaction can be expressed as

$$b_c = \frac{2.303\, RT}{\alpha_c\, zF}$$

The mixed potential diagram and Tafel extrapolation are described in the Figure 2.2. From the obtained current densities, the percentage of inhibition can be calculated by the following equation

$$\eta_{pol}\,\% = \frac{I_{corr} - I'_{corr}}{I_{corr}} X100 \qquad (16)$$

where i_{corr} and i'_{corr} are uninhibited and inhibited corrosion current densities respectively.

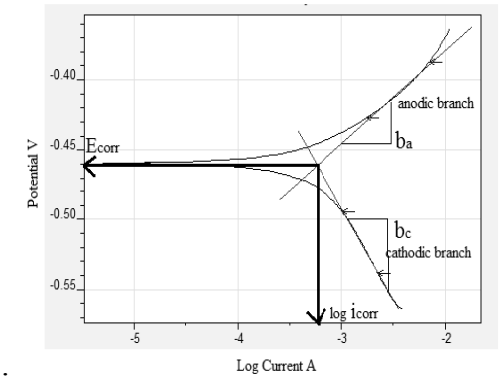

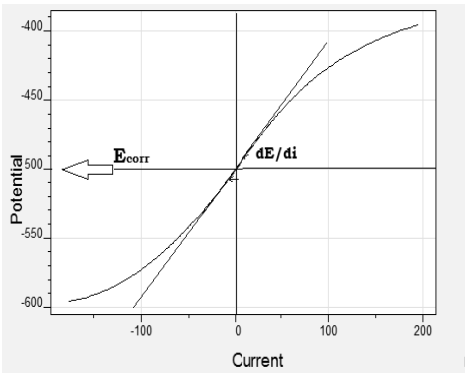

Fig. 2.2 Tafel extrapolation method

Fig. 2.3 Linear polarization method

The slopes of Tafel lines have a significant role in interpreting the mechanism of inhibitor. By comparing the Tafel slopes of the uninhibited and the inhibited solutions, one will get the idea about the nature of inhibition. If the anodic slope (b_a) of the inhibited solution only deviates considerably from the anodic slope of the uninhibited solution, it can be assumed that inhibitor molecule affect on anodic process of corrosion. Similarly, the change of cathodic slope (b_c) alone is an indication of the adsorption of the inhibited molecules on the cathodic sites. An appreciable change in both b_a and b_c assures that the inhibitor molecule affect both anodic and cathodic process of corrosion. Tafel extrapolation as well as other polarization techniques badly affect by several factors such as ohmic

resistance (arises from the resistivity of the solution) cell geometry, location of the reference electrode, magnitude of the applied current etc, which are few among this. Ohmic resistance may also contribute to overvoltage error sometimes [35,36,47,48].

Linear polarization resistance method

For small overpotential reactions with respect to E_{corr}, Stern and Geary modified the kinetic equation [43]. For the activation controlled process the equation can be linearized as

$$i_{corr} = \left(\frac{\Delta i_{app}}{2.303\,\Delta E}\right)\left(\frac{b_a b_c}{b_a + b_c}\right) \quad (17)$$

Rearranging the above equation

$$i_{corr} = \left(\frac{1}{2.303\,R_p}\right)\left(\frac{b_a b_c}{b_a + b_c}\right) = \frac{B}{R_p} \quad (18)$$

where R_p is $\frac{\Delta E}{\Delta i}$, called the polarization resistance and 'B' is a constant obtained by all the constant terms in the above equation. Most often i_{app} shows approximate linearity with potential. When one determine the slope of this plot(Figure 2.3) at E_{corr}, it may call as polarization resistance and it will be inversely proportional to the corrosion rate [49-50].

Linear polarization technique can be applied for the corrosion monitoring studies in the sense that the polarization resistance (R_p) increases with the inhibitor concentration. The rate of charge transfer process will be decreased considerably as the inhibitor molecules 'work' on the surface of the corroding metal by adsorption. In this scenario the rate of corrosion decreases appreciably.

From the slope analysis of the linear polarization curves at the corrosion potential, the polarization resistances were obtained.

The corrosion inhibition efficiency can be calculated using the equation

$$\eta_{R_p}\,\% = \frac{R'_p - R_p}{R'_p}\,X100 \qquad (19)$$

where R'_p and R_p are the polarization resistance in the presence and absence of inhibitor respectively [51]

Electrochemical impedance spectroscopy (EIS)

Impedance measurements are of key importance in predicting the corrosion rate of the metal in the aggressive solutions. Studies like corrosion behavior of metals which are coated with protective layers and of the inhibitive role of corrosion inhibitors on the metal surface etc can be easily performed with EIS measurements. In EIS technique, the working electrode is subjected to a small amplitude sinusoidal potential at a number of discrete frequencies ω. The resulting currents at each frequency will display sinusoidal response that is out of phase with applied potential signal by an amount Φ. The amplitude of the current is now inversely proportional to the impedance of the interface Z(ω). Electrochemical impedance is thus related to excitation voltage and the current response of the system by the following equation

$$Z(\omega) = V(\omega)/i(\omega) \qquad (20)$$

where V(ω) is the excitation voltage and can be expressed as a function of time i.e., $V = V_0 \sin(\omega t)$. Here V_0 is the amplitude of the signal. In equation 20, 'i' is the time varying current density and is given by $i = i_0 \sin(\omega t + \Phi)$, where i_0 is the amplitude of the current signal.

Impedance Z(ω) can be expressed as a complex function with the real and imaginary components whose values are frequency dependent

$$Z(\omega) = Z'(\omega) + jZ''(\omega) \quad (21)$$

where Z'(ω) is the real component of the impedance and given by $Z'(\omega) = Z_0 \cos\Phi$. Z''(ω) is the imaginary part of the impedance i.e., $Z''(\omega) = Z_0 \sin\Phi$, j is the imaginary number $\sqrt{-1}$ and Z_0 is the magnitude of the impedance.

The impedance response of a corroding system enables us to determine the equivalent circuit that exactly fit to the electrochemical system under examination. In many cases the simple equivalent circuit which mimic the corroding system consists of two resistances and one capacitance which are aligned in the following manner [52]

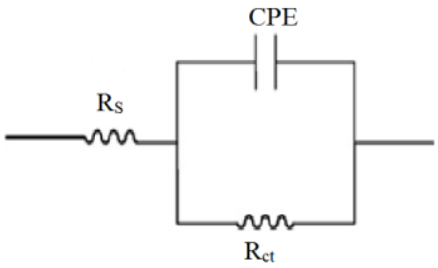

Fig. 2.4 Equivalent circuit fitting

where R_s is the solution resistance, R_{ct} is the charge transfer resistance and C_{dl} is the double layer capacitance. According to the above model circuit, at very low frequencies impedance will be equal to the sum of charge transfer resistance R_{ct} and solution resistance R_s while at higher frequencies impedance will be very close to the solution resistance R_s.

Representation of Impedance Data

Impedance data can be well represented by the Nyquist (Cole-Cole) plot, Bode plot and impedance plot.

Nyquist plot

In this method, the real part of the impedance (x-axis) is plotted against the imaginary component of the impedance (y-axis). The obtained curves will have semicircle shapes. At high frequencies, the impedance of the system is almost equal to the ohmic resistance R_s (or solution resistance). The frequency reaches its high limit at the leftmost end of the semicircle, where the semicircle touches the x- axis. The frequency reaches its low limit at the rightmost end of the semicircle where the impedance of the system will be R_s+R_{ct} (Figure 2.5).

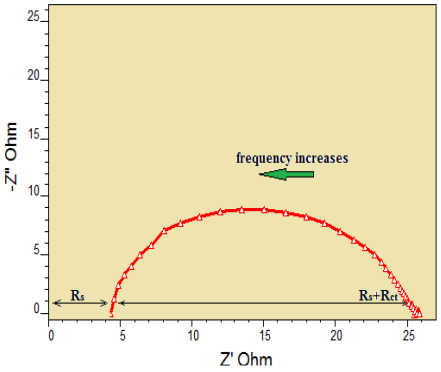

Fig. 2.5 Nyquist or Cole-Cole plot

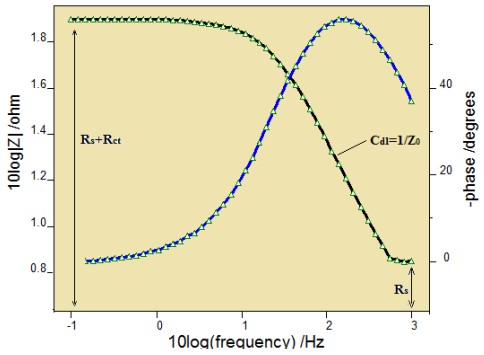

Fig. 2.6 Combined impedance and Bode plot

Each point on the Nyquist plots is the impedance at one frequency. It is estimated that if a compound has a corrosion inhibition capacity, the charge transfer resistance of the corroding metal in the presence of that compound will be higher than that of charge transfer resistance of the metal in the absence of the inhibitor in a corroding medium. From the values of the charge transfer

resistances the inhibition efficiency of a particular compound can be calculated by the following equation.

$$\eta_{EIS}\,\% = \frac{R_{ct} - R'_{ct}}{R_{ct}} X100 \qquad (22)$$

where R_{ct} and R'_{ct} are the charge transfer resistances of working electrode with and without inhibitor, respectively [51]. Nyquist plots have one serious disadvantage that one can't obtain the frequency at a particular point from the curve.

Bode plot and impedance plot

For a simple equivalent circuit represented in Figure 2.4, Bode plot is obtained by drawing the phase angle as a function of frequency. In this plot the absolute impedance and the phase angle, θ, of the resultant wave form is plotted as a function of frequency. The curve representing log|Z| versus log frequency is called the impedance plot. The absolute value of impedance Z is calculated from the equation $|Z| = \sqrt{Z'^2 + Z''^2}$. Analysis of the impedance plot will provide the values of R_s and R_{ct}. The break point of the impedance curve should lie on a straight line (at intermediate frequency) whose slope will be -1. Extrapolation of this straight line to the y-axis at f=1 or logf = 0 gives the value of C_{dl}.

$$|Z| = \frac{1}{C_{dl}} \qquad (23)$$

The combined Bode and impedance model plot is given in the Figure 2.6.

CHAPTER 3

CORROSION INHIBITION INVESTIGATIONS ON SCHIFF BASES DERIVED FROM 3-ACETYLPYRIDINE ON CARBON STEEL IN ACIDIC MEDIA

Three novel Schiff bases, 3-acetylpyridine semicarbazide (APSC), 3-acetylpyridine thiosemicarbazide (APTSC) and 3-acetylpyridine phenylhydrazine (APPH) have been synthesized and characterized as described in part I and their corrosion inhibition efficiencies on carbon steel (CS) in hydrochloric acid and sulphuric acid medium were explored by the conventional gravimetric studies, potentiodynamic polarization studies and electrochemical impedance spectroscopic studies. The mechanism of corrosion inhibition by these heterocyclic Schiff bases were evaluated by adsorption studies and this was further verified by surface morphological analysis. The temperature effect on the rate of corrosion in the presence and absence of the Schiff bases was studied in detail at a temperature range 30-60^{0}C. The synergistic effect of iodide ions on the corrosion inhibition response of compounds was also investigated. The details are provided in this chapter.

The entire chapter is divided into two sections. Section I deals with the corrosion investigations of CS in the presence of Schiff bases in HCl. The details of corrosion inhibition response of the heterocyclic Schiff bases on CS in 0.5M sulphuric acid is well documented in Section II.

SECTION I

CORROSION BEHAVIOUR OF CARBON STEEL IN 1.0 M HCl IN THE PRESENCE OF SCHIFF BASES DERIVED FROM 3-ACETYL PYRIDINE

The corrosion inhibition studies of the three Schiff bases, 3-acetylpyridine semicarbazone (APSC), 3-acetylpyridine thiosemicarbazone (APTSC) and 3-acetylpyridine phenylhydrazone (APPH) were conducted in 1.0 M HCl by preparing inhibitor solutions in the range 0.2 mM-1.0 mM. The CS specimens adopted for the study were prepared in accordance with ASTM standards which are described in chapter 2 in detail.

Gravimetric Corrosion Studies

Mass loss corrosion studies of CS were conducted by immersing the CS specimens in 1.0 M HCl medium for 24 h in the absence and presence of the Schiff bases at various concentrations. Table 2.1 and 2.2 represent the corrosion rates in mmy^{-1} and inhibition efficiencies (%) of the three heterocyclic Schiff bases APSC, APTSC and APPH on CS in HCl medium. The comparison of corrosion rates and inhibition efficiencies of these heterocyclic compounds can more clearly be visualized from Figures 2.7 and 2.8.

Table 2.1 Corrosion rates of CS in mmy^{-1} in the presence and absence of Schiff bases, APSC, APTSC and APPH in 1.0 M HCl

Schiff base	Concentration (mM)					
	0	0.2	0.4	0.6	0.8	1.0
APSC	6.54	2.6	1.91	1.15	0.933	0.932
APTSC	6.54	1.79	1.82	0.89	0.82	0.72
APPH	6.54	0.940	0.733	0.702	0.632	0.58

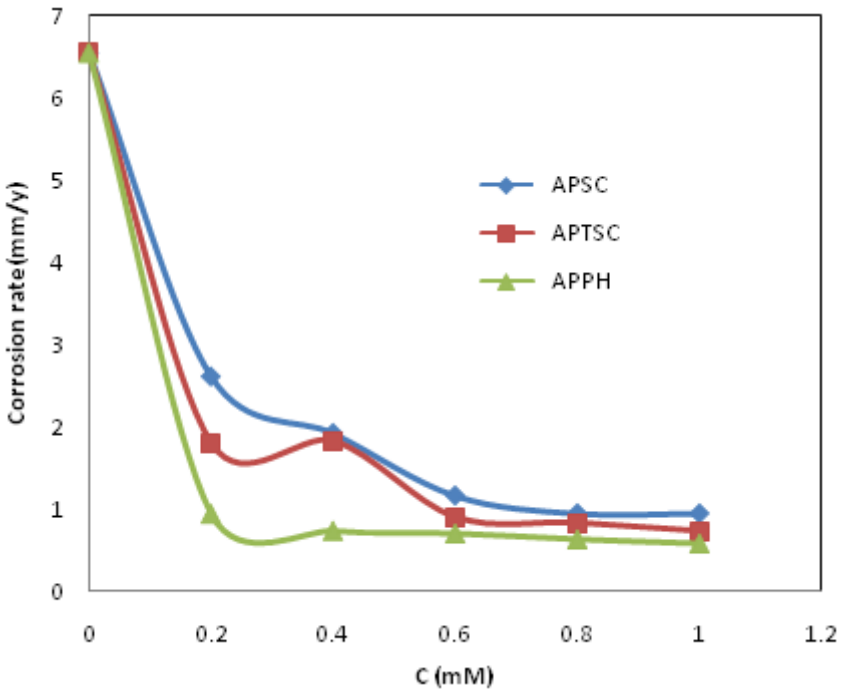

Fig. 2.7 Variation of corrosion rates of CS with the concentration of Schiff bases APSC, APTSC and APPH in 1.0 M HCl

Table 2.2 Corrosion inhibition efficiencies (η_w%) of Schiff bases, APSC, APTSC and APPH on CS in 1.0 M HCl

	Concentration (mM)				
Schiff base	0.2	0.4	0.6	0.8	1.0
APSC	60.33	70.77	82.40	85.73	85.75
APTSC	75.56	72.19	86.39	87.39	88.94
APPH	85.63	88.80	89.26	90.34	91.47

It is evident from the tables and figures that corrosion rate of the carbon steel in hydrochloric acid medium was considerably decreased in the presence of the heterocyclic Schiff bases. Even at low concentrations, these compounds inhibit the metallic dissolution appreciably in the acidic medium. All the three Schiff bases showed marked rise in the corrosion inhibition capacity with concentration.

The mechanism of corrosion inhibition by potential organic inhibitors can be explained as follows. It is well known that the surface of the metal is positively charged in acidic media [53]. It is believed that the Cl^- ions can be specifically adsorbed on the metal surface and creates an excess of negative charge on the surface. This will favour the adsorption of protonated Schiff bases on the surface and hence reduce the dissolution of Fe to Fe^{2+} [54]. Besides this electrostatic attraction between the protonated Schiff base and the metal surface, other possible interactions are i) interaction of unshared electron pairs in the molecule with the metal ii) interaction of π-electrons with the metal and iii) a combination of types (i–ii) [55,56]. On close examination of the molecular structures of these compounds, one can find various potential probes responsible for the inhibition capability. The heteroatom, azomethine moiety, π electron cloud of the aromatic rings, nitrogen atoms present on the other parts of the molecule etc will help to bind the molecules on the corroding metal surface through chloride ion. The unshared pair of electrons present on N atoms is of key importance in making coordinate bond with the metal. The π-electron cloud of the aromatic rings and the azomethine linkage also participate in the inhibition mechanism. Furthermore, the double bonds in the inhibitor molecule permit the back donation of metal d electrons to the π*-orbital and this type of interaction is not possible with amines [57].

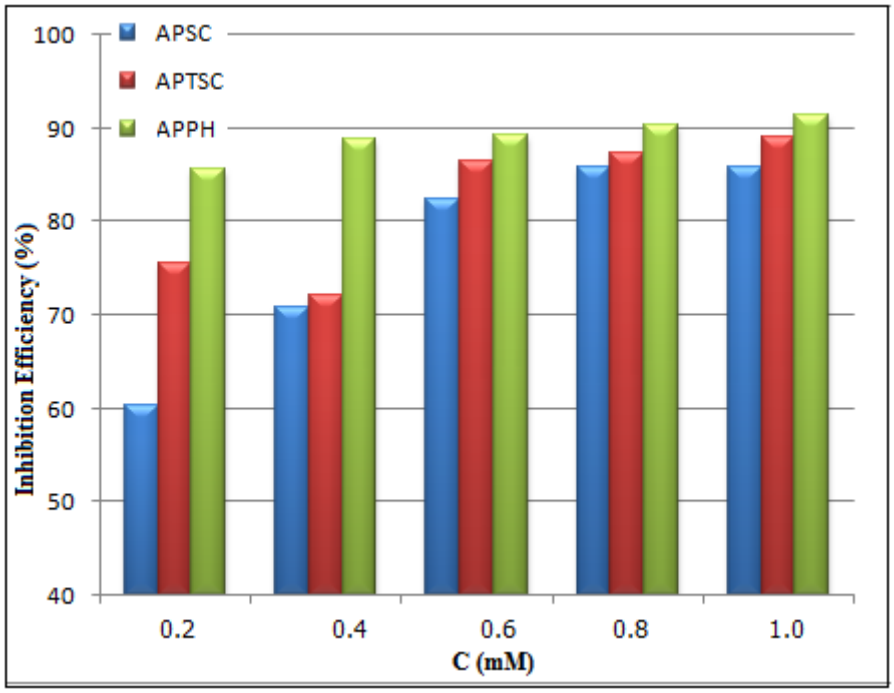

Fig. 2.8 Comparison of corrosion inhibition efficiencies (η_w%) of Schiff bases, APSC, APTSC and APPH on CS in 1.0 M HCl

To get a more insight into the mechanism of corrosion inhibition, Schiff bases were subjected to UV spectral studies in hydrochloric acid medium. It was confirmed by the study that all the three compounds undergo slow hydrolysis into their parent compounds in acidic medium. Figure 2.9 is the UV-visible spectrum of APPH in HCl, which exemplifies the hydrolysis of Schiff base. To answer the question ‘‘did the hydrolyzed products participate in the inhibition process?’’, gravimetric corrosion studies were performed by choosing the parent ketone and parent amine as the test compounds in acidic medium (Figure 2.11). Results showed that the parent compounds are scarcely inhibitive than Schiff bases. It may be concluded from the above investigations that the imines which are directly attached to the metal surface (via adsorption) do not undergo hydrolysis. These molecules thus reduce the rate of corrosion of CS specimens in acidic medium by

making a protective barrier without any hydrolysis. On the other hand, the molecules present in the bulk of the solution are more susceptible to hydrolysis and will be converted into parent compounds. This study also establishes the significant role of halide ion (chloride) in the corrosion inhibition process, which will be discussed in detail in the subsequent sessions.

On examination of Table 2.2 and Figure 2.8, it is evident that the Schiff bases followed the corrosion inhibition efficiency in the order APSC < APTSC < APPH at all studied concentrations. A maximum of 91.5% inhibition efficiency was achieved by APPH at 1.0 mM concentration. The remarkable corrosion preventing ability of this molecule when compared to the other two may be attributed to the presence of highly delocalized π electron cloud of the benzene ring. The molecular geometries obtained for the Schiff bases after the 'minimum energy' calculations show that perfect planar geometry was acquired for the APPH molecule, which might have caused the strong interaction of the molecule on the metal surface by means of two aromatic ring systems more efficiently, in addition to the azomethine linkage. The geometries of the three Schiff bases obtained after the minimum energy calculations are depicted in Figure 2.10. The only difference between the structures of APSC and APTSC is that the former one contains oxygen atom instead of the sulphur atom present in the later one. Since the electron cloud present on the sulphur atom is more polarizable than the oxygen atom, increased interaction is possible with the unsatisfied valencies on the metal surface, which will lead to an elevated corrosion inhibition capacity of APTSC than APSC.

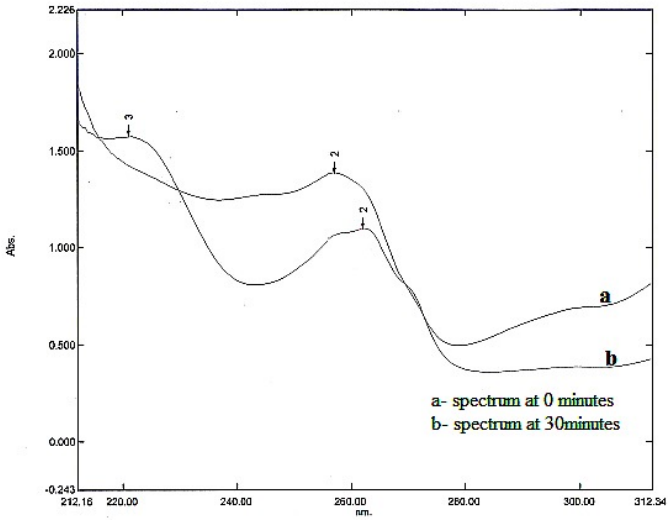

Fig. 2.9 UV-Vis spectrum of APPH in HCl at
a) 0 minute b) 30 minutes

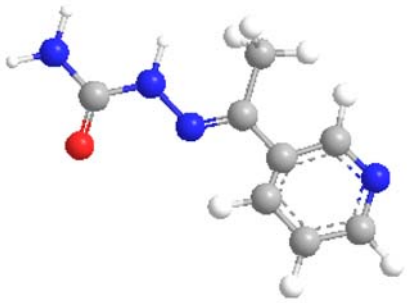

3-acetylpyridine semicarbazide (APSC)

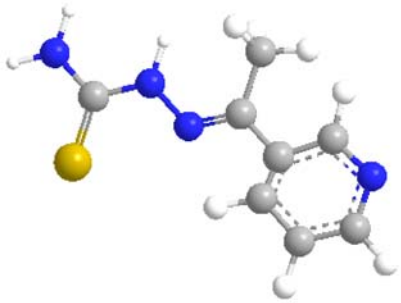

3-acetylpyridine thiosemicarbazide (APTSC)

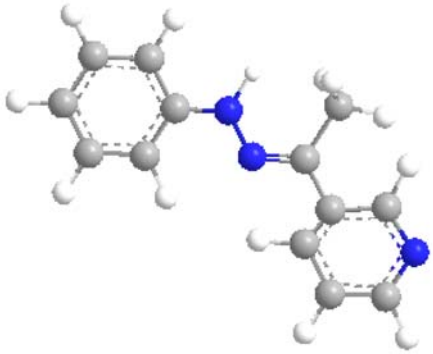

3-acetylpyridine phenyl hydrazine (APPH)

Fig. 2.10 Geometries of Schiff base molecules derived from 3-acetylpyridine

Corrosion inhibition studies of parent compounds

The parent ketone 3-acetylpyridine (3AP) and the amines such as semicarbazide (SC), thiosemicarbazide (TSC) and phenyl hydrazine (PH) were screened for the corrosion inhibition studies on CS in order to establish the significant role of azomethine linkage. The results are summarized in Figure 2.11. It was confirmed that all the Schiff bases exhibited much higher corrosion inhibition efficiencies than their parent compounds at all the studied concentrations. These studies ascertain that the azomethine moiety present in the Schiff base molecules has a marked role in preventing the dissolution of iron in acid medium.

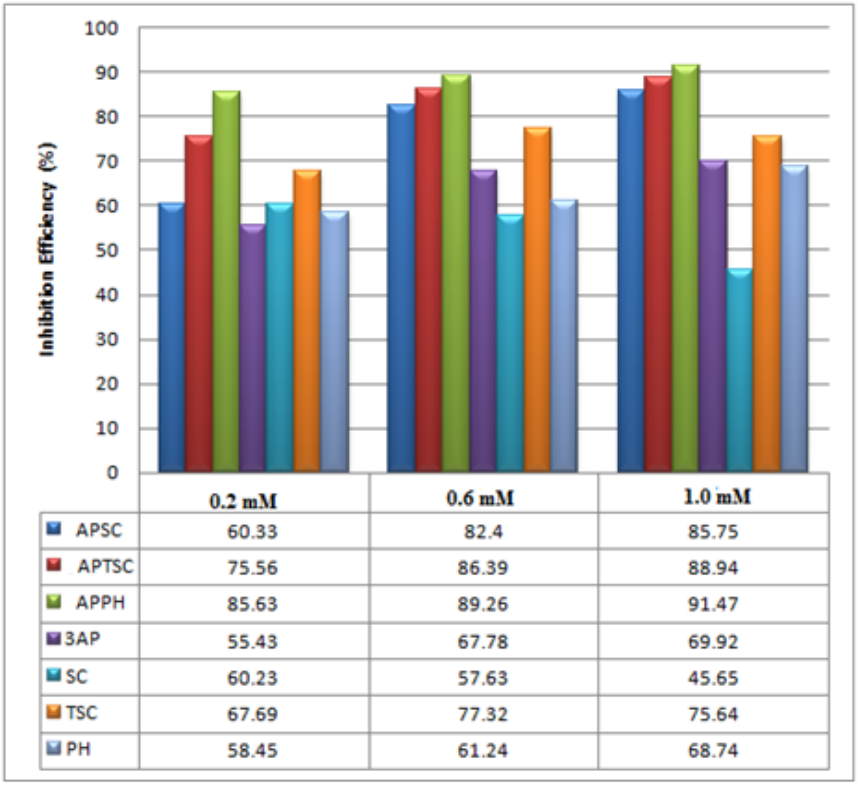

	0.2 mM	0.6 mM	1.0 mM
APSC	60.33	82.4	85.75
APTSC	75.56	86.39	88.94
APPH	85.63	89.26	91.47
3AP	55.43	67.78	69.92
SC	60.23	57.63	45.65
TSC	67.69	77.32	75.64
PH	58.45	61.24	68.74

Fig. 2.11 Comparison of corrosion inhibition efficiencies (η_w%) of Schiff bases, APSC, APTSC and APPH and their parent compounds 3AP, SC, TSC and PH in 1.0 M HCl

Adsorption isotherms

The inhibitory action of organic molecules on the surface of metal specimens is due to the phenomenon adsorption. To verify the mechanism of inhibition, various adsorption isotherms were plotted and the most suitable one was selected with the aid of correlation coefficient (R^2). In the present investigation, adsorption isotherms considered are Langmuir, Freundlich, Frumkin, El-awady and Temkin adsorption isotherms. Analysis of the adsorption isotherms was useful in predicting the important parameters such as adsorption equilibrium constant K_{ads} and free energy of adsorption ΔG_{ads}. From the adsorption studies it was found that all the three Schiff bases followed Langmiur adsorption isotherm during the inhibition process on the CS surface. The adsorption isotherms are represented in the Figures 2.12, 2.13 and 2.14 and the parameters obtained by the analysis of isotherms are listed in Table 2.3.

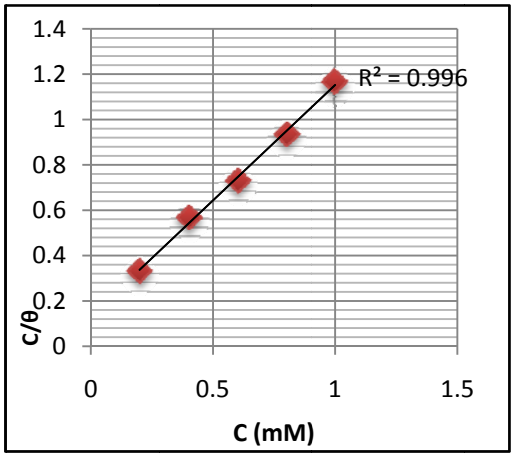

Fig. 2.12 Langmuir adsorption isotherm for APSC on CS in 1.0 M HCl

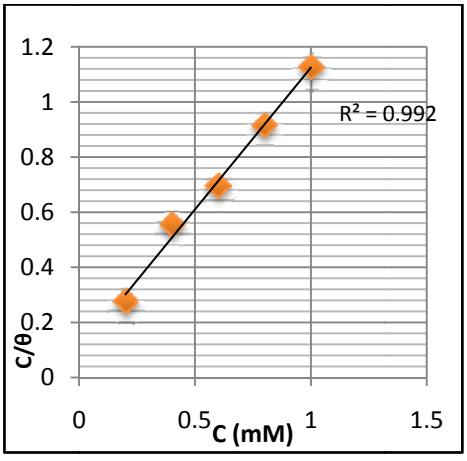

Fig. 2.13 Langmuir adsorption isotherm for APTSC on CS in 1.0 M HCl

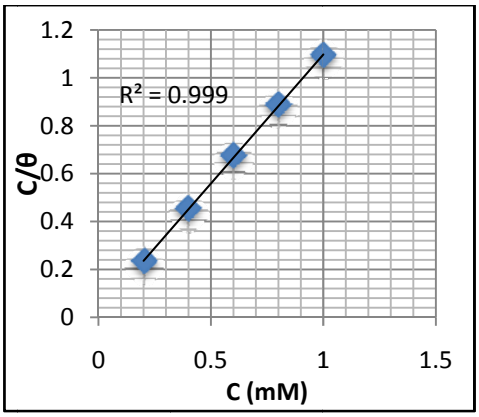

Fig. 2.14 Langmuir adsorption isotherm for APPH on CS in 1.0 M HCl

Table 2.3 Thermodynamic parameters for the adsorption of APSC, APTSC and APPH on CS in 1.0 M HCl

Schiff base	R^2	K_{ads}	ΔG_{ads} ($kJmol^{-1}$)
APSC	0.996	7519	-33.4
APTSC	0.992	1056	-27.66
APPH	0.999	48356	-37.04

All adsorption isotherms exhibited high correlation coefficient (approaches to unity). ΔG^0_{ads} for the Schiff bases on CS showed negative values indicating the spontaneity of the process. The value of ΔG^0_{ads} up to $-20 kJmol^{-1}$ is an indication of the electrostatic interaction of the charged molecule on the positively charged surface of the metal (physisorption), while ΔG^0_{ads} is more negative than $-40 kJmol^{-1}$, implies that inhibitor molecules are adsorbed strongly on the metal surface through co-ordinate type bond (chemisorption) [58-59]. In the present investigation, the three Schiff bases displayed ΔG^0_{ads} values in between -27 to $-37 kJmol^{-1}$, suggesting that the adsorption of Schiff bases involves both electrostatic-adsorption and chemisorption. On examining the free energies of adsorption, it is obvious that the Schiff base APPH has a strong chemical interaction on the metal surface than the other two Schiff bases.

Effect of temperature

The effect of temperature on corrosion was evaluated by the weight loss studies for the three Schiff bases in the temperature range 30-60^0C. The activation

energy of corrosion with and without the inhibitor could calculate by Arrhenius equation, which is given below.

$$K = A \exp\left(-\frac{E_a}{RT}\right) \quad (24)$$

where K is the rate of corrosion, E_a the activation energy, A the frequency factor, T the temperature in Kelvin scale and R is the gas constant. Arrhenius curves were obtained by plotting logK against 1000/T for the three Schiff bases and are displayed in the Figures 2.15, 2.17 and 2.19. Regression coefficients of these straight lines were close to unity indicates that the corrosion of CS in HCl can be explained by the simple kinetic model. The activation energy of corrosion and frequency factor were deduced using Arrhenius equation.

Enthalpy and entropy of activation (ΔH*, ΔS*) were calculated from the transition state theory, which can be represented by the following equation, [60]

$$K = \left(\frac{RT}{Nh}\right)\exp\left(\frac{\Delta S*}{R}\right)\exp\left(\frac{-\Delta H*}{RT}\right) \quad (25)$$

where N is the Avogadro number and h is the Planks constant. A plot of log(K/T) Vs 1/T gave straight lines for the corrosion of CS in 1.0 M HCl in the presence and absence of the Schiff bases (Figures 2.16, 2.18, 2.20).

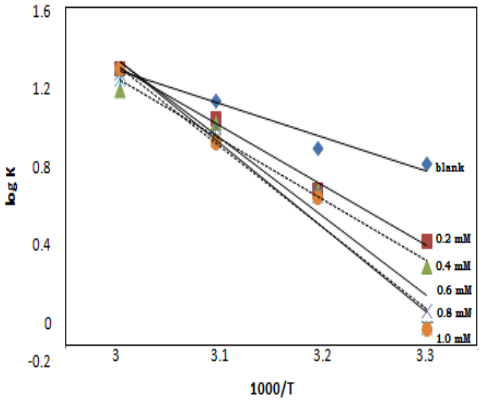

Fig. 2.15 Arrhenius plots for the corrosion of CS in the absence and presence of APSC

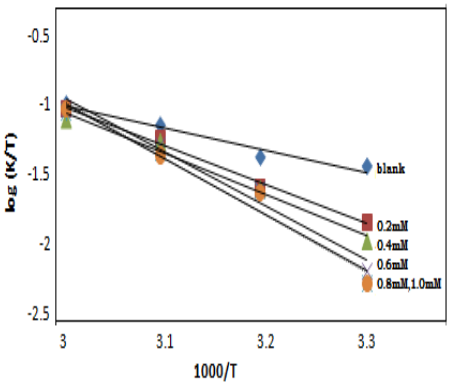

Fig. 2.16 Plots of log(K/T) vs 1000/T for the corrosion of CS in the absence and presence of APSC

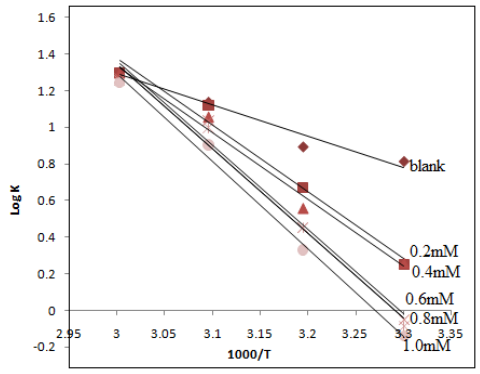

Fig. 2.17 Arrhenius plots for the corrosion of CS in the absence and presence of APTSC

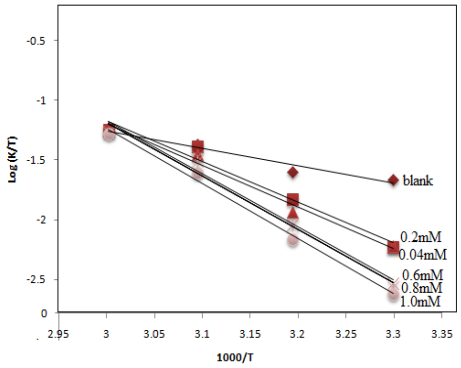

Fig. 2.18 Plots of log(K/T) vs 1000/T for the corrosion of CS in the absence and presence of APTSC

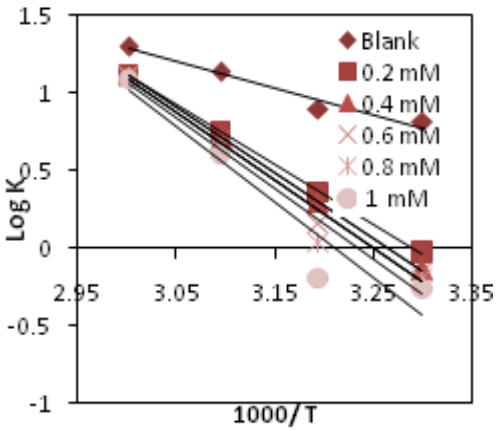

Fig. 2.19 Arrhenius plots for the corrosion of CS in the absence and presence of APPH

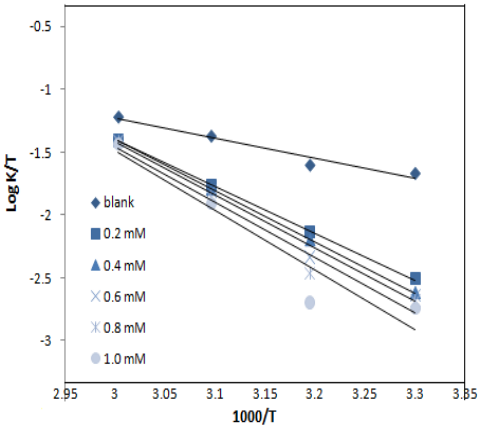

Fig. 2.20 Plots of log(K/T) vs 1000/T for the corrosion of CS in the absence and presence of APPH

Table 2.4 explores the activation energy and thermodynamic parameters of corrosion of CS in 1.0 M HCl in the presence and absence of various Schiff bases. It is apparent from the results that activation energy of dissolution of metal increased with the Schiff base concentration. This implies that the reluctance of dissolution of metal was increased with the inhibitor concentration, which can be attributed to the considerable intervention of Schiff base molecules during the metallic dissolution. Positive signs of enthalpies in three cases with a regular rise,

reflect the endothermic nature of corrosion and the increasing difficulty for dissolution with the inhibitor concentration. The energy of activation and also enthalpy of corrosion regularly increased with the concentration for APSC and APPH. But for APTSC, these parameters reached to a limit at a higher concentration of the Schiff base (0.6 mM).

Table 2.4 Thermodynamic parameters of corrosion of CS in the presence and absence of Schiff bases, APSC, APTSC and APPH in 1.0 M HCl

Schiff base	C (mM)	E_a (kJ mol^{-1})	A	ΔH* (kJ mol^{-1})	ΔS* (J mol^{-1} K^{-1})
APSC	Blank	32.86	2.76×10^{6}	30.21	-100.88
	0.2	58.59	3.09 x0[10]	54.19	-20.26
	0.4	59.62	3.89×10^{10}	56.98	-12.62
	0.6	77.12	2.69×10^{13}	74.48	41.76
	0.8	79.96	7.08×10^{13}	77.32	49.61
	1.0	82.87	2.13×10^{14}	78.68	54.02
APTSC	0.2	69.48	1.82×10^{12}	65.31	-23.87
	0.4	69.59	1.70×10^{12}	66.96	-19.53
	0.6	88.08	1.44×10^{15}	85.45	36.38
	0.8	89.99	1.55×10^{15}	85.74	36.95
	1.0	88.38	3.98×10^{15}	88.70	44.99
APPH	0.2	73.73	4.68×10^{12}	71.10	-11.14
	0.4	80.5	5.37×10^{13}	77.90	8.99
	0.6	83.61	1.58×10^{14}	81.01	17.99
	0.8	87.02	5.01×10^{14}	84.41	27.57
	1.0	93.17	4.27×10^{15}	90.50	45.38

When comparing the E_a and ΔH* at a higher concentration of 1.0 mM, it is obvious that the metal dissolution process has got higher activation energy and enthalpy of dissolution in the presence of APPH. This data strongly support the argument that APPH molecules are more strongly adsorbed on the metal surface than the other two Schiff bases. It is also evident from Table 2.4 that the entropy

of activation was increased with the inhibitor concentration. For the blank and low concentrations of the inhibitor, the entropy of activation was large and negative. This implies that in the rate determining step, a decrease in disordering takes place on going from reactants to the activated complex. But as the concentration of inhibitor increased, the disordering of activated complex elevated and the entropy of activation acquired positive values.

Surface Morphological Studies

To authenticate the mechanism of Schiff bases on the surface of carbon steel, morphological studies were performed by capturing the SEM images of steel specimens. Figures 2.21 to 2.23 respectively show the SEM images of bare CS surface, CS specimen in 1.0 M HCl and CS specimen in 1.0 M HCl containing APSC (1.0 mM, 48h treatment). On close inspection and comparison of the Figures 2.22 and 2.23, it is evident that the surface of CS was severely corroded in the acidic solution. Small pits and mild cracks on the bare metal surface were due to the irregularity of the metal surface and the effect of surface polishing. These polishing lines and cracks were totally lacking on the surface of the metal in HCl in the absence of the inhibitor due to intensive corrosion. Comparison of the textures of images 2.22 and 2.23, revealed that less damage of the surface of CS happened in the presence of APSC. This implies that the corrosion was suppressed considerably by the formation of a good protective film of APSC through adsorption.

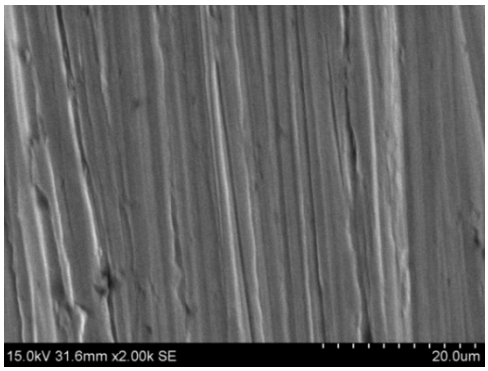

Fig. 2.21 SEM image of bare CS surface

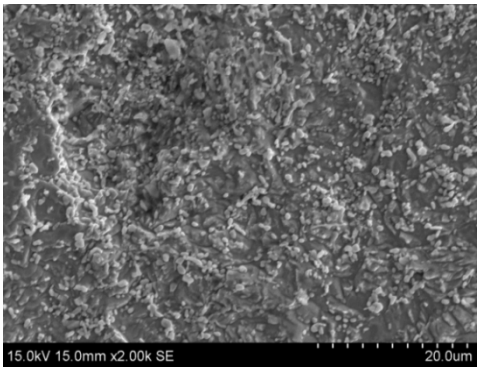

Fig. 2.22 SEM image of CS surface in 1.0 M HCl (blank)

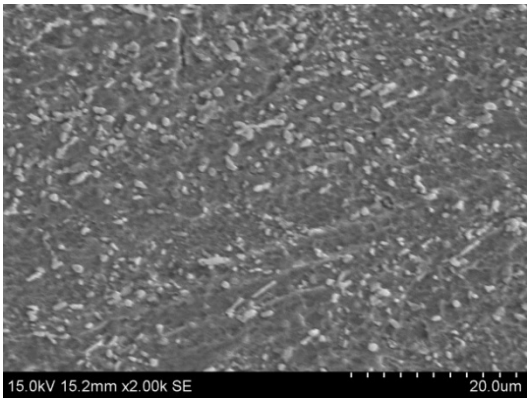

Fig. 2.23 SEM image of CS surface in 1.0 M HCl and APSC (1.0 mM, 48h)

Electrochemical Corrosion Investigations

Electrochemical investigations were performed in a three electrode cell assembly, in which saturated calomel electrode (SCE) was the reference electrode and platinum electrode having $1cm^2$ area was the working electrode. Carbon steel specimen with an exposed area of $1cm^2$ acted as the working electrode. Ac impedance measurements and potentiodynamic studies were conducted with the help of Ivium compactstat-e electrochemical system.

Electrochemical impedance spectroscopic studies

The corrosion response of CS in 1.0 M HCl in the presence and absence of Schiff bases has been investigated using ac impedance measurements at 30^0C. Figures 2.24a, 2.25a and 2.26a represent the Nyquist plots of the three Schiff bases APSC, APTSC, APPH respectively and Figures 2.24b, 2.25b and 2.26b denote the corresponding Bode plots in the absence and presence of the Schiff bases in 1.0 M HCl.

It is evident from the plots that the impedance response of metal specimens showed a marked difference in the presence and absence of Schiff bases. The semicircles showed slight irregularities which may be attributed to the roughness or non homogeneous nature of the metal surface [61-64]. Impedance behaviour can be well explained by pure electric models that could verify and enable to calculate numerical values corresponding to the physical and chemical properties of electrochemical system under examination [65]. The simple equivalent circuit that fit to many electrochemical system is composed of a double layer capacitance C_{dl}, solution resistance R_s and charge transfer resistance R_{ct} [66-67]. To reduce the effects due to surface irregularities of metal, constant phase element (CPE) was introduced into the circuit instead of a pure double layer capacitance which gave more accurate fit as shown in the Figure 2.4 [68].

The impedance of CPE can be expressed as $Z_{CPE} = \frac{1}{Y_0 \ (j\omega)^n}$ (26)

where Y_0 is the magnitude of CPE, n is the exponent (phase shift), ω is the angular frequency and j is the imaginary unit. CPE may be resistance, capacitance and inductance depending upon the values of n [69]. In all experiments, the

observed value of n ranges between 0.75 and 1.0, suggesting the capacitive response of CPE. The EIS parameters such as charge transfer resistance (R_{ct}), solution resistance (R_s) and double layer capacitance (C_{dl}) and the percentage of inhibition efficiency were depicted in Tables 2.5. The percentage of corrosion inhibition ($\eta_{EIS\%}$) on CS specimens can be calculated by the charge transfer resistance using the equation

$$\eta_{EIS}\,\% = \frac{R_{ct} - R'_{ct}}{R_{ct}} X100 \qquad (22)$$

where R_{ct} and R'_{ct} are the charge transfer resistances of the corroding electrode with and without inhibitor respectively.

From Table 2.5 and impedance plots, it is unambiguous that the charge transfer values (R_{ct}) were increased with increasing Schiff base concentration due to the increased adsorption. The value of R_{ct} is a measure of electron transfer across the exposed area of the metal surface and it is inversely proportional to rate of corrosion [70]. Decrease in capacitance values C_{dl} with inhibitor concentration can be attributed to the decrease in local dielectric constant and /or increase in the thickness of the electrical double layer. This emphasis the action of inhibitor molecules by adsorption at the metal–solution interface [71]. The percentage of inhibition ($\eta_{EIS\%}$) for all Schiff bases showed a regular increase with increasing Schiff base concentration.

Table 2.5 Electrochemical impedance parameters of CS in the absence and presence of Schiff bases, APSC, APTSC and APPH in 1.0 M HCl

Schiff base	C (mM)	R_{ct} (Ωcm^2)	C_{dl} ($\mu F\ cm^{-2}$)	$\eta_{EIS\%}$
	0	23.08	76.36	-
APSC	0.2	58.32	63.87	60.43
	0.4	72.17	81.59	68.02
	0.6	136.1	51.06	83.04
	0.8	144.7	54.18	84.05
	1.0	177.3	50.98	86.98
APTSC	0.2	95.1	53.8	75.73
	0.4	97.5	57.7	76.33
	0.6	118.9	52.2	80.59
	0.8	132.8	46.0	82.62
	1.0	339.9	44.2	93.21
APPH	0.2	85.01	54.3	72.85
	0.4	166.24	45.87	86.11
	0.6	177.18	43.45	86.92
	0.8	369.2	43.11	93.70
	1.0	599.44	40.28	96.14

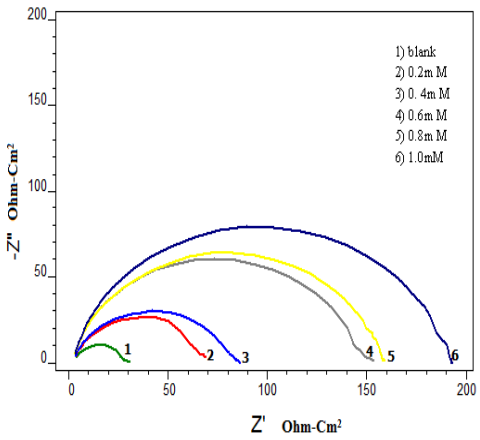

Fig. 2.24a Nyquist plots of CS in the presence and absence of APSC in 1.0 M HCl

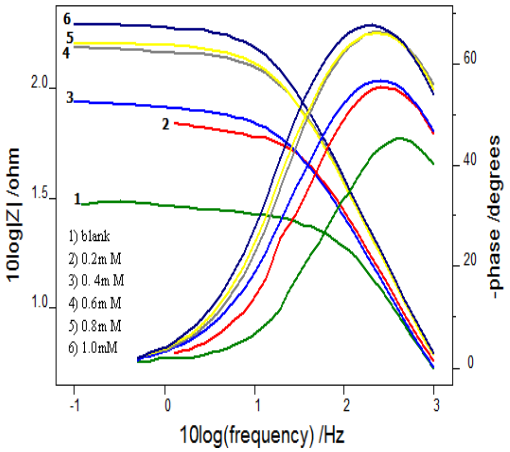

Fig. 2.24b Bode plots of CS in the presence and absence of APSC in 1.0 M HCl

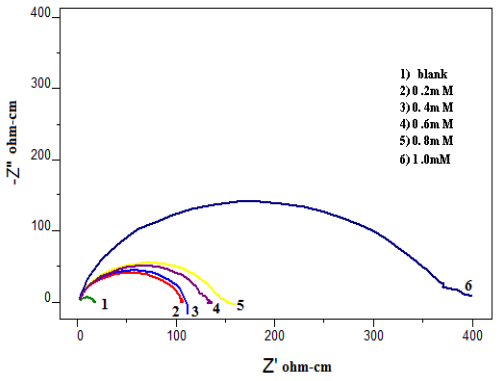

Fig. 2.25a Nyquist plots of CS in the presence and absence of APTSC in 1.0 M HCl

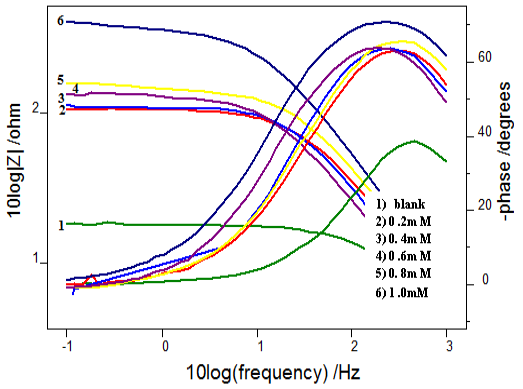

Fig. 2.25b Bode plots of CS in the presence and absence of APTSC in 1.0 M HCl

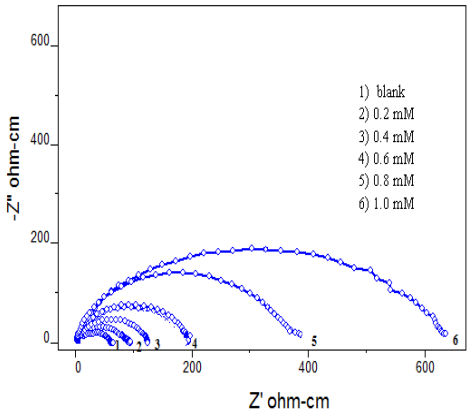

Fig. 2.26a Nyquist plots of CS in the presence and absence of APPH in 1.0 M HCl

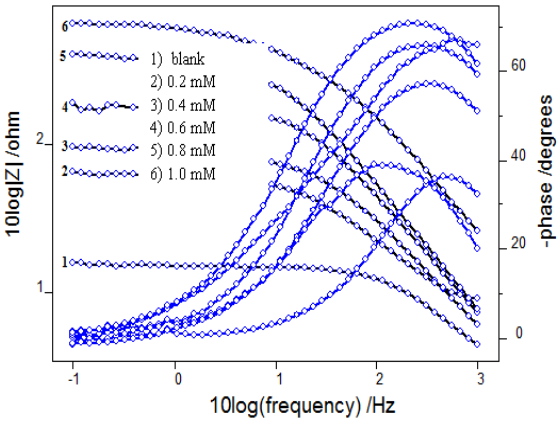

Fig. 2.26b Bode plots of CS in the presence and absence of APPH in 1.0 M HCl

Figure 2.27 depicts the comparison of the corrosion inhibition efficiencies of three Schiff bases by EIS measurements. From the figure it is obvious that the inhibition efficiency of the three Schiff bases derived from 3-acetylpyridine follows the order APSC < APTSC < APPH generally. This trend finds good agreement with the results obtained from the gravimetric weight loss studies.

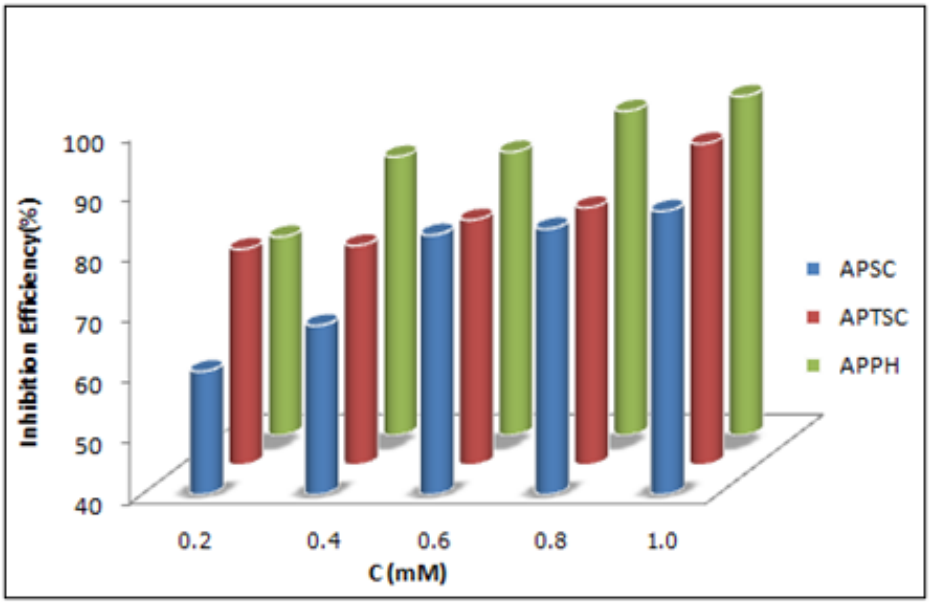

Fig. 2.27 Comparison of the corrosion inhibition efficiencies ($\eta_{EIS\%}$) of Schiff bases, APSC, APTSC and APPH on CS in 1.0 M HCl

Nearly all the $\eta_{EIS\%}$ values of APPH at various concentrations demonstrated higher values than the other two Schiff bases. The higher $\eta_{EIS\%}$ of APPH may be due to the presence of phenyl ring in the molecule. Due to the enhanced delocalization of π electrons in this molecule, the interaction between the molecules and the surface atoms of the metal specimen significantly rises. A maximum of 96% of inhibition efficiency was exhibited by APPH at 1.0 mM in HCl medium.

Potentiodynamic polarization studies

Potentiodynamic polarization studies on CS specimens at room temperature were conducted in HCl medium in the presence and absence of three different Schiff bases. Tafel polarization and linear polarization analyses were performed separately. Potential scan range for the working electrode was selected between +100 mV to -100 mV and a sweep rate of 1mV/sec was maintained

throughout the experiment with the help of Ivium compactsat-e electrochemical system. The linear polarization plots and Tafel plots for CS specimens in the presence and absence of Schiff bases in acidic medium are displayed in Figures 2.28 to 2.30. Polarization parameters like corrosion current densities (I_{corr}), corrosion potential (E_{corr}), cathodic Tafel slope (b_c), anodic Tafel slope (b_a), and polarization resistance (R_p) of CS specimens in HCl medium containing various Schiff bases are listed in Tables 2.6.

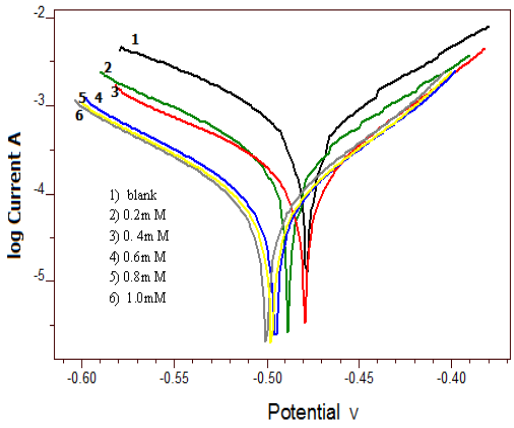

Fig. 2.28a Tafel plots of CS in in the presence and absence of APSC 1.0 M HCl

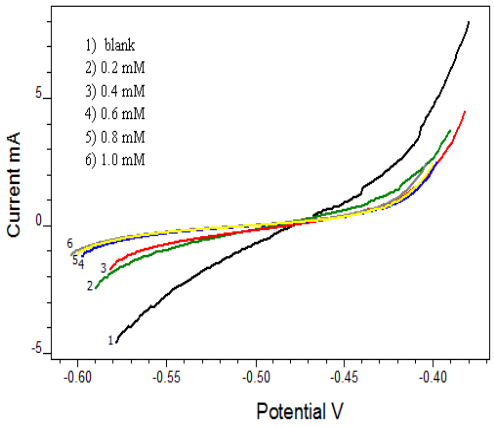

Fig. 2.28b Linear polarization curves of CS in the presence and absence of APSC in 1.0 M HCl

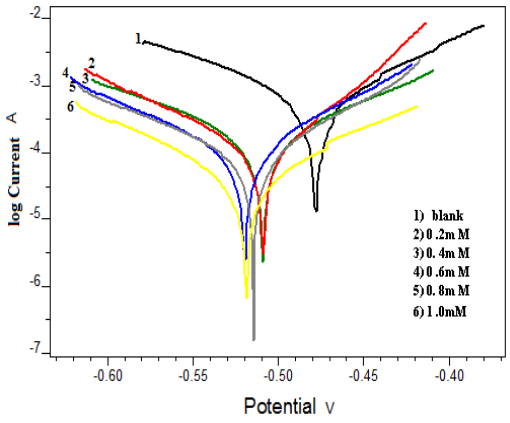

Fig. 29a Tafel plots of CS in the presence and absence of APTSC in 1.0 M HCl

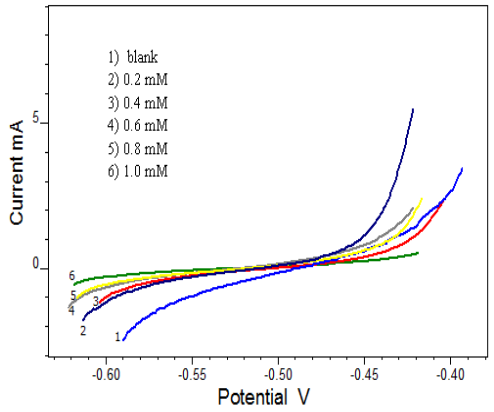

Fig. 2.29b Linear polarization curves of CS in the presence and absence of APTSC in 1.0 M HCl

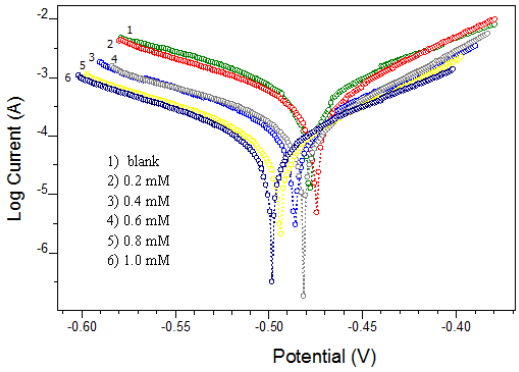

Fig. 2.30a Tafel plots of CS in the presence and absence of APPH in 1.0 M HCl

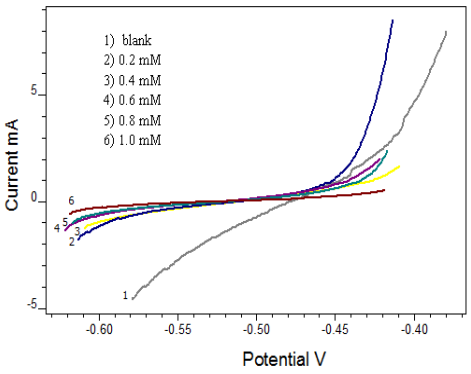

Fig. 2.30b Linear polarization curves of CS in the presence and absence of APPH in 1.0 M HCl

Table 2.6 Potentiodynamic polarization parameters of CS in the presence and absence of Schiff bases, APSC, APTSC and APPH in 1.0 M HCl

		Tafel data					Linear polarization data	
Schiff Base	C (mM)	E_{corr} (mV/SCE)	I_{corr} ($\mu A/cm^2$)	$-b_c$ (mV/dec)	b_a (mV/dec	$\eta_{pol\%}$	R_p(ohm)	$\eta_{Rp\%}$
	0	-474	499.6	102	77	-	38.14	-
	0.2	-484	207.4	101	74	58.49	89.54	57.40
	0.4	-476	150.2	106	65	69.94	117.2	67.46
APSC	0.6	-492	71.13	89	65	85.76	230.6	83.32
	0.8	-498	66.88	88	64	86.61	241.1	84.18
	1.0	-495	65.99	88	64	86.79	244.3	84.39
	0.2	-509	138.2	104	77	72.30	154.7	75.34
	0.4	-504	91.6	86	65	81.64	149.5	74.49
APTSC	0.6	-522	91.47	90	77	81.67	197	80.64
	0.8	-515	76.44	96	73	84.68	234	83.70
	1.0	-515	31.47	83	73	93.69	534	92.86
	0.2	472	130.18	101	62	73.94	137.62	72.29
	0.4	486	89.92	100	69	82.00	198.11	80.75
APPH	0.6	477	60.88	111	61	87.81	275.86	86.17
	0.8	490	49.01	97	69	90.19	359.47	89.39
	1.0	496	35.59	95	75	92.87	481.78	92.08

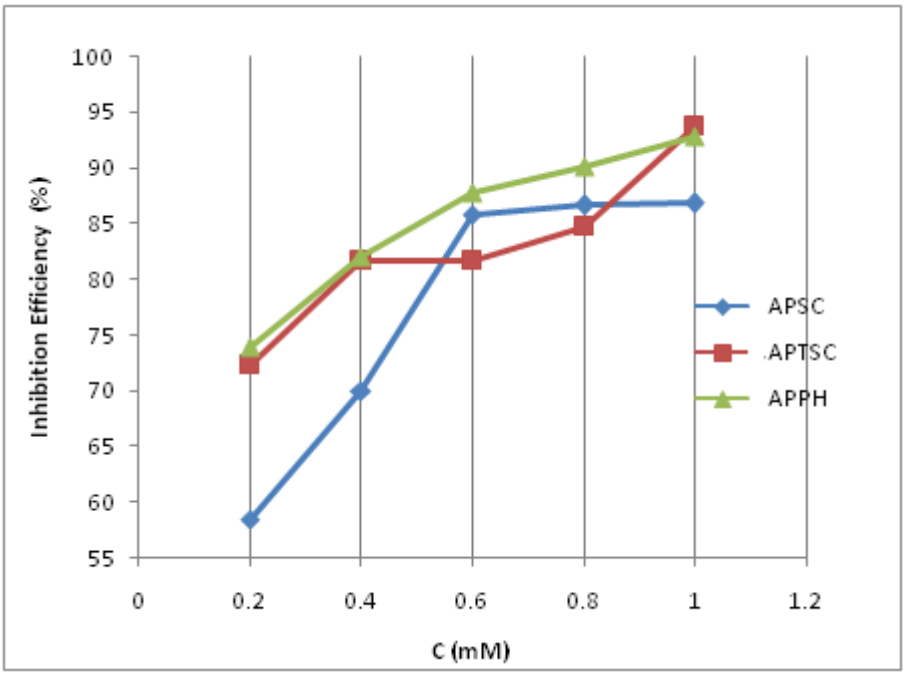

Fig. 2.31 Comparison of the corrosion inhibition efficiencies ($\eta_{pol\%}$) of Schiff bases, APSC, APTSC and APPH on CS in 1.0 M HCl

From Table 2.6 it is apparent that, a prominent decrease in the corrosion current density (I_{corr}) was observed in the presence of all Schiff bases when compared to the I_{corr} of the CS specimen in the absence of inhibitor (blank). The corrosion inhibition efficacy of the Schiff bases on CS gradually increased with concentration. On close examination of Table 2.6 and Figure 2.31, it is quite clear that in general, the Schiff base APPH displayed higher inhibitive action on CS surface when compared to the other two according to Tafel polarization studies. Linear polarization analysis also supports this observation. The inhibition efficiency of the Schiff bases follows the order APSC < APTSC < APPH. This trend is in good agreement with the observations of gravimetric corrosion studies and EIS measurements. In all cases, the cathodic slopes b_c and anodic slopes b_a of the Tafel curves were affected and therefore it may be concluded that these

heterocyclic Schiff bases act as a mixed type inhibitors in 1.0 M HCl on CS surface. Furthermore, the E_{corr} with respect to the blank experiment didn't altered considerably (>85) in all investigations and these compounds can be assumed as mixed type inhibitor [72,73]. But, since the cathodic slopes affected considerably than the anodic slopes, one can obviously make a statement that all the three Schiff bases are more adsorbed on the cathodic sites than the anodic sites during the inhibition process.

SECTION II

CORROSION BEHAVIOUR OF CARBON STEEL IN 0.5 M SULPHURIC ACID IN THE PRESENCE OF SCHIFF BASES DERIVED FROM 3-ACETYL PYRIDINE

The corrosion response of carbon steel in sulphuric acid and the inhibitive effect of the three Schiff bases derived from 3-acetylpyridine on CS surface were investigated in detail and reported in this section. The performance of the Schiff bases on CS surface was entirely different in sulphuric acid medium when compared to their response in HCl medium. To enhance the corrosion inhibition capacity of the Schiff bases in this medium, potassium iodide was added into the corrodent. The addition of iodide ions caused to exhibit synergistic effect in some cases. This augmentation of the corrosion inhibition efficiencies were also studied quantitatively and presented in this section. The three corrosion monitoring techniques such as gravimetric corrosion studies, EIS measurements and potentiodynamic polarization investigations were used to evaluate the corrosion response of CS in sulphuric acid medium.

Gravimetric Corrosion Studies

The well polished CS specimens were immersed in the sulphuric acid medium in the presence and absence of the Schiff bases. The weight loss occurred for the specimens after 24 h were determined and corrosion rates were evaluated. Table 2.7 and Figure 2.32 show and compares the corrosion rates of CS specimens in 0.5 M H_2SO_4 in the presence and absence of the three Schiff bases derived from 3-acetylpyridine. The corrosion inhibition efficiencies of the

heterocyclic Schiff bases on CS surface are listed in the Table 2.8 and depicted in Figure 2.33.

Table 2.7 Corrosion rates of CS in mmy^{-1} in the presence and absence of Schiff bases, APSC, APTSC and APPH in 0.5 M H_2SO_4

Schiff base	Concentration (mM)					
	0	0.2	0.4	0.6	0.8	1.0
APSC	23.53	23.23	22.14	21.39	19.67	18.42
APTSC	23.53	21.39	18.21	6.33	2.89	2.00
APPH	23.53	19.4	27.83	32.67	44.77	45.31

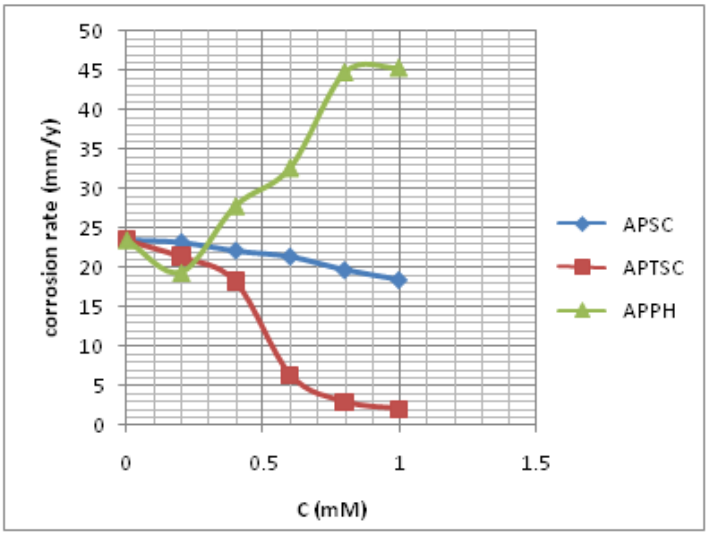

Fig. 2.32 Comparison of the corrosion rates of CS in the presence and absence of Schiff bases, APSC, APTSC and APPH in 0.5 M H_2SO_4

Table 2.8 Corrosion inhibition efficiencies (η_w%) of Schiff bases, APSC, APTSC and APPH on CS in 0.5 M H_2SO_4

Schiff base	Concentration (mM)				
	0.2	0.4	0.6	0.8	1.0
APSC	1.27	5.94	9.11	16.40	21.74
APTSC	9.09	22.59	73.07	87.69	91.49
APPH	24	-18.28	-38.83	-90.26	-92.54

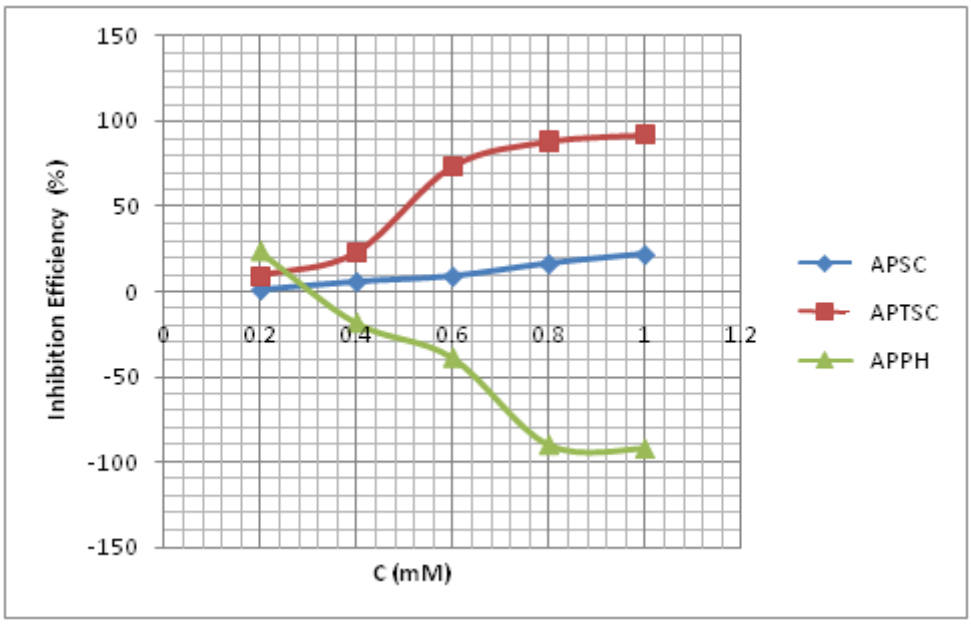

Fig. 2.33 Comparison of corrosion inhibition efficiencies (η_w%) of Schiff bases, APSC, APTSC and APPH on CS in 0.5 M H_2SO_4

From the above tables and figures, it is evident that the corrosion rates of CS specimens in sulphuric acid in the presence of the Schiff bases APSC and APTSC diminish with the concentration. Beyond 0.4 mM concentration, an abrupt decrease in the corrosion rate was noticed for the APTSC system, while a regular but a slow decrease in the corrosion rate was noticed for CS immersed in sulphuric acid with APSC. Contrary to the expectation, the CS specimens showed a rise in the corrosion rate with the concentration of Schiff base APPH in sulphuric acid medium i.e., the molecule worked as a corrosion accelerator (antagonistic nature) in sulphuric acid at 24 h. This behaviour of the Schiff base APPH was dissimilar to its behaviour in HCl medium. APPH acted as a good corrosion inhibitor in HCl medium and the rate of corrosion was decreased regularly with the inhibitor concentration. Thus by examining the results of

corrosion inhibition studies on CS by various Schiff bases in sulphuric acid medium at 24 h the following generalizations can be drawn out.

a) APSC possess poor corrosion inhibition efficiency

b) APTSC has significant corrosion inhibition efficiency and

c) APPH exhibits corrosion accelerating (antagonistic) behavior.

To investigate a detailed corrosion inhibition response of the APPH on CS, the gravimetric measurements were performed at every 2 h interval. The corrosion rate of CS was found to decrease regularly with the APPH concentration up to 8 h or η_w% showed a regular increase with the concentration. Beyond this period, APPH exhibited corrosion accelerating effect. From the UV-visible spectral studies it was confirmed that the inhibitor molecules undergo slow hydrolysis in sulphuric acid medium at room temperature. The hydrolyzed products of APSC and APTSC (3AP, SC and TSC) were less inhibited on the CS surface when compared to the parent molecule, which was confirmed by performing the gravimetric corrosion studies of CS in sulphuric acid by taking parent amine and ketone as the inhibitor (Table 2.9).

The mechanism of antagonistic behaviour of APPH i.e., increase of corrosion rate with the inhibitor concentration can be accounted as follows. Initially the inhibitor molecules are firmly adsorbed on the metal surface to inhibit the corrosion. Due to the polarity of the inhibitor molecules, large number of hydronium ions would have surrounded these molecules. The parent molecules get hydrolyzed by one of the hydronium ion around it and immediately the product molecules formed were desorbed from the surface. This state will cause to an increased interaction of the adjacent hydronium ions with the metal surface and

to enhance the corrosion rate. In actual practice, the hydronium ions have to replace the adsorbed water molecules from the surface of the metal and to react with the metal atoms [74]. But in the presence of the APPH molecules, an ample possibility is obtained for the hydronium ions to reach the metal surface.

To answer the question "why molecules other than APPH (APSC and APTSC) behave in a dissimilar way"?, one has to observe closely the corrosion response of parent ketone 3-acetylpyridine and parent amines such as semicarbazide and thiosemicarbazide in sulphuric acid on CS and has to compare with the inhibition efficiencies of the corresponding Schiff bases. It is evident from Table 2.8 that APSC exhibited very poor inhibition efficiency on CS in sulphuric acid medium. This may be attributed to the hydrolysis of the Schiff base in acidic medium. Also the hydrolyzed products i.e., 3-acetylpyridine and semicarbazide are less obstructed the corrosion of CS as obtained by the gravimetric studies (Table 2.9). In sulphuric acid, the Schiff base APTSC behaved as a good corrosion inhibitor on CS and the inhibition efficiency was enhanced with the inhibitor concentration. Similar to the other Schiff base, APTSC also undergo hydrolysis in acidic medium, but one of the hydrolyzed product i.e., thiosemicarbazide displayed good inhibition on the CS corrosion in sulphuric acid medium (Table 2.9). Similar results were reported by A.B. D. Silva et al [27]

Table 2.9 Corrosion inhibition efficiencies (η_w%) of parent ketone (3AP) and parent amines (SC, TSC and PH) on CS in 0.5 M H_2SO_4

C (mM)	3-acetylpyridine (3AP)	Semicarbazide (SC)	Thiosemicarbazide (TSC)	Phenylhydrazine (PH)
0.2	0.82	0.89	10.75	28.88
0.6	1.57	10.14	37.56	35.63
0.8	1.84	7.368	80.07	43.02

Even if hydrolysis occurred for the Schiff base molecules in hydrochloric acid medium, they showed appreciable corrosion inhibition efficiency on CS. This phenomenon can be explained by the synergistic type mechanism. At first the chloride ions adsorb on the positively charged metal surface, following this protonated Schiff base molecules interact with the metal surface through the halide ion. Of course, majority of the molecules stay in the diffusion layer undergo slow hydrolysis in acidic medium, but can assume that the firmly adsorbed Schiff base molecules on the metal surface show reluctance to hydrolysis. The role of halide ions in preventing the hydrolysis of the adsorbed Schiff bases may cause to improve the corrosion inhibition efficiency and was verified by performing a separate corrosion inhibition investigation of APPH in 0.5 M H_2SO_4 and in the presence of small amount of KI (0.2mM). The subsequent session deals with the effect of iodide ions on the corrosion behavior of APPH in sulphuric acid medium.

Synergistic effect studies

To check the synergistic effect of I^-, the gravimetric corrosion analysis of the system, APPH+KI were performed independently for a period of 24 h and compared with systems like APPH, phenylhydrazine (PH) +KI, 3-acetylpyridine (3AP) +KI and PH+3AP+KI in sulphuric acid medium. (Figure2.34). From the previous examination it was established that APPH molecule behaved as a corrosion antagonist in sulphuric acid medium at 24 h on CS. Apart from this performance, APPH molecule showed very high inhibition efficiency in the presence of KI at all concentrations (Table 2.10). This phenomenon can be

explained by the synergistic mechanism. The iodide ions which are already adsorbed on the metal surface will firmly held the inhibitor molecules by chemical interaction and thus prevent the attached inhibitor molecules from hydrolysis. The product molecules generated after hydrolysis of the inhibitor (phenylhydrazine and 3-acetylpyridine), showed low inhibition efficiency in the presence of I^- ions when compared to the APPH/KI system, which was confirmed by the gravimetric corrosion studies of individual phenylhydrazine/KI and 3-acetylpyridine/KI systems (Figure 2.34). This study also emphasizes that inhibitor molecules attaching through the I^- ions on CS surface do not undergo hydrolysis by hydronium ions.

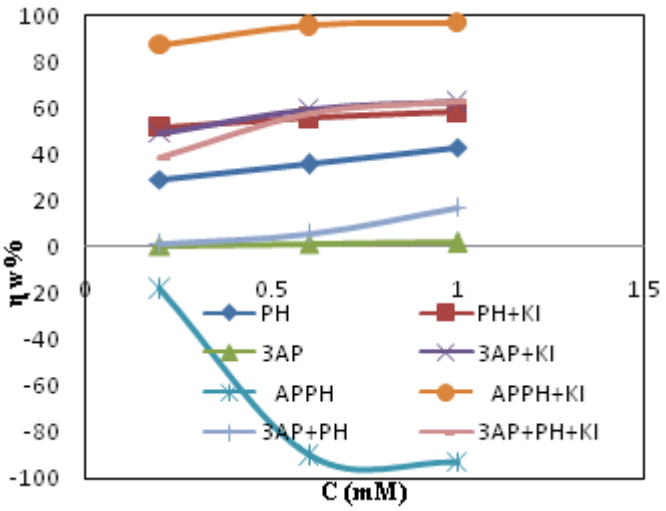

Fig 2.34 Comparison of corrosion inhibition efficiencies (η_w%) of APPH and its parent compounds in the presence and absence of KI on CS in 0.5 M H_2SO_4

It has been found that the addition of halide ions to sulphuric acid enhances the corrosion inhibition capacity of the organic molecules on carbon steel synergistically. The synergistic effect of the halides have been observed to

increase in the order $Cl^- < Br^- < I^-$ [75,76]. Due to large size and ease of polarizability, iodide (I^-) shows the highest synergistic effect [77-79].

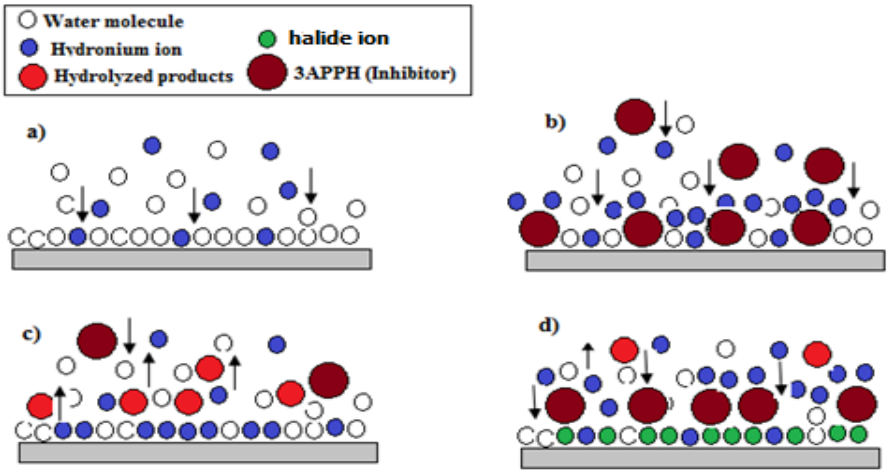

Fig. 2.35 a) Metal in acid **b)** Adsorption of APPH molecules on the surface and interaction of hydronium ions with the inhibitor **c)** Desorption of the hydrolyzed product from the surface and increased interaction of hydronium ions on the surface **d)** Synergism of I^- with the inhibitor

Table 2.10 Corrosion inhibition efficiency (η_w%) of systems APPH and APPH+KI on CS at 24 h in 0.5 M H_2SO_4

System/Conc.	Corrosion rate (ν)	Inhibition efficiency (η_w %)
Blank	23.53	-
Blank + 0.2 mM KI	19.40	24.0
0.2 mM APPH	27.83	-18.28
0.4 mM APPH	32.67	-38.83
0.6 mM APPH	44.77	-90.26
0.8 mM APPH	45.31	-92.54
1.0 mM APPH	45.48	-93.27
0.2 mM APPH + 0.2 mM KI	2.84	87.90
0.4 mM APPH + 0.2 mM KI	2.50	89.38
0.6 mM APPH + 0.2 mM KI	1.06	95.47
0.8 mM APPH + 0.2 mM KI	0.99	95.80
1.0 mM APPH + 0.2 mM KI	0.82	96.50

To examine the corrosion response of carbon steel in 0.5 M H_2SO_4 containing Schiff bases APSC and APTSC, along with iodide ions, gravimetric studies were performed. It was understood from the investigations that the two Schiff bases didn't exhibit appreciable elevation in the corrosion inhibition efficiencies on the CS surface on the addition of KI. In other words the synergistic effect was absent for the systems APSC+KI and APTSC +KI. At all concentrations the system APPH +KI exhibited higher inhibition efficiency than the sum of the inhibition efficiencies of KI and APPH alone in sulphuric acid medium on CS surface. This response is called the synergistic effect. The inhibition mechanism of APPH can be more clearly visualized from Figure 2.35.

Adsorption isotherms

To find out the nature of adsorption by the heterocyclic molecules on CS surface, adsorption isotherms were plotted and thermodynamic parameters such as adsorption equilibrium constant and free energy of adsorption were evaluated. From the various isotherms tried, the best one was selected with the aid of correlation coefficient. The most suitable adsorption isotherm for APSC was Freundlich isotherm, while APTSC followed El-Awady adsorption isotherm on CS surface at 24 h in 0.5 M H_2SO_4. Since the Schiff base APPH displayed corrosion acceleration in sulphuric acid it was not possible to assign a suitable adsorption isotherm to this molecule on CS surface. Figures 2.36 and 2.37 respectively portrait the adsorption isotherms for APSC and APTSC.

Table 2.11 Thermodynamic parameters for the adsorption of Schiff bases, APSC and APTSC on CS in 0.5 M H_2SO_4

Schiff base	Isotherm	K_{ads}	$-\Delta G_{ads}$ (kJ/mol)
APSC	Freundlich	257	23.94
APTSC	El-Awady	2153	29.25

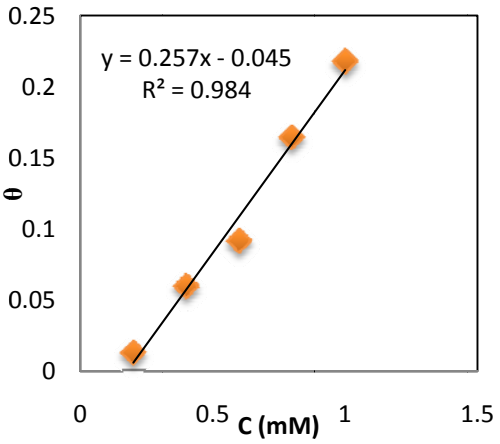

Fig.2.36 Freundlich adsorption isotherm for APSC on CS in 0.5 M H_2SO_4

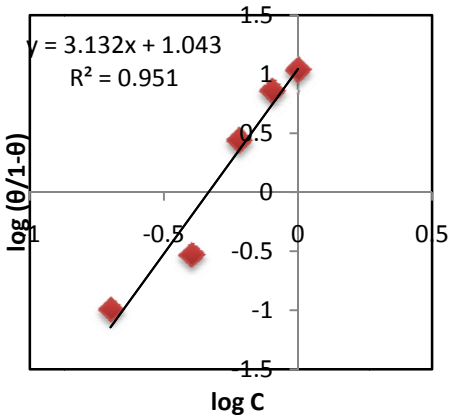

Fig. 2.37 El-Awady adsorption isotherm for APTSC on CS in 0.5 M H_2SO_4

It is obvious from the above table that the two Schiff base molecules interact on the metal surface by both physisorption and chemisorption. Since the ΔG_{ads} for APSC was near to -20kJ, the main interactive force that is responsible for the corrosion inhibition is electrostatic in nature. Moreover the K_{ads} value for this Schiff base on CS surface was very small, which is an indication of the weak interaction between the CS surface and the inhibitor molecules in sulphuric acid.

Electrochemical Corrosion Investigations

The corrosion response of carbon steel was investigated by electrochemical corrosion monitoring techniques. The working area of the metal specimens was exposed to the electrolyte for 30 minutes prior to the measurement for attaining equilibrium. The details are given in the subsequent paragraphs.

Electrochemical impedance spectroscopic studies

The EIS experiments were carried out by Ivium compactstat-e electrochemical system. Impedance measurements were performed at constant potential (OCP) in the frequency range 1 KHz to 100 mHz with an amplitude of 10 mV as excitation signal. Since it was confirmed by electronic spectral studies that the three Schiff base molecules undergo slow hydrolysis in acidic medium, the electrochemical corrosion studies only will give answer to the question " how do Schiff base molecules behave towards the carbon steel corrosion in sulphuric acid at a period of 30 minutes?"

The impedance parameters along with the inhibition efficiencies of various Schiff bases are listed Table 2.12. The Nyquist and Bode plots for the Schiff bases are displayed in Figures 2.38, 2.39 and 2.40.

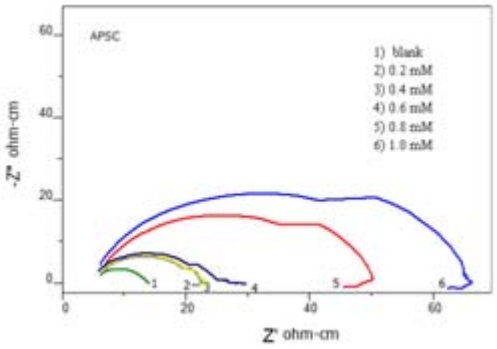

Fig. 2.38a Nyquist plots for CS in the presence and absence of APSC in 0.5 M H_2SO_4

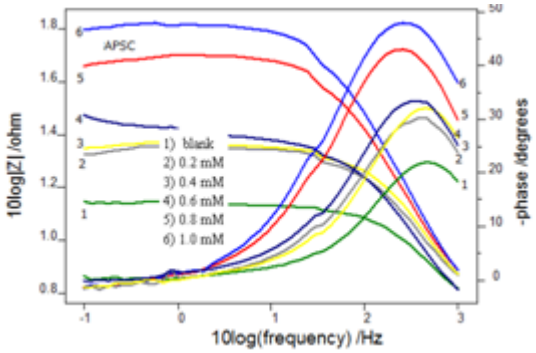

Fig. 2.38b Bode plots for CS in the presence and absence of APSC in 0.5 M H_2SO_4

From Tables and Figures, one can arrive into following conclusions

1) All Schiff bases displayed moderate (sometimes marked) corrosion inhibition efficiencies on CS surface at 30 minutes.

2) Among the studied Schiff bases, APPH showed highest inhibition efficiency nearly at all concentrations.
3) At lower concentrations the inhibition efficiency of APSC was approximately equal to that of APTSC, but the former one showed better efficiency at higher concentrations.

Table 2.12 Electrochemical impedance parameters of CS in the presence and absence of Schiff bases, APSC, APTSC and APPH in 0.5 M H_2SO_4

Schiff base	C (mM)	R_{ct} (Ωcm^2)	C_{dl} ($\mu F\ cm^{-2}$)	$\eta_{EIS\%}$
	0	9.72	133	-
	0.2	14.68	79.58	33.78
	0.4	15.46	64.93	37.13
APSC	0.6	18.08	65.68	46.24
	0.8	39.86	67.85	75.61
	1.0	54.18	60.75	82.06
	0.2	12.2	87.66	20.33
	0.4	15.01	83.82	35.24
APTSC	0.6	22.56	79.04	56.91
	0.8	27.89	90.54	65.15
	1.0	31.04	75.08	68.69
	0.2	19.54	134	50.25
	0.4	22.77	121	57.31
APPH	0.6	24.09	119	59.65
	0.8	41.39	118	76.51
	1.0	48.22	116	79.84

These results are quite not in agreement with observations obtained by gravimetric corrosion studies for 24 h. The molecule APPH showed corrosion antagonistic response as per weight loss studies, but the same Schiff base displayed good inhibition efficiency on CS surface as per EIS measurements.

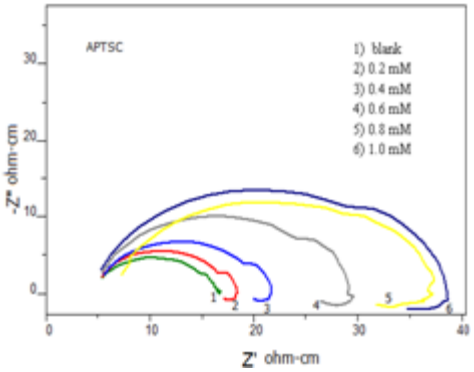

Fig. 2.39a Nyquist plots for CS in the presence and absence of APTSC in 0.5 M H_2SO_4

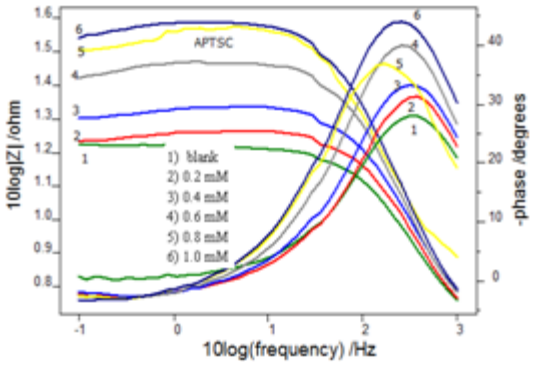

Fig. 2.39b Bode plots for CS in the presence and absence of APTSC in 0.5 M H_2SO_4

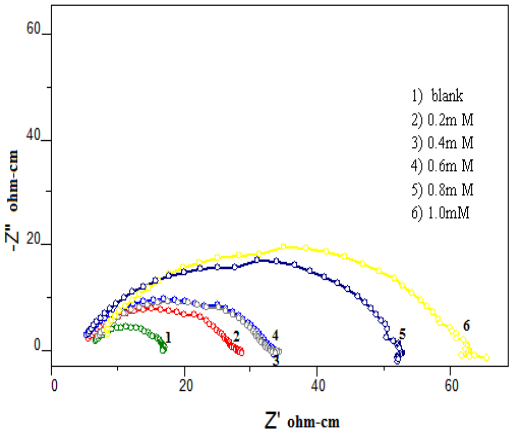

Fig. 2.40a Nyquist plots for CS in the presence and absence of APPH in 0.5 M H_2SO_4

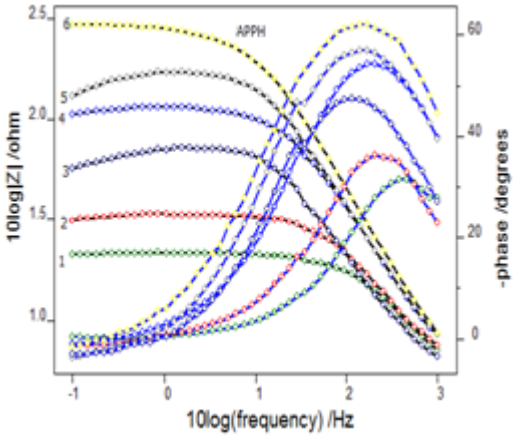

Fig. 2.40b Bode plots for CS in the presence and absence of APPH in 0.5 M H_2SO_4

Comparison of gravimetric and EIS studies, gave solid evidence for the corrosion accelerating response of the APPH, which is solely due to the hydrolysis in acidic medium, even though this molecule is equipped with active probes for corrosion inhibition (azomethine group, pyridine ring, benzenoid ring etc). A period of 30 minutes is not at all sufficient for the Schiff base molecules to convert completely into their parent compounds by hydrolysis. In a similar manner other two Schiff bases showed appreciable corrosion inhibition efficiency in sulphuric acid medium (Figure 2.41).

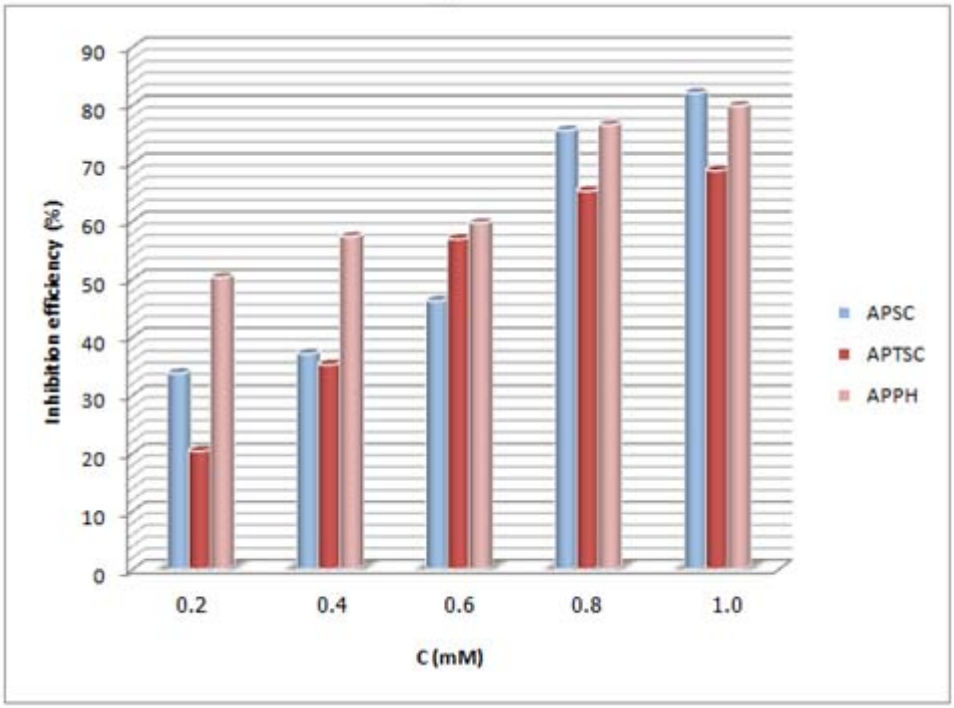

Fig. 2.41 Comparison of the inhibition efficiencies ($\eta_{EIS\%}$) of Schiff bases, APSC, APTSC and APPH on CS 0.5 M H_2SO_4

As per the gravimetric studies, the Schiff base APSC exhibited very poor inhibitive response on CS surface, but showed good inhibition by EIS measurements. The inhibitive response of the Schiff base APTSC as per EIS studies was almost comparable to the gravimetric analysis. This can be attributed to the very slow hydrolysis of the molecule in acid medium. Moreover the parent molecules obtained by the hydrolysis of this Schiff base was effective to reduce the rate of corrosion of CS in sulphuric acid medium.

Synergistic effect studies using EIS analysis

To emphasize the role of iodide ions on the corrosion inhibition of CS by APPH, impedance study was performed by exposing the corroding metal surface towards the APPH and APPH+ KI in 0.5 M H_2SO_4, for 30 minutes. Figure 2.42

represents the Nyquist plots of CS specimens in 0.5 M H_2SO_4 in the presence of various concentrations of APPH+ KI. It is evident from the plots that the impedance response of metal specimens exhibited marked difference in the presence and absence of the KI with APPH. Equivalent circuit that fit to many electrochemical systems, composed of a C_{dl}, R_s and R_{ct}, can be accepted in this study too.

The impedance parameters and the percentage of inhibition (η_{EIS}%) are listed in Table 2.13. On comparing the data presented in the table 2.12 and 2.13, it is clear that the capacitance values (C_{dl}) decreased with APPH concentration and this decrease was enhanced by the addition of I^- ions to the corrosive environment. These results suggest that the APPH molecules function by adsorption at the metal/solution interface and this adsorption is reinforced by I^- ions. A drastic increase in the η_{EIS}% values was observed by the addition of KI. From Tables 2.12 and 2.13 it is also evident that η_{EIS}% for KI in combination with APPH is higher than the sum of η_{EIS}% for single KI and single APPH, which is considered as synergistic effect. Using the results obtained by the EIS measurements, adsorption isotherms were plotted for APPH and APPH+KI systems. Both systems obeyed Langmuir adsorption isotherms on CS surface. The adsorption parameters are summarized in Table 2.14.

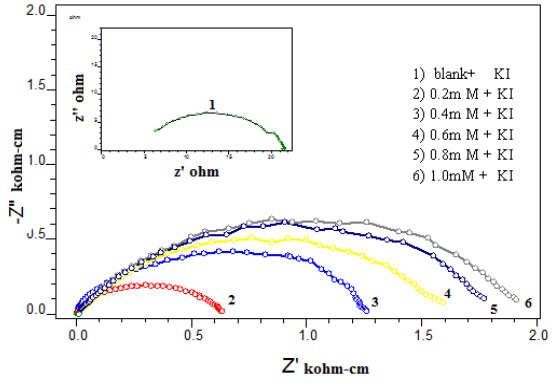

Fig. 2.42 Nyquist plots of CS in the presence of APPH+ KI in 0.5 M H_2SO_4

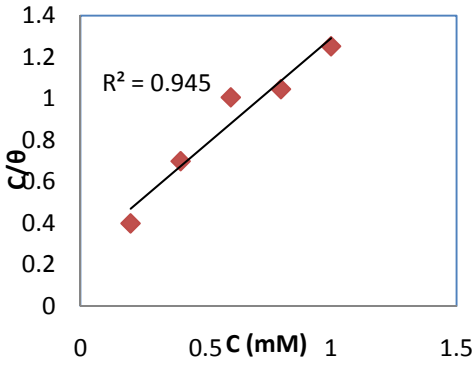

Fig. 2.43 Langmuir adsorption isotherm for APPH on CS in 0.5 M H_2SO_4

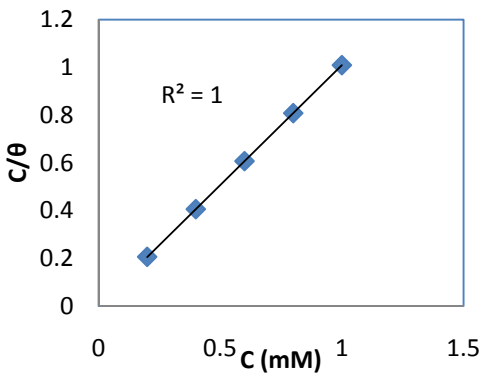

Fig. 2.44 Langmuir adsorption isotherm for APPH+ KI on CS in 0.5 M H_2SO_4

Free energy of adsorption (ΔG^0_{ads}) was negative for both investigations, which suggest the spontaneity of the processes. For the inhibition process by APPH on CS without KI, ΔG^0_{ads} value implies that the mechanism of adsorption involve both physisorption and chemisorption. Since ΔG^0_{ads} exhibited for the APPH solution containing KI was more than -40 kJ, the chemisorption is the sole factor responsible for the inhibition process. This investigation clearly establishes the synergistic effect of I^- ions with APPH, which may cause to adsorb firmly the

Schiff base molecules (without hydrolysis) on the metal surface by a strong chemical interaction

Table 2.13 Electrochemical impedance parameters of CS in the absence and presence of APPH + 0.2 mM KI in 0.5 M H_2SO_4

C (mM)	R_{ct} (Ωcm^2)	C_{dl} ($\mu F\ cm^{-2}$)	η_{EIS}%
Blank +KI	12.21	128	20.39
0.2+KI	518.4	28.9	98.13
0.4+KI	1071	26.2	99.09
0.6+KI	1301	20.2	99.25
0.8+KI	1499	21.5	99.35
1.0+KI	1607	14.3	99.39

Table 2.14 Thermodynamic parameters for the adsorption of APPH and APPH+KI on CS in 0.5 M H_2SO_4

System	Isotherm	K_{ads}	ΔG^0_{ads} (kJ/mol)
APPH	Langmuir	$3.80x10^3$	-30.90
APPH + KI	Langmuir	$2.32x10^5$	-41.25

Potentiodynamic polarization studies

Polarization studies are the conventional electrochemical technique employed for the investigation of corrosion response of various metals in different environment. To investigate the intervention of the Schiff bases during the corrosion process, potentiodynamic polarization studies were conducted by allowing the metal specimens to come in contact with the corrodent for 30 minutes. Polarization plots were obtained in the electrode potential range from -100 to +100 mV vs corrosion potential (E_{corr}) at a sweep rate of 1mV/sec. Polarization parameters like corrosion current densities (I_{corr}), corrosion potential (E_{corr}), cathodic Tafel slope (b_c), anodic Tafel slope (b_a), and inhibition efficiency (η_{pol}%) for various Schiff bases in 0.5 M sulphuric acid are listed in Table 2.15.

Percentage of inhibition efficiencies obtained by linear polarization technique (η_{Rp}%) are also listed in this table.

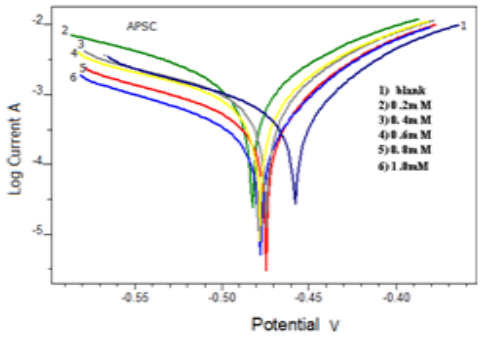

Fig. 2.45a Tafel plots of CS in the presence and absence of APSC in 0.5 M H_2SO_4

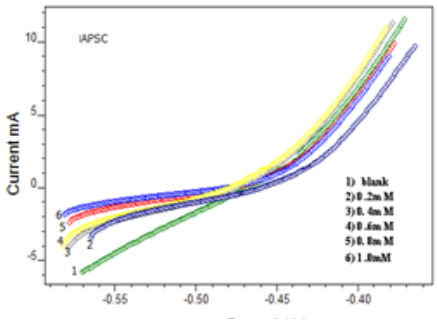

Fig. 2.45b Linear polarization curves of CS in the presence and absence of APSC in 0.5 M H_2SO_4

Table 2.15 Potentiodynamic polarization data of CS in the presence and absence of Schiff bases, APSC, APTSC and APPH in 0.5 M H_2SO_4

		Tafel data					Linear polarization data	
Schiff Base	C (mM)	E_{corr} (mV/SCE)	I_{corr} ($\mu A/cm^2$)	$-b_c$ (mV/dec)	b_a (mv/dec)	η_{pol}%	R_p(ohm)	η_{Rp}%
APSC	0	482	1041	126	85	-	14.09	-
	0.2	477	724	157	76	30.45	24.3	42.01
	0.4	482	671	157	78	35.54	26.8	47.42
	0.6	461	559	144	68	46.30	30.0	53.14
	0.8	480	314	138	66	69.83	37.4	62.30
	1.0	458	243	129	61	76.66	49.7	71.62
APTSC	0.2	542	428	115	72	58.88	34.18	58.95
	0.4	542	338	112	66	67.56	41.96	66.56
	0.6	536	319	117	65	69.39	45.66	69.27
	0.8	530	205	110	52	80.35	65.24	78.49
	1.0	521	139	104	55	86.62	92.86	84.89
APPH	0.2	461	591	131	67	43.1	26.67	47.39
	0.4	464	432	123	63	58.5	34.67	59.53
	0.6	455	395	124	68	62.0	38.79	63.83
	0.8	465	255	114	54	75.5	56.83	75.31
	1.0	462	175	106	46	83.2	72.91	80.76

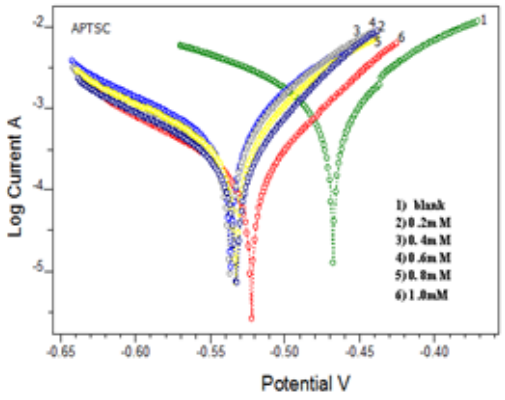

Fig. 2.46a Tafel plots of CS in the presence and absence of APTSC in 0.5 M H_2SO_4

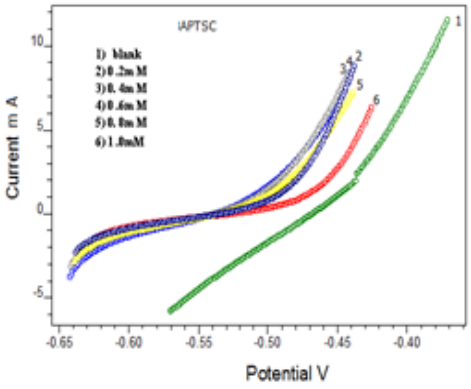

Fig. 2.46b Linear polarization curves of CS in the presence and absence of APTSC in 0.5 M H_2SO_4

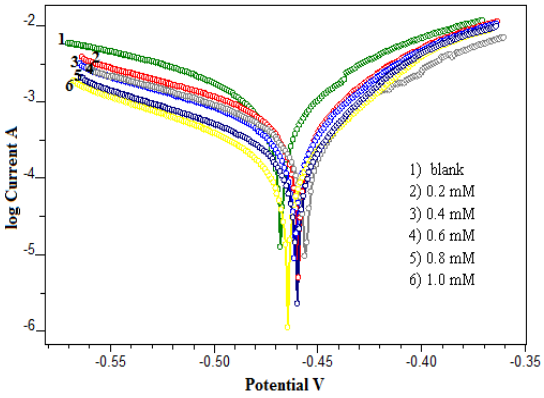

Fig. 2.47a Tafel plots of CS in the presence and absence of APPH in 0.5 M H_2SO_4

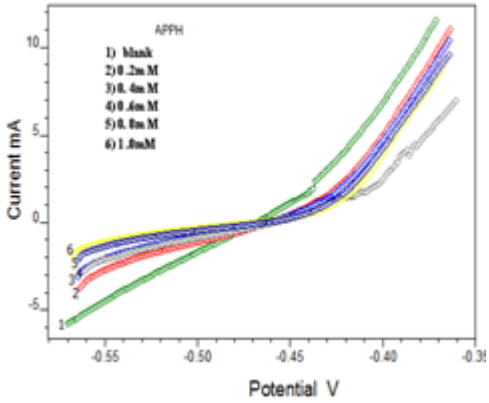

Fig. 2.47b Linear polarization curves of CS in the presence and absence of APPH in 0.5 M H_2SO_4

On examining the data of potantiodynamic polarization curves of Schiff bases (Figures 2.45 to 2.47), it is obvious that the findings are in good agreement with the results obtained by EIS measurements. On the addition of the Schiff bases to the sulphuric acid medium, the corrosion current density significantly lowered with the concentration. The Schiff base APSC displayed appreciable corrosion inhibition efficiency at 30 minutes. The inhibition efficiency of this Schiff base was poor as per gravimetric studies (at 24 h), due to the hydrolytic effect in sulphuric acid medium. The hydrolysis of the molecules was confirmed

by electronic spectral studies. The Schiff base APTSC also undergoes hydrolysis in sulphuric acid medium into its parent compounds but showed good corrosion inhibition efficiency on CS in sulphuric acid medium as per polarization analyses. η_w% and η_{pol}% of APTSC were comparable in 0.5 M H_2SO_4. The first result was solely due to the corrosion inhibition of the hydrolyzed product while the results of polarization studies demonstrated the inhibition efficiency of the Schiff base at 30 minutes. At this period, the Schiff base APPH displayed substantial corrosion inhibition efficiency on CS according to potentiodynamic polarization studies, but the same compound showed antagonistic behavior towards the end of 24 h as per gravimetric corrosion studies.

Figure 2.48 compares the corrosion inhibition efficiencies of the three Schiff bases derived from 3-acetylpyridine obtained by polarization studies. From the figure it may be concluded that η_{pol}% of these Schiff bases follows the order APTSC > APPH > APSC.

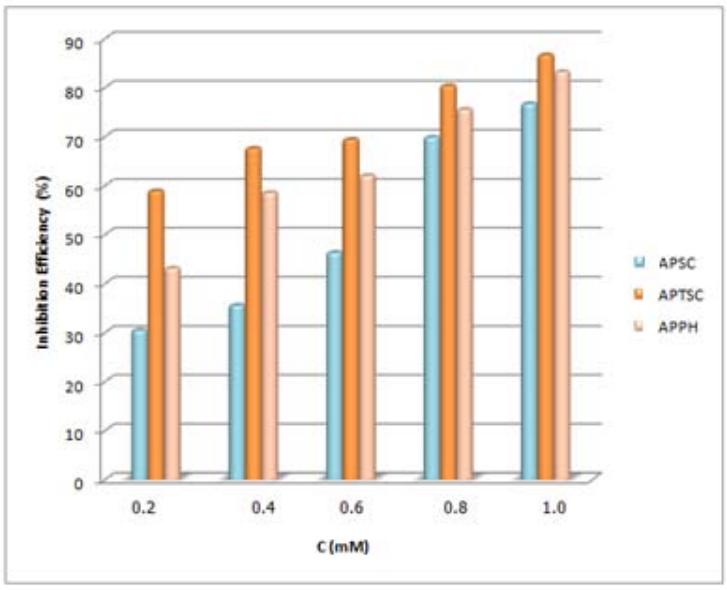

Fig. 2.48 Comparison of the corrosion inhibition efficiencies (η_{pol}%) of Schiff bases, APSC, APTSC and APPH on CS in 0.5 M H_2SO_4

On examining the anodic and cathodic slopes of Tafel curves, one can claim that the three Schiff bases act as mixed type inhibitor on the corrosion of CS in sulphuric acid medium, since the value of the anodic and cathodic slopes were altered more or less uniformly by these molecules when compared to the uninhibited solution. In other words, the Schiff bases obstructed the cathodic and anodic process of corrosion appreciably for a period of 30 minutes in sulphuric acid medium.

Synergistic effect studies using polarization analysis

Potentiodynamic polarization curves for CS in 0.5 M H_2SO_4 at 30^0C in the presence of various concentrations of APPH + KI are shown in Figure 2.49 and the corresponding polarization parameters like corrosion current densities (I_{corr}), corrosion potential (E_{corr}), cathodic Tafel slope (b_c), anodic Tafel slope (b_a), and inhibition efficiency (η_{pol}%) are listed in Table 2.16.

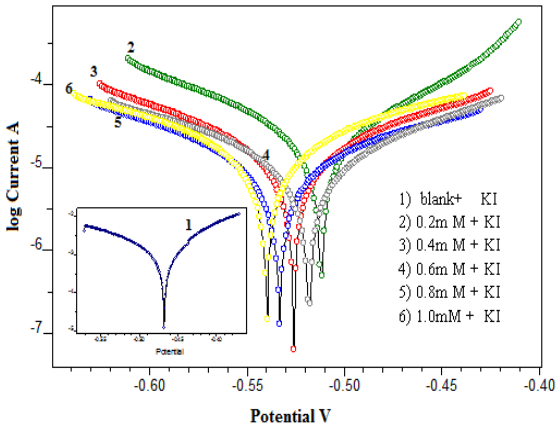

Fig. 2.49 Tafel plots of CS in the presence of KI and APPH + KI in 0.5 M H_2SO_4

Addition of I^- ions to APPH/H_2SO_4 systems resulted in marked decrease in the corrosion current density (I_{corr}), compared to the system containing only APPH. The values establish that the η_{pol}% of APPH was increased in presence of KI and these results also assure the existence of strong synergism between APPH and KI in the corrosion inhibition process of CS.

Table 2.16 Potentiodynamic polarization parameters of CS in the presence of KI and APPH+KI in 0.5 M H_2SO_4

C (mM)	E_{corr} (mV/SCE)	I_{corr} ($\mu A/cm^2$)	b_a (mV/dec)	$-b_c$ (mV/dec)	η_{pol}%
Blank +KI	-475	799	80	123	23.3
0.2 +KI	-507	18.8	85	102	98.2
0.4+KI	-540	12.6	118	121	98.8
0.6+KI	-526	11.8	117	105	98.9
0.8+KI	-515	8.9	102	119	99.1
1.0+KI	-534	8.5	127	106	99.2

Surface Morphological Studies

To examine the effect of APPH molecules on CS surface, SEM analyses were performed [80,81]. SEM images of CS surfaces are given in Figures 2.50a-d. On comparison of the Figures 2.50a and 2.50b, it is clear that the surface of CS was seriously corroded in the acidic solution. Figure 2.50c represents the surface image of the metal in the presence of the APPH (0.8 mM, 24 h). Assessment of the textures of images 2.50b and 2.50c revealed that severe damage on the surface of CS happened in the presence of the APPH due to the antagonistic behaviour. Figure 2.50d is the image of CS surface treated with APPH and KI (0.8 mM+0.2 mM KI for 24 h). Morphology of this image is entirely different from that of other

images and least damage occurred for the surface. This suggests that an increased inhibition of the APPH molecules occurred on the CS surface through I^- ions.

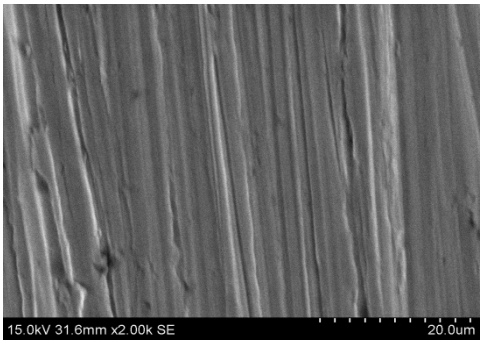

Fig. 2.50a SEM image of bare CS surface

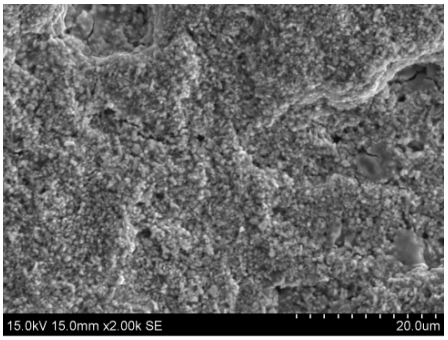

Fig. 2.50b SEM image of CS surface in 0.5 M H_2SO_4

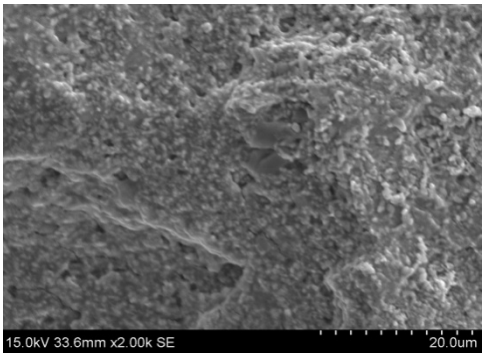

Fig. 2.50c SEM image of CS surface in 0.5 M H_2SO_4 with APPH (0.8mM)

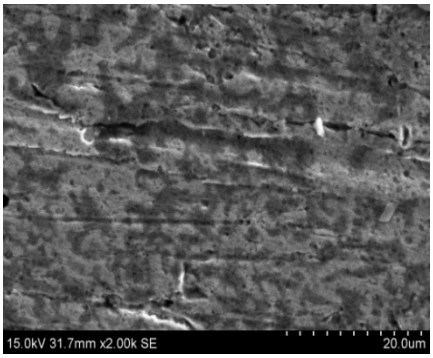

Fig. 2.50d SEM image of CS surface in 0.5 M H_2SO_4 with APPH (0.8mM) + 0.2 mM KI

CHAPTER 4

CORROSION INHIBITION INVESTIGATIONS ON SCHIFF BASES DERIVED FROM FURAN-2-ALDEHYDE AND THIOPHENE-2-ALDEHYDE ON CARBON STEEL IN ACIDIC MEDIA

Novel Schiff bases such as furan-2-aldehyde-3-aminobenzoic acid (FAABA), carboxyphenyl furan-2-aldehyde semicarbazone (CPFASC), carboxyphenyl furan-2-aldehyde phenylhydrazone (CPFAPH), nitrophenyl furan-2-aldehyde semicarbazone (NPFASC) and carboxyphenyl thiophene-2-aldehyde semicarbazone (CPTASC) were synthesized and characterized. Details of the synthesis, characterization and molecular structures of FAABA, CPFASC, CPFAPH and CPTASC were reported in part I.

The Schiff base NPFASC was prepared in two stages. First step was the arylation of furan-2-aldehyde with p-nitro aniline as explained in part I (Meerwin arylation). This arylated product was refluxed with equimolar amount of semicarbazide hydrochloride in ethanol medium for 4h in a water bath. The precipitated yellow coloured product was filtered, washed with hot water and dried. M.P = 220^0C. CHN data, found: (calc.), C:52.78(52.55)%, H:3.99(3.65)%, N:21.01(20.43)%. Mass spectrum of this compound gave a signal at m/z 274, which was due to the molecular ion peak. Base peak observed in the spectrum at m/z 231 can be assigned to the fragment $[C_{11}H_9O_3N_3]^+$, which was formed by losing CONH moiety from the molecular ion. Loss of the amino part from the molecule gave a fragment having m/z 201. The furfural moiety $[C_5H_3O]^+$ displayed a signal at m/z 79. FTIR spectrum of the Schiff base gave characteristic

stretching frequencies due to bond vibrations. The intense peaks appeared at 1693 and 1597cm^{-1} were due to $\upsilon_{C=O}$ and $\upsilon_{C=N}$ respectively. Stretching frequencies of N-O group appeared as medium bands at 1527 and 1332cm^{-1}. UV-visible spectrum of the ligand in DMSO displayed two bands at 29615 and 32011cm^{-1}, which can be assigned to the n→π* and π→π* transitions respectively. The spectral analysis of the compound NPFASC established the molecular structure as given in the Figure 2.51

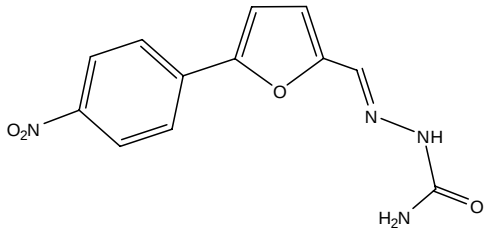

Fig. 2.51 Structure of NPFASC

The corrosion inhibition performance of these five Schiff bases on carbon steel surface in hydrochloric acid and sulphuric acid medium were studied in detail and accounted in this chapter as two sections. In the first section, details of corrosion inhibition response of Schiff bases, FAABA, CPFASC, CPFAPH NPFASC and CPTASC on CS in 1.0 M HCl solution is represented. Second section contains the corrosion inhibition studies of the five Schiff bases on CS surface in 0.5 M H_2SO_4 and synergistic effect of iodide ions in enhancing the corrosion inhibition efficiency of certain molecules. An attempt to correlate the molecular structure with the corrosion inhibition efficiency of the Schiff bases on CS has also been done in this section.

SECTION I

CORROSION BEHAVIOUR OF CARBON STEEL IN 1.0 M HCl IN THE PRESENCE OF SCHIFF BASES DERIVED FROM FURAN-2-ALDEHYDE AND THIOPHENE-2-ALDEHYDE

As explained in the previous chapters, the corrosion response of the CS specimens was investigated in HCl medium in the presence and absence of the Schiff bases, FAABA, CPFASC, CPFAPH, NPFASC and CPTASC, by conventional gravimetric studies, EIS measurements and potentiodynamic polarization studies.

Gravimetric Corrosion Studies

The five Schiff bases were screened for their corrosion inhibition efficiency on CS in HCl medium using weight loss measurements. Since the solubility of these heterocyclic furan/thiophene based Schiff bases were generally low in acidic medium, compared to the solubility of Schiff bases derived from 3-acetylpyridine, studies were done with inhibitor solutions having low concentrations. The range of concentration selected for the present corrosion study was 0.1mM-0.5 mM. The solutions having different inhibitor concentrations were treated with CS metal specimens for 24 h and the gravimetric studies were conducted. The rate of corrosion was determined from the weight loss occurred for the metal specimens after 24 h. For the blank specimen, the rate of corrosion in 1.0 M HCl, was 6.5mmy^{-1}. The variation of corrosion rate of CS specimens with Schiff base concentration is displayed in Table 2.17 and depicted in Figure 2.52.

Table 2.17 Corrosion rates of CS in mmy^{-1} in the presence and absence of Schiff bases, FAABA, CPFASC, CPFAPH, NPFASC and CPTASC in 1.0 M HCl

C (mM)	FAABA	CPFASC	CPFAPH	NPFASC	CPTASC
0.1	1.95	4.91	1.72	4.15	1.66
0.2	1.71	3.71	1.52	3.62	1.56
0.3	1.70	2.67	1.30	1.45	1.12
0.4	0.68	1.67	1.06	1.39	0.99
0.5	0.66	0.96	0.72	1.01	0.74

Table 2.18 Corrosion inhibition efficiencies (η_w%) of Schiff bases, FAABA, CPFASC, CPFAPH, NPFASC and CPTASC on CS in 1.0 M HCl

C (mM)	FAABA	CPFASC	CPFAPH	NPFASC	CPTASC
0.1	70.17	24.95	73.70	36.54	74.65
0.2	73.93	43.24	76.80	44.65	76.19
0.3	73.99	58.72	80.11	77.83	82.93
0.4	89.55	74.54	83.79	78.75	84.92
0.5	89.95	85.37	88.96	84.59	88.74

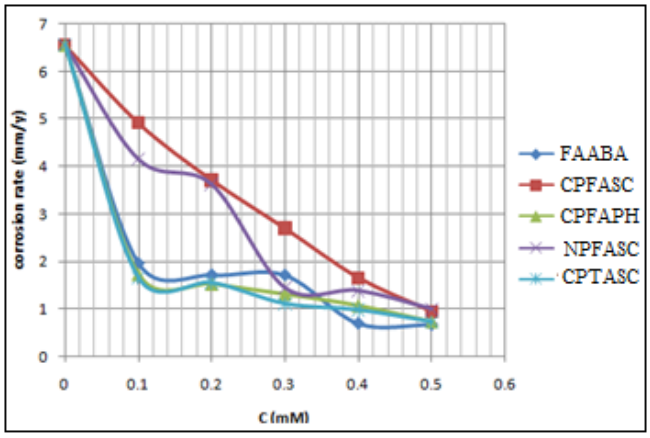

Fig. 2.52 Variation of corrosion rate of CS with concentration of Schiff bases, FAABA, CPFASC, CPFAPH, NPFASC and CPTASC in 1.0 M HCl

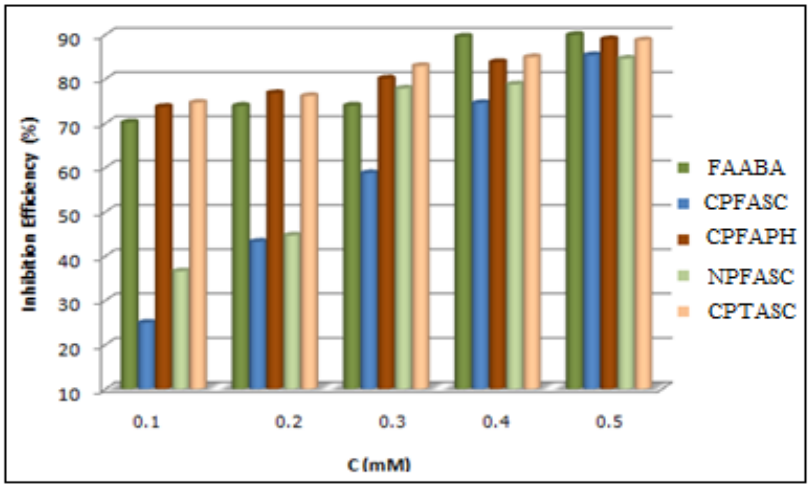

Fig. 2.53 Comparison of corrosion inhibition efficiencies (η_w%) of Schiff bases, FAABA, CPFASC, CPFAPH, NPFASC and CPTASC on CS in 1.0 M HCl

From Figure 2.52, it is understandable that the rate of corrosion of CS considerably decreased with the concentration of the Schiff bases. An abrupt decrease in the corrosion rate was noticed for CS in the presence of FAABA, CPFAPH and CPTASC, while a gradual decrease in the corrosion rate was observed in the presence of CPFASC and NPFASC in HCl medium. All the Schiff bases displayed >80% of corrosion inhibition efficacy on CS at 0.5 mM concentration. On examining the Figure 2.53 and Table 2.18, it is quite clear that the corrosion inhibition efficiency of the three Schiff bases FAABA, CPFAPH and CPTASC were significantly higher than the other two molecules CPFASC and NPFASC and were almost equal at all concentrations. The elevated inhibition efficiency of the FAABA and CPFAPH molecules can be attributed to the presence of electron rich aromatic rings in the molecules (especially in the amino part). It was already understood from the corrosion inhibition studies of Schiff bases derived from 3-acetylpyridine, that the presence of a phenyl ring is one of the key factors responsible for the enhanced corrosion inhibition efficiency. In the

second series of the compounds derived from furan-2-aldehyde, the same generalization can be applicable. The highly delocalized electron clouds of the benzene ring interact with the metal surface greatly and thus prevent the metallic dissolution appreciably. The planarity of the furan ring and the benzene ring of these molecules and overall coplanarity of these molecules (except NPFASC) helped for the firm attachment on the CS surface without excessive sterric hindrance. Molecular geometries obtained after minimum energy calculation of various Schiff bases are given in Figures 2.54-2.58.

Though phenyl ring was absent in the amino part of the molecule, CPTASC showed appreciable inhibition efficiency, which was comparable to the inhibition efficiencies of FAABA and CPFAPH. This can be illustrated by the presence of sulphur atom in the thiophene ring system, instead of oxygen atom of furan ring system of FAABA and CPFAPH. The highly poalarizable lone pair present on the sulphur atom act as a soft base, which can donate electrons to the vacant orbitals of Fe atoms (which can be considered as soft acid). According to Pearson's concept, soft bases strongly interact with soft acids. This soft-soft interaction is thus possible between CPTASC and the Fe atoms, which may be responsible for the higher inhibition efficiency.

When considering the Schiff bases CPFASC and NPFASC, it is obvious from the tables and figures that the rate of corrosion of CS in both cases have similar trend i.e., gradually decreased with the Schiff base concentration. This similar response can be attributed to the structural similarity of the molecules. The only difference between the structures of CPFASC and NPFASC is that the

former contain a –COOH group attached to the phenyl ring which is replaced by the $–NO_2$ group in later. The corrosion inhibition efficiency of these two Schiff bases was inferior to the other three on CS in HCl medium especially at lower concentrations.

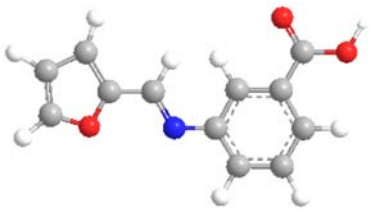

Fig. 2.54 Geometry of FAABA

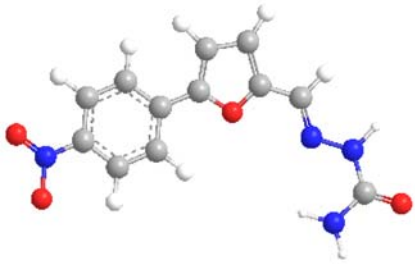

Fig. 2.55 Geometry of CPFASC

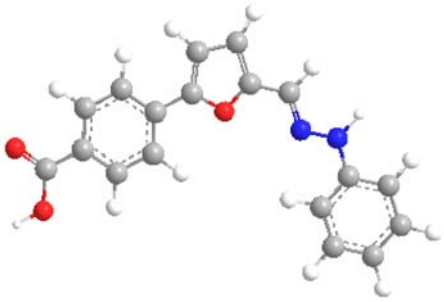

Fig.2.56 Geometry of CPFAPH

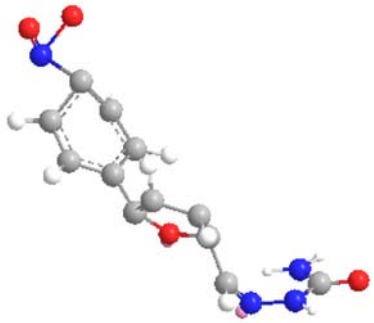

Fig. 2.57 Geometry of NPFASC

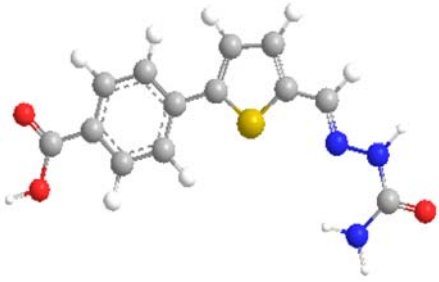

Fig. 2.58 Geometry of CPTASC

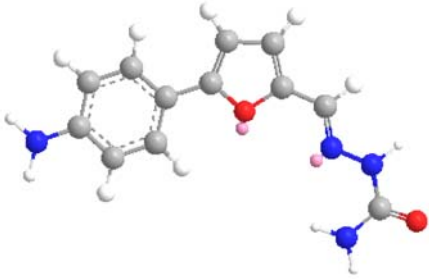

Fig. 2.59 Geometry of APFASC

But the inhibition efficiencies of these Schiff bases approached to the range 75- 80% at higher concentrations and were comparable to the inhibition efficiencies of the Schiff bases FAABA, CPFAPH and CPTASC. The lower values for the inhibition efficiency can be attributed to the absence of additional aromatic ring systems, originate from the parent amine as in the case of FAABA and CPFAPH.

Among the Schiff bases CPFASC and NPFASC, CPFASC displayed lesser efficiency than NPFASC on CS surface in acidic medium. It is quite evident that $–NO_2$ group has higher electro negativity than the carboxylic acid group. Moreover considerable deviation can be observed from the coplanar nature of NPFASC (geometry of NPFASC, Figure 2.57), which may lead to provide only poor inhibition on the metal surface. If one explain the corrosion inhibition efficiency of molecules in terms of their structures, it is worthwhile to mention the electron denser probes on the molecule which are mainly responsible for the inhibitive action on the metal surface. But on comparing the structures of two molecules CPFASC and NPFASC, evidently the electron density of the aromatic ring systems and also that of azomethine linkage will be poorer in NPFASC than in CPFASC due to the highly electron withdrawing group $–NO_2$ and the NPFASC molecule may be expected to display deprived corrosion inhibition efficiency on CS surface. Contrary to expectation NPFASC molecule showed better efficiency than CPFASC molecule at all concentrations. This can be accounted by the following probable mechanism.

It was Bechamp who succeeded first to reduce aromatic nitro compounds into the corresponding amino compounds by using iron and HCl [82]. He used this reaction mainly to convert nitronaphthalenes to naphthyl amines and nitro benzene to aniline. Here, one can think the possibility of Bechamp's reaction for the NPFASC molecule in HCl medium and in the presence of Fe metal (Figure 2.60). The simple conversion of NPFASC molecule into amino compound (APFASC) in the presence of Fe and HCl can be shown as follows.

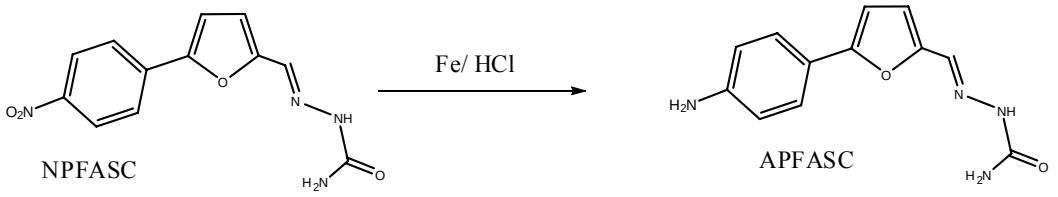

Fig. 2.60 Conversion of NPFASC into APFASC

Thus, on approaching to the metal surface, majority of NPFASC molecules may be converted into amino compound due to reduction. In the present scenario, the nature of the Schiff base molecules will be completely altered since the electron withdrawing $-NO_2$ group is replaced by the electron rich (activating) amino group. This helps to improve the corrosion inhibition efficiency of the NPFASC molecule appreciably than CPFASC molecule. Molecular minimum energy calculations showed that upon reduction, the molecule get a complete planar structure (Figure 2.59) and can interact with the metal surface more effectively. This will also facilitate the corrosion inhibition efficiency of the molecule. (A detailed investigation regarding the reduction process of NPFASC in the presence of Fe and HCl is in progress).

Adsorption isotherms

The mechanism of corrosion inhibition by organic molecules can be explained well with the help of the adsorption. Among the various adsorption isotherms considered, the most fit one for each Schiff base was selected with the aid of correlation coefficient (Figures 2.61-2.65). Out of the five Schiff bases investigated, three i.e., FAABA, CPFAPH and CPTASC displayed Langmuir adsorption isotherms on CS surface in HCl medium. CPFASC followed Freundlich adsorption isotherm while Temkin isotherm was obeyed by NPFASC Schiff base. All Schiff bases except CPFASC exhibited large and negative value (approximately -35kJ/mol, Table 2.19) for free energy of adsorption, indicating the spontaneity of the process and also strong interaction between the metal surface and Schiff bases, which is mainly chemical in nature. These four Schiff base molecules hinder the dissolution of the metal considerably by making a passive monolayer on the metal surface.

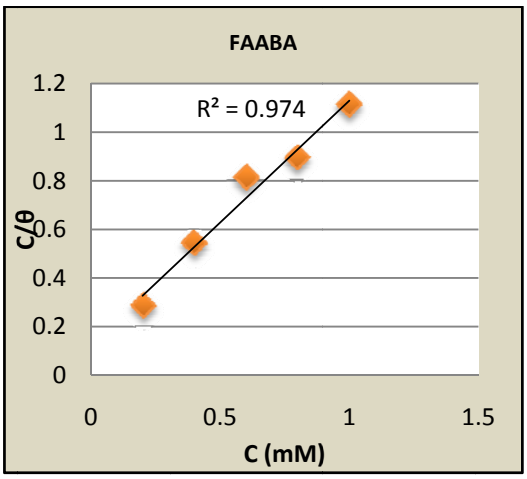

Fig. 2.61 Langmuir adsorption isotherm for FAABA on CS in 1.0 M HCl

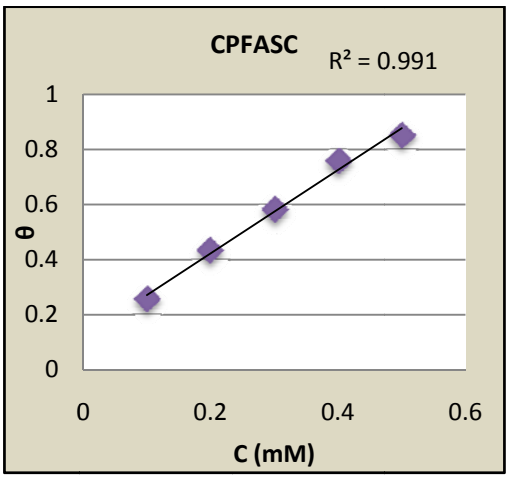

Fig. 2.62 Freundlich adsorption isotherm for CPFASC on CS in 1.0 M HCl

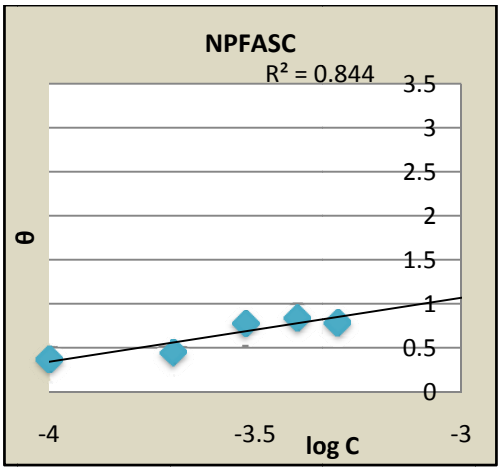

Fig. 2.63 Temkin adsorption isotherm for NPFASC on CS in 1.0 M HCl

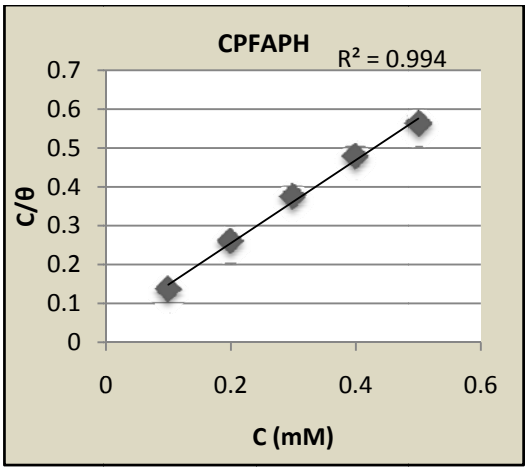

Fig. 2.64 Langmuir adsorption isotherm for CPFAPH on CS in 1.0 M HCl

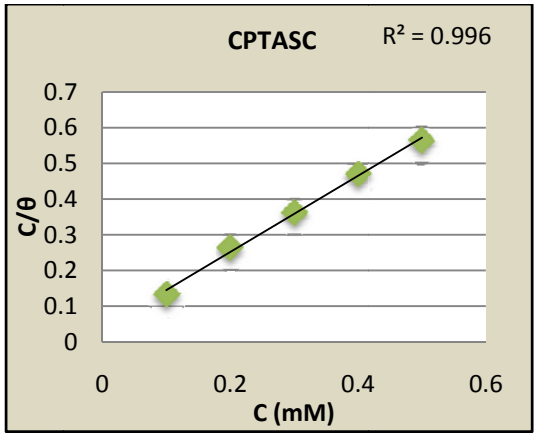

Fig. 2.65 Langmuir adsorption isotherm for CPTASC on CS in 1.0 M HCl

Table 2.19 Thermodynamic parameters for the adsorption of Schiff bases, FAABA, CPFASC, CPFAPH, NPFASC and CPTASC on CS in 1.0 M HCl

Schiff base	Adsorption isotherm	K_{ads}	ΔG_{ads} (kJ/mol)
FAABA	Langmuir	15873	-34.48
CPFASC	Freundlich	1515	-28.6
CPFAPH	Langmuir	24390	-35.56
NPFASC	Temkin	29218	-36.02
CPTASC	Langmuir	26315	-35.76

The most fit isotherm model for NPFASC molecule was Temkin isotherm. The molecular interaction parameter obtained by the Temkin model was a=-0.6868, which shows that repulsive force exists between the adsorbed NPFASC molecules.

Freundlich adsorption isotherm was shown by CPFASC molecule on CS surface in 1.0 M HCl. The low value of adsorption equilibrium constant and free energy of adsorption, compared to the other molecules, indicates that only a weak interaction occurs between CPFASC molecules and CS surface. The small value of corrosion inhibition efficiency especially at lower concentrations compared to other molecules supports this argument.

Electrochemical Corrosion Investigations

To investigate the inhibitive response of the Schiff bases on CS, electrochemical corrosion techniques such as EIS measurements and potentiodynamic polarization studies were performed. Tafel polarization studies was very useful in predicting the site of adsorption i.e., whether the molecules act on cathodic, anodic or both sites. Apart from the conventional weight loss corrosion studies, electrochemical analyses are rapid and reproducible. The carbon steel specimens were treated with the corroding solution for 30 minutes prior to the analysis with and without the inhibitor. Three electrode assembly was used for electrochemical analyses, in which platinum electrode and SCE were acted as the inert electrode and reference electrode respectively. 1 cm^2 area of the exposed metal specimen was performed as the working electrode.

Electrochemical impedance spectroscopic studies

Nyquist plots and the combined Bode-impedance plots of the five Schiff bases FAABA, CPFASC, CPFAPH, NPFASC and CPTASC are given in Figures 2.66-2.70. Nyquist plots were slightly depressed semi circles with some irregularity at low frequency regions. This irregularities observed in the depressed semi circles can be attributed to the roughness of the metal surface. The analyses of each Nyquist plots were done with the assistance of the most suitable equivalent circuit which contains two resistances and one capacitance. Among the three elements in the equivalent circuit, solution resistance (R_s) was not found to vary with the concentration of inhibitor during the analysis. Table 2.20 shows the impedance parameters such as charge transfer resistance and double layer capacitance and corrosion inhibition efficiency obtained by the EIS measurements for five Schiff bases.

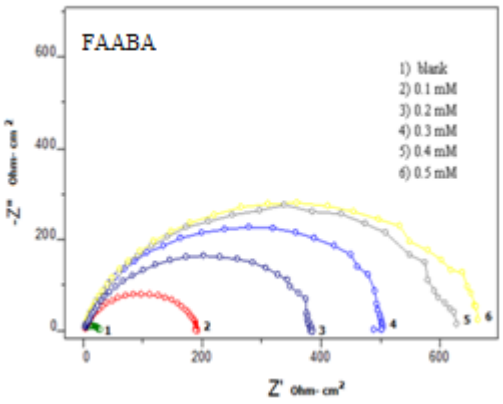

Fig. 2.66a Nyquist plots of CS in in the presence and absence of FAABA 1.0 M HCl

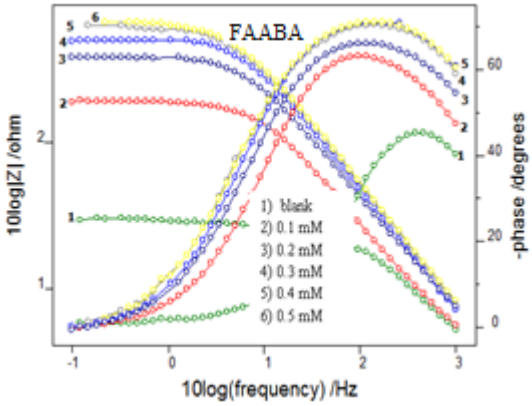

Fig. 2.66b Bode plots of CS in the presence and absence of FAABA in 1.0 M HCl

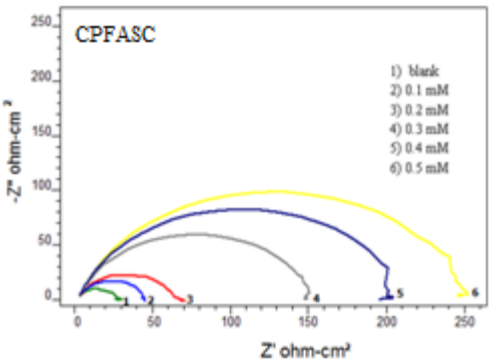

Fig. 2.67a Nyquist plots of CS in the presence and absence of CPFASC in 1.0 M HCl

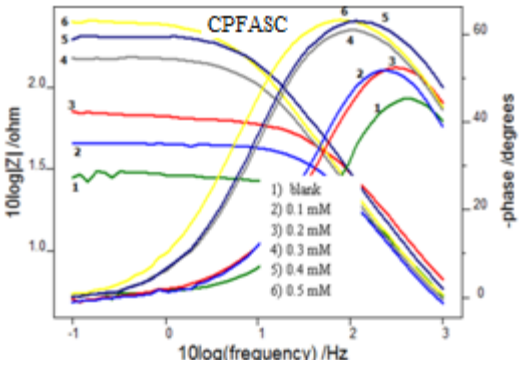

Fig. 2.67b Bode plots of CS in the presence and absence of CPFASC in 1.0 M HCl

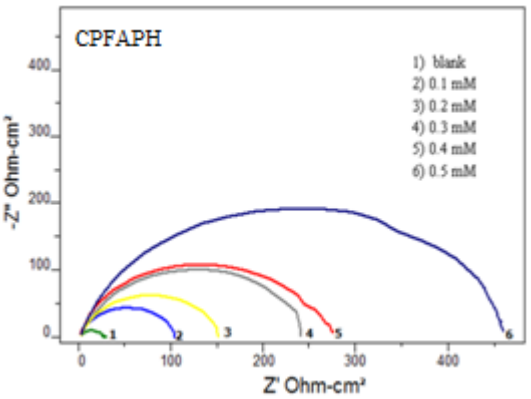

Fig. 2.68a Nyquist plots of CS in the presence and absence of CPFAPH in 1.0 M HCl

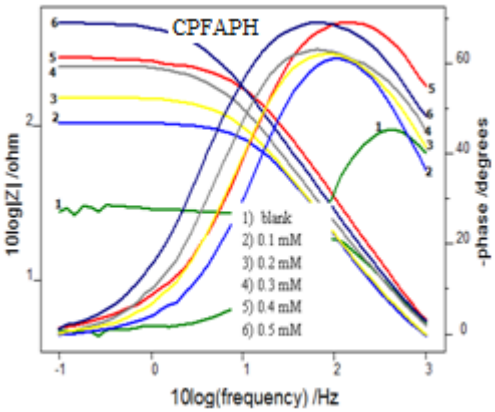

Fig. 2.68b Bode plots of CS in the presence and absence of CPFAPH HCl in 1.0 M HCl

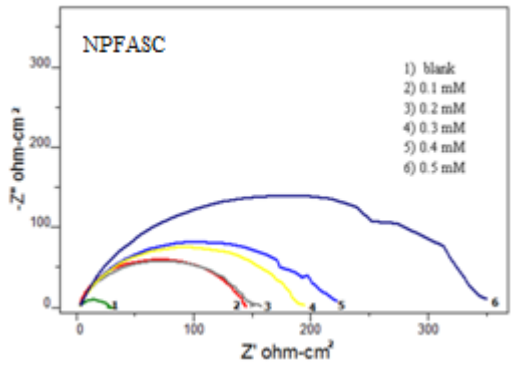

Fig. 2.69a Nyquist plots of CS in the presence and absence of NPFASC in 1.0 M HCl

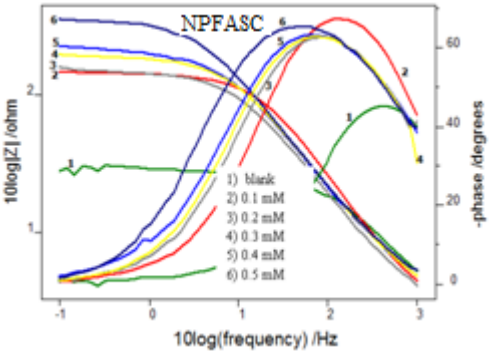

Fig. 2.69b Bode plots of CS in the presence and absence of NPFASC in 1.0 M HCl

Table 2.20 Electrochemical impedance parameters of CS in the presence and absence of Schiff bases, FAABA, CPFASC, CPFAPH, NPFASC and CPTASC in 1.0 M HCl

Schiff base	C (mM)	C_{dl} ($\mu F\ cm^{-2}$)	R_{ct} ($\Omega\ cm^{-2}$)	η_{EIS}%
	0	76.36	23.08	-
FAABA	0.1	74.44	177.50	87.00
	0.2	56.73	362.20	93.63
	0.3	48.01	484.60	95.24
	0.4	47.63	589.10	96.08
	0.5	45.38	621.80	96.29
CPFASC	0.1	72.00	38.96	40.76
	0.2	60.69	55.88	58.70
	0.3	58.80	136.50	83.09
	0.4	56.00	187.80	87.71
	0.5	56.10	227.40	89.85
CPFAPH	0.1	66.84	96.18	76.00
	0.2	64.86	139.70	83.48
	0.3	52.73	224.80	89.73
	0.4	50.65	249.10	90.73
	0.5	48.19	429.30	94.62
NPFASC	0.1	75.89	132.80	82.68
	0.2	72.87	134.10	82.85
	0.3	69.43	171.40	86.58
	0.4	43.75	192.40	88.05
	0.5	43.67	315.00	92.70
CPTASC	0.1	75.40	40.01	42.3
	0.2	68.20	70.20	68.16
	0.3	64.00	129.5	82.17
	0.4	62.30	145.28	84.11
	0.5	59.80	151.87	84.82

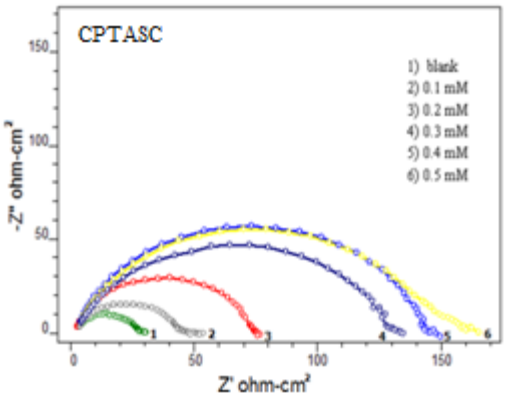

Fig. 2.70a Nyquist plots of CS in the presence and absence of CPTASC in 1.0 M HCl

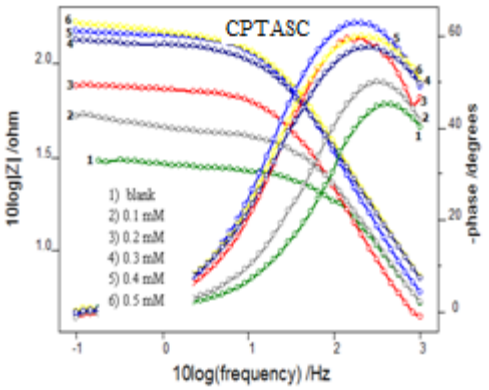

Fig. 2.70b Bode plots of CS in the presence and absence of CPTASC in 1.0 M HCl

Impedance parameters derived clearly establish that the charge transfer resistance (R_{ct}) for each Schiff base increased considerably with the concentration. This trend of R_{ct} values shows that all the Schiff base molecules effectively hinder the charge transfer process of corrosion, which is regarded as the rate controlling process taking place during the dissolution of metal in acid. In all measurements, double layer capacitance values were found to decrease with increasing concentration of Schiff bases, suggesting that increased adsorption of the inhibitor molecules on the metal specimen took place with concentration.

On examining the above table, it is obvious that maximum percentage of corrosion inhibition efficiency was shown by the Schiff base FAABA. Even at low concentrations, this molecule displayed better inhibition efficiency on CS. It showed η_{EIS}% of 87 at a low concentration of 0.1 mM. This value gradually increased with the concentration and reached a saturation value of 96% at 0.4 mM. Beyond this concentration an appreciable rise in the inhibition efficiency was not observed. Presence of azomethine linkage which is bridged through two aromatic systems (benzene ring and furan ring), of course enhances the

delocalization of π electron cloud in the molecule, which will definitely favour the interaction of the molecule on the metal surface. The results obtained from the gravimetric studies were also in good agreement with the EIS measurements.

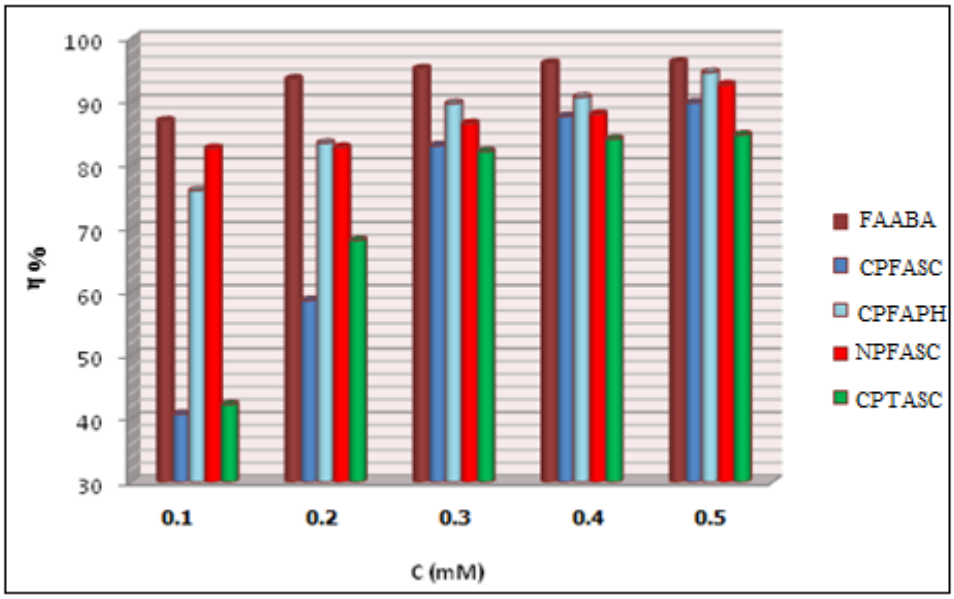

Fig. 2.71 Comparison of corrosion inhibition efficiencies (η_{EIS}%) of Schiff bases, FAABA, CPFASC, CPFAPH, NPFASC and CPTASC on CS in 1.0 M HCl

CPFAPH molecule also exhibited good corrosion inhibition efficiency, but just below that of FAABA as obtained by EIS studies. This molecule too possesses three aromatic rings (two benzene rings and one furan ring), which have significant role in reducing the rate of corrosion of CS appreciably in HCl medium. A maximum of 95% of efficiency was noted for this molecule at 0.5 mM concentration. Due to the presence of a N-N bond, extended conjugation was not possible in the molecule. This may be the reason why CPFAPH shows slightly lesser η_{EIS}% than FAABA in HCl medium.

From the Figure 2.71 it is unambiguous that the corrosion inhibition efficiency of NPFASC is principally greater than that of CPFASC at all concentrations on CS in HCl medium. This trend is unexplainable in terms of the electronegativity of nitro group and carboxylic group. As explained in gravimetric corrosion inhibition studies, this enhancement in the inhibition efficiency of NPFASC molecules on CS surface can be attributed to the formation of amino compound in the medium by the reduction of the nitro group of NPFASC molecule. The greater electron density around the amino group helped the reduced molecule to adsorb on the metal surface firmly.

The Schiff base CPTASC also displayed good corrosion inhibition efficiency especially at higher concentrations, but showed less efficiency than the similarly structured CPFASC molecules as per EIS studies. At lower concentrations its inhibition efficiency exceeds that of CPFASC but at higher concentrations it showed little bit lesser efficiency than CPFASC. This observation is dissimilar with the observation obtained from gravimetric studies i.e., CPTASC displayed higher corrosion inhibition efficiency than CPFASC at all concentrations. The higher inhibition efficiency of this molecule can be attributed to the presence of highly polarizing sulphur atom in the thiophene ring system in addition to the azomethine linkage.

Potentiodynamic polarization studies

To emphasize the corrosion inhibitory role of the Schiff bases derived from furan-2-aldehyde and thiophene-2-aldehyde on carbon steel and to propose the electrochemical site of interaction, potentiodynamic polarization studies were performed with the help of three electrode system. Carbon steel with an exposed

area of 1cm^2 was used as the working electrode. Linear polarization and Tafel polarization studies were performed using Ivium electrochemical system. Polarization resistance and corrosion current density were calculated from each analysis and inhibition efficiency was determined.

Figures 2.72 to 2.76 represent the Tafel plots and polarization curves of the five Schiff bases derived from furan-2-aldehyde and thiophene-2-aldehyde. All the Tafel plots were exhibited considerable difference from the Tafel plots of the uninhibited solution. Table 2.21 provides the Tafel data and linear polarization data obtained by the potentiodynamic polarization studies. On close observation of the data it is unequivocal that the corrosion current densities of CS specimens decreased significantly with the concentration of the Schiff bases. This is due to the fact that these molecules hinder the metal dissolution process appreciably by either intervening in the anodic or cathodic process of corrosion or both. Studies revealed that all the Schiff bases exhibited good corrosion inhibition efficiency on CS in 1.0 M HCl solution. The Schiff base FAABA showed excellent inhibition on the corroding metal. The results obtained by the potentiodynamic polarization studies were in good agreement with the ac impedance studies.

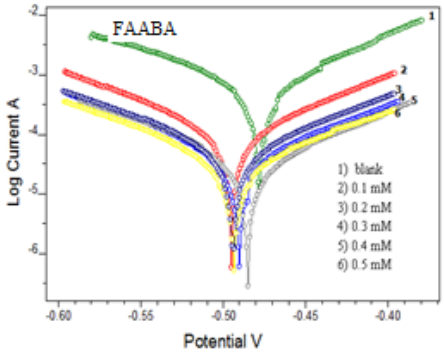

Fig. 2.72a Tafel plots of CS in the presence and absence of FAABA in 1.0 M HCl

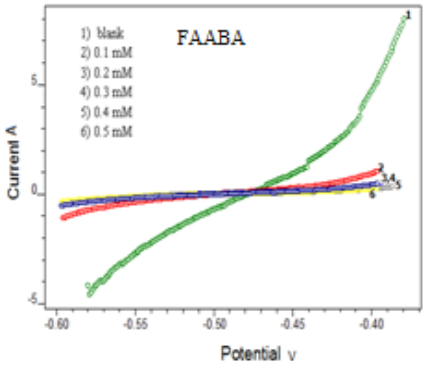

Fig. 2.72b Linear polarization curves of CS in the presence and absence of FAABA in 1.0 M HCl

Table2.21 Potentiodynamic polarization parameters of CS in the presence and absence of Schiff bases, FAABA, CPFASC, CPFAPH, NPFASC and CPTASC in 1.0 M HCl

Schiff Base	Tafel Data						Linear polarization data	
	C (mM)	$-E_{corr}$ (mV/SCE)	I_{corr} ($\mu A/cm^2$)	$-b_c$ (mV/dec)	b_a (mv/dec)	$\eta_{pol\%}$	R_p(ohm)	$\eta_{Rp\%}$
FAABA	0	474	499.6	102	77	-	38.14	-
	0.1	492	80.25	88	85	83.93	188.9	79.81
	0.2	489	43.21	97	88	91.35	377	89.88
	0.3	488	32.91	87	92	93.41	463.8	91.78
	0.4	478	28.82	94	86	94.23	567.1	93.27
	0.5	489	25.28	90	88	94.94	651.2	94.14
CPFASC	0.1	474	215.6	54	87	56.85	77.98	51.09
	0.2	498	146	64	94	70.78	106.5	64.19
	0.3	507	102	79	93	79.58	155.98	75.55
	0.4	493	76.84	77	94	84.62	197.6	80.70
	0.5	492	61.9	75	93	87.61	247.5	84.59
CPFAPH	0.1	478	116.6	83	61	76.66	113.8	66.49
	0.2	478	88.98	81	78	82.19	161.4	76.37
	0.3	488	62.62	84	78	87.47	234.9	83.76
	0.4	496	50.04	76	74	89.98	294	87.03
	0.5	481	35.08	85	91	92.98	432.2	91.18
NPFASC	0.1	489	95.29	82	94	80.93	185.1	79.39
	0.2	498	73.12	85	92	85.36	213.2	82.11
	0.3	480	66.44	82	86	86.70	226.5	83.16
	0.4	487	65.55	74	62	86.88	193.1	80.25
	0.5	475	37.36	84	79	92.52	397.4	90.40
CPTASC	0.1	479	172	90	66	65.57	96.45	60.46
	0.2	502	156.4	84	74	68.69	109	65.01
	0.3	492	99.53	106	71	80.08	186.2	79.52
	0.4	500	82.99	87	74	83.39	209	81.75
	0.5	495	77.44	94	78	84.50	238.7	84.02

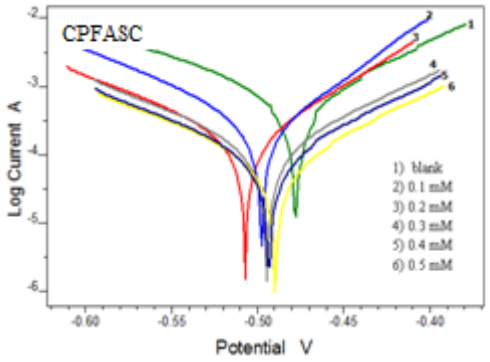

Fig. 2.73a Tafel plots of CS in the presence and absence of CPFASC in 1.0 M HCl

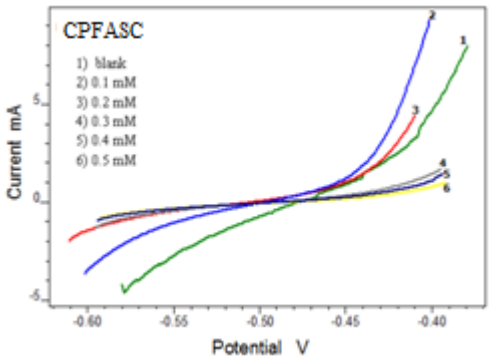

Fig. 2.73b Linear polarization curves for CS in the presence and absence of CPFASC in 1.0 M HCl

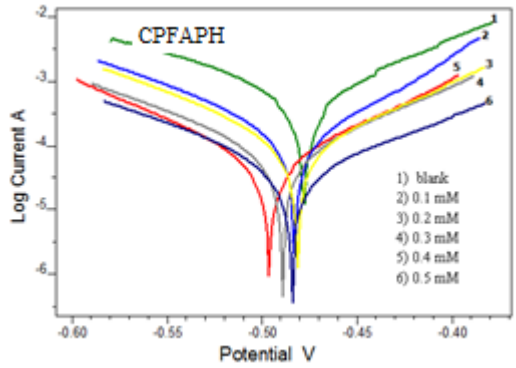

Fig. 2.74a Tafel plots of CS in the presence and absence of CPFAPH in 1.0 M HCl

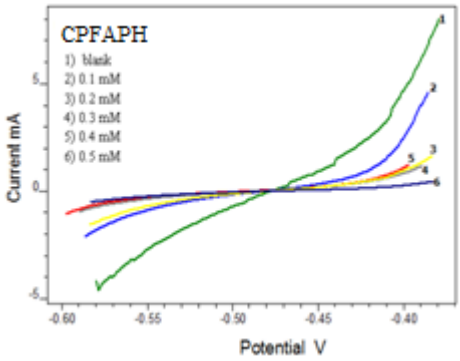

Fig. 2.74b Linear polarization curves of CS in the presence and absence of CPFAPH in 1.0 M HCl

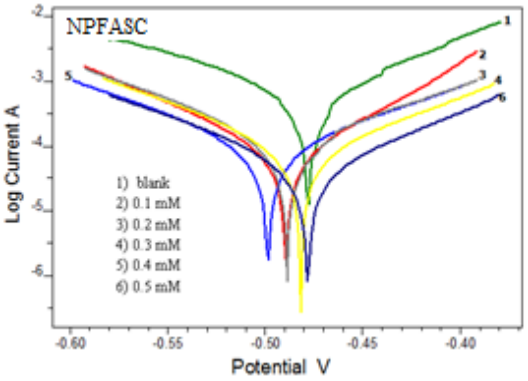

Fig. 2.75a Tafel plots of CS in the presence and absence of NPFASC in 1.0 M HCl

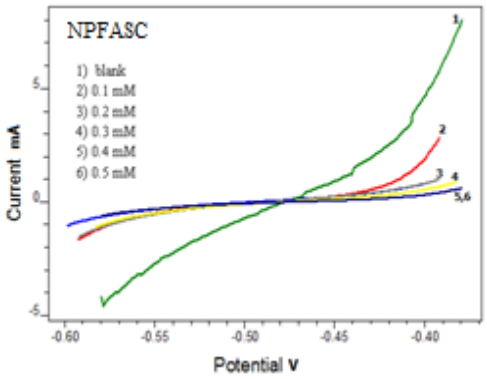

Fig. 2.75b Linear polarization curves of CS in the presence and absence of NPFASC in 1.0 M HCl

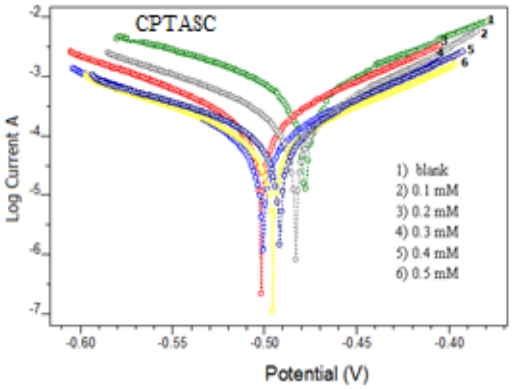

Fig. 2.76a Tafel plots of CS in the presence and absence of CPTASC in 1.0 M HCl

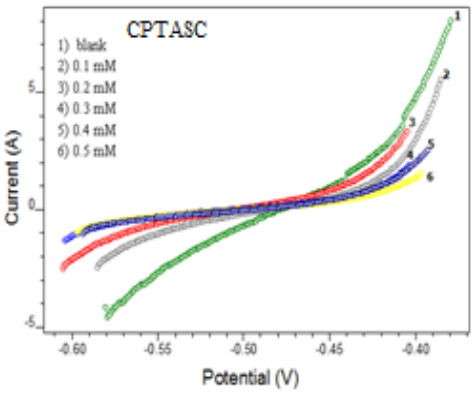

Fig. 2.76b Linear polarization curves of CS in the presence and absence of CPTASC in 1.0 M HCl

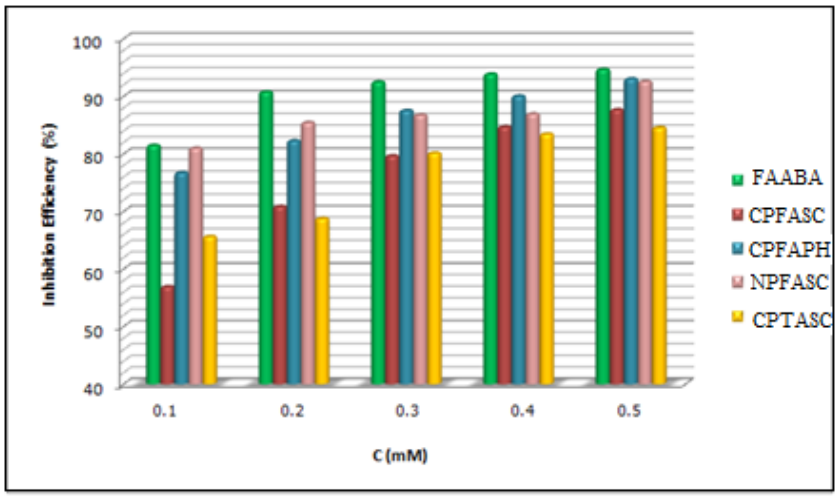

Fig. 2.77 Comparison of corrosion inhibition efficiencies (η_{pol}%) of Schiff bases, FAABA, CPFASC, CPFAPH, NPFASC and CPTASC in 1.0 M HCl

A comparison between the inhibition efficiencies were done and portrayed in Figure 2.77. It is clear from the figure that at all concentrations the Schiff base FAABA displayed good corrosion inhibition efficiency. A highest of 94% of the inhibition efficiency was observed at a low concentration of 0.5 mM. Presence of two aromatic rings in this molecule in which one of them is directly linked to the azomethine group helps the molecule to a make strong interaction with the metal surface. The involvement of the benzenoid ring in the corrosion prevention

process can further be justified by demonstrating the inhibition efficiency of CPFAPH molecule. CPFAPH molecule showed the higher corrosion inhibition efficiency very near to FAABA in acidic medium, due to the presence of two benzenoid rings. The two similarly structured Schiff bases CPFASC and NPFASC also displayed good corrosion inhibition efficiency on CS surface, but at all concentrations it is well clear that NPFASC showed higher efficiency than CPFASC even though it bear a electron withdrawing moiety i.e., nitro group. Most probably the electron withdrawing groups in an organic molecule is a curse for the corrosion inhibition response, since these groups will worsen the electron densities of the active probes of the molecule. As explained in the previous sections, this anomalous behavior of NPFASC molecule can be attributed to the reduction of the nitro group into the amino group in the presence of Fe and HCl, which became a boon to the molecule to enhance the electron density. Even though CPTASC molecule did not exhibit an expected level of corrosion inhibition, it showed comparatively good corrosion inhibition efficiency on CS surface. A maximum of 84% of inhibition efficiency was showed by this molecule at 0.5 mM. Results of the linear polarization analysis showed good agreement with Tafel analysis in all investigations.

The potentiodynamic polarization studies can be employed for predicting the nature of the corrosion inhibitor. On analyzing the data presented in Table 2.21, it can be ensure that most of the Schiff bases appreciably changed the slope of the Tafel lines, compared to the Tafel lines of uninhibited solution. If both the slopes of Tafel lines are affected considerably the inhibitor molecule can be

regarded as a mixed type one. Alternatively, if the anodic or cathodic slopes alter from the slope of the uninhibited solution, the inhibitor can be considered as anodic or cathodic type. In the present investigation the three Schiff bases namely FAABA, CPFASC and NPFASC affects the anodic and cathodic slopes in a uniform fashion and therefore these molecules can be regarded as mixed type inhibitors. On examining the Tafel slopes of the Schiff bases CPFAPH and CPTASC it is evident that the anodic slopes almost remain undisturbed during the polarization analysis, suggesting that they are mainly acting on the cathodic sites and thus reduces the rate of cathodic process of corrosion considerably. Thus these Schiff bases are believed to act as cathodic inhibitor.

SECTION II

CORROSION BEHAVIOUR OF CARBON STEEL IN 0.5 M H_2SO_4 IN THE PRESENCE OF SCHIFF BASES DERIVED FROM FURAN-2-ALDEHYDE AND THIOPHENE-2-ALDEHYDE

To investigate the corrosion inhibition response of Schiff bases derived from furan-2-aldehyde and thiophene-2-aldehyde, on carbon steel in sulphuric acid medium, analytical methods such as gravimetric corrosion inhibition studies and electrochemical studies were carried out.

Gravimetric Corrosion Studies

Weight loss studies of CS specimens in the presence and absence of the Schiff bases for 24 hours were performed as described in the previous sections. The rate of corrosion and the inhibition efficiencies obtained are displayed in Table 2.22 and 2.23. A corrosion rate of 23.5 mm/y was exhibited by the CS specimens in 0.5 M sulphuric acid (blank). Figures 2.78 and 2.79 respectively portrait the variation of corrosion rate and inhibition efficiency with the concentration of the Schiff bases.

Table 2.22 Corrosion rates (mmy^{-1}) of CS in the presence of Schiff bases, FAABA, CPFASC, CPFAPH, NPFASC and CPTASC in 0.5 M H_2SO_4

C(mM)	FAABA	CPFASC	CPFAPH	NPFASC	CPTASC
0.1	19.64	10.23	21.18	11.71	8.69
0.2	18.66	11.23	20.01	9.38	4.82
0.3	13.81	13.91	18.02	7.52	4.14
0.4	12.91	13.02	17.13	6.48	3.10
0.5	11.45	14.47	15.71	5.89	1.47

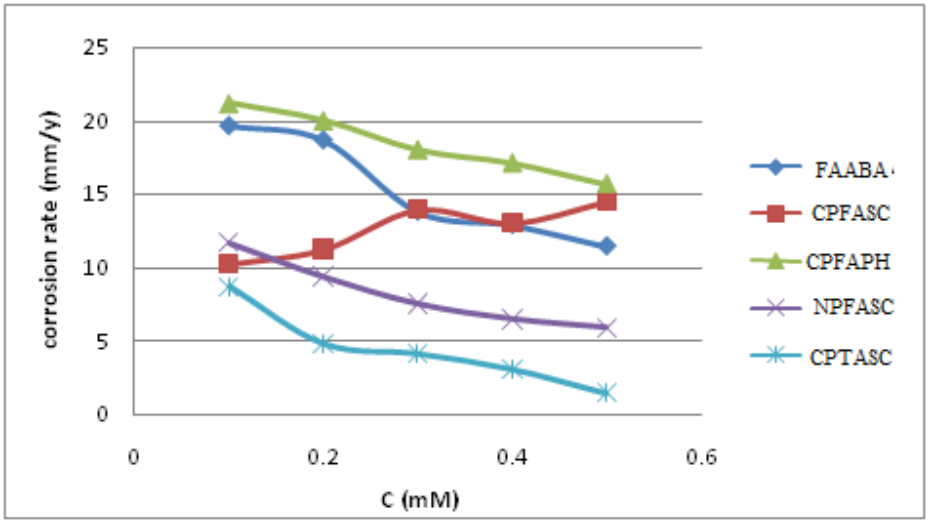

Fig. 2.78 Variation of corrosion rates of CS with the concentration of Schiff bases, FAABA, CPFASC, CPFAPH, NPFASC and CPTASC in 0.5 M H_2SO_4

Table 2.23 Corrosion inhibition efficiencies (η_w%) of Schiff bases, FAABA, CPFASC, CPFAPH, NPFASC and CPTASC on CS in 0.5 M H_2SO_4

C (mM)	FAABA	CPFASC	CPFAPH	NPFASC	CPTASC
0.1	16.44	56.51	9.99	50.23	63.04
0.2	20.59	52.27	14.96	60.15	79.50
0.3	41.25	40.88	23.40	68.04	82.39
0.4	45.07	44.66	27.20	72.46	86.83
0.5	51.30	38.50	33.28	74.97	93.74

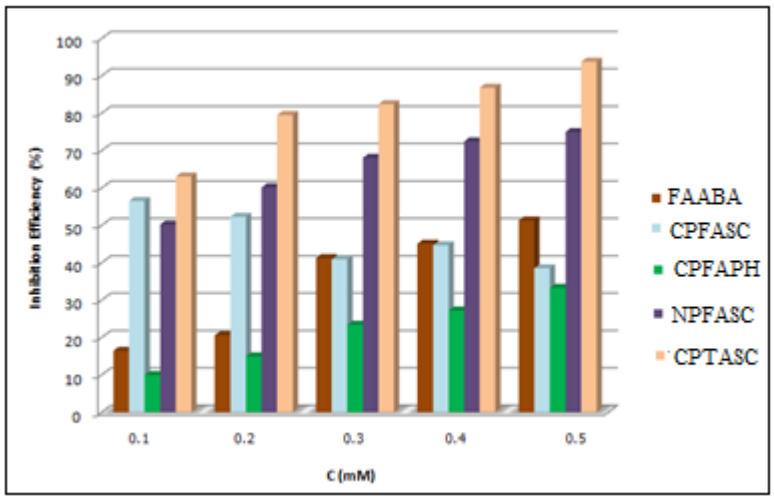

Fig. 2.79 Comparison of corrosion inhibition efficiencies (η_w%) of Schiff bases, FAABA, CPFASC, CPFAPH, NPFASC and CPTASC on CS in 0.5 M H_2SO_4

On examining the above figures and tables it is apparent that the corrosion rate of CS in the presence of the Schiff bases other than NPFASC and CPTASC were reasonably high and decreased gradually with concentration. The three Schiff bases derived from furan-2-aldehyde namely FAABA, CPFASC and CPFAPH exhibited low corrosion inhibition efficiencies on CS in sulphuric acid medium. As the concentration of the Schiff bases increased, these molecules were unsuccessful to enhance the inhibition appreciably. Among the three Schiff bases, FAABA exhibited comparatively fair η_w%. A maximum of 51% of η_w was shown by this molecule at a concentration of 0.5 mM. Apart from the normal behavior of Schiff bases, the CPFASC molecule showed slight increase in the corrosion rate with concentration. This may be due to the tendency of the CPFASC molecules to form complex with the ferrous ions produced as a result of metal dissolution. The tendency for chelation may lead to considerable desorption of the molecules from the metal surface and hence to raise the rate of corrosion with concentration. Thus the corrosion inhibition efficiency of CPFASC molecules decreased with concentration. Additional factors such as elevated rate of corrosion of CS in sulphuric acid medium and slow hydrolysis of the Schiff base molecules may also lead to the increased dissolution of metal in sulphuric acid or the poor inhibition efficiency, even though these molecules are equipped with active probes such as azomethine linkage, hetero atom and aromatic rings in their structure.

The remaining two Schiff bases namely NPFASC and CPTASC showed good corrosion inhibition efficiency on CS surface. Maximum η_w% shown by NPFASC molecule at a concentration of 0.5 mM was 75%. The higher inhibition

efficiency of this molecule, compared to the previously discussed molecules, can be believed to the reduction of nitro group into the amino group which takes place in sulphuric acid medium containing Fe metal.

The Schiff base derived from thiophene-2-aldehyde i.e., CPTASC showed matchless corrosion inhibition efficiency than all other studied molecules in sulphuric acid medium. The η_w% varied from 63 to 94% for concentrations 0.1 to 0.5 mM respectively. Even at these very low concentrations, this molecule exhibited its unique inhibition efficiency values on CS surface. The effective role of CPTASC as a very good corrosion inhibitor can be explained due to the presence of the sulphur atom in the thiophene ring. The highly polarizable sulphur atom, bearing appreciable electron density, will lead to a strong interaction between the metal surface and protonated Schiff bases in acidic medium.

Mechanism of inhibition

It has been proposed that anions such as Cl^-, I^-, $SO_4^{2-}$and S^{2-}may take part in forming reaction intermediates on the corroding metal surface, which either inhibit or stimulate corrosion [83]. The suppression or stimulation of the dissolution process is initiated by the specific adsorption of the anions on the metal surface. According to the Bockris mechanism, the dissolution of Fe in acidic sulphate solutions depends primarily on the adsorbed intermediate $FeOH_{ads}$ [84].

Ashassi-Sorkhabi and Nabavi-Amri proposed the following mechanism involving two adsorbed intermediates to account for the retardation of Fe anodic dissolution in the presence of an inhibitor [85]:

$$Fe + H_2O \leftrightarrow FeH_2O_{ads}$$

$$FeH_2O_{ads} + A \leftrightarrow FeOH^-_{ads} + H^+ + A$$

$$FeH_2O_{ads} + A \leftrightarrow FeA_{ads} + H_2O$$

$$FeOH^-_{ads} \leftrightarrow FeOH_{ads} + e$$

$$FeA_{ads} \leftrightarrow FeA^+_{ads} + e$$

$$FeOH_{ads} + FeA^+_{ads} \leftrightarrow FeA_{ads} + Fe\,OH^+$$

$$Fe\,OH^+ + H^+ \leftrightarrow F\,e^{2+} + H_2O$$

where A represents the inhibitor species. A corroding metal surface is generally characterized by multiple adsorption sites having activation energies and heats of adsorption. Inhibitor molecules may thus be adsorbed more readily at surface active sites having suitable adsorption enthalpies. According to the mechanism proposed above, displacement of some adsorbed water molecules on the metal surface by inhibitor species to yield the adsorbed intermediate FeA_{ads}. This species will reduce the amount of $FeOH_{ads}$ available for the rate determining steps and consequently retards Fe anodic dissolution [86,87].

Owing to the complex nature of adsorption and inhibition of a given inhibitor, it is not possible for single adsorption mode between inhibitor and metal surface. Generally, two types of adsorption could be considered. In one mode, the neutral Schiff base molecules may be on the surface of carbon steel through the chemisorption mechanism involving the displacement of water molecules from the carbon steel surface and the sharing of electrons between the heteroatoms and iron. The inhibitor molecule can also adsorb on the carbon steel surface on the basis of donor-acceptor interactions between π electrons of the heterocyclic ring and vacant d-orbitals of surface iron. It is well known that the steel surface bears positive charge in acid solution [88] and it is difficult for the protonated Schiff

base to approach the positively charged mild steel surface (H_3O^+/metal interface) due to the electrostatic repulsion. Thus, the presence of sulphate ions which have excess negative charges in the vicinity of the interface could favour the adsorption of the positively charged inhibitor molecules. The protonated Schiff base could then adsorb through electrostatic interactions between the positively charged molecules and the steel surface which now has negatively charged sulphate ions on it. Thus there is a synergism between sulphate ions and the protonated Schiff base molecules [89]. This can be considered as the second mode of interaction between the inhibitor and metal surface.

Adsorption isotherms

The mechanism of interaction of the Schiff base on the surface of CS specimens was verified with the help of adsorption isotherms. The best fit model of isotherm was selected with the aid of correlation coefficient (Figures 2.80-2.83). Among the five Schiff bases studied FAABA and CPFAPH followed Freundlich adsorption isotherm, while the molecule NPFASC and CPTASC obeyed Langmuir adsorption isotherm. Since the molecule CPFASC did not exhibit a regular increase in the corrosion inhibition efficiency with concentration on carbon steel, its interaction on the metal surface in the corroding medium could not verify with any adsorption isotherms. The Schiff bases FAABA and CPFAPH which showed poor corrosion inhibition efficiency on CS, exhibited low value of adsorption equilibrium constants and displayed low free energy of adsorption (Table 2.24).

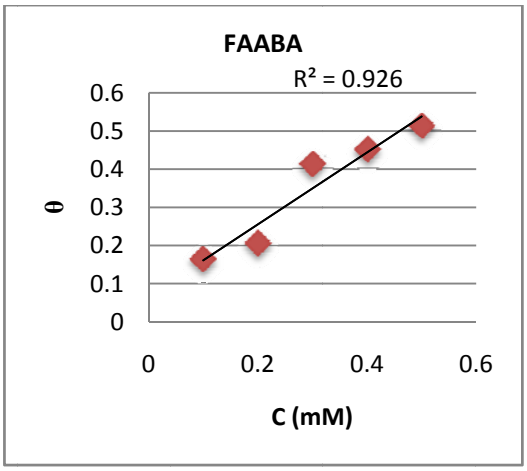

Fig. 2.80 Freundlich adsorption isotherm for FAABA on CS in 0.5 M H_2SO_4

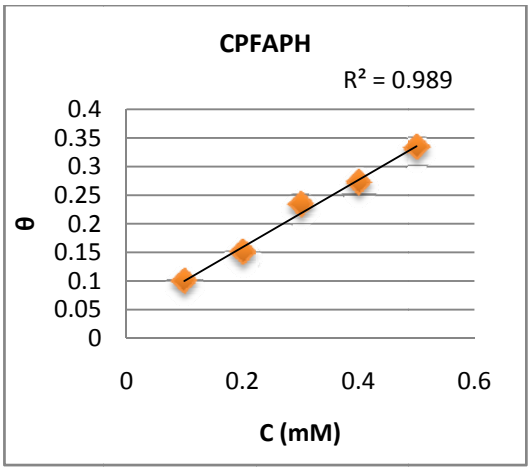

Fig. 2.81 Freundlich adsorption isotherm for CPFAPH on CS in 0.5 M H_2SO_4

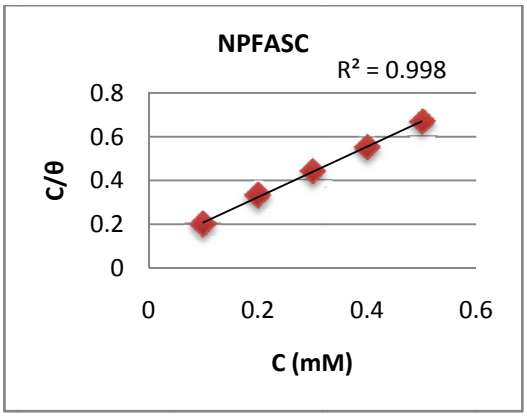

Fig. 2.82 Langmuir adsorption isotherm for NPFASC on CS in 0.5 M H_2SO_4

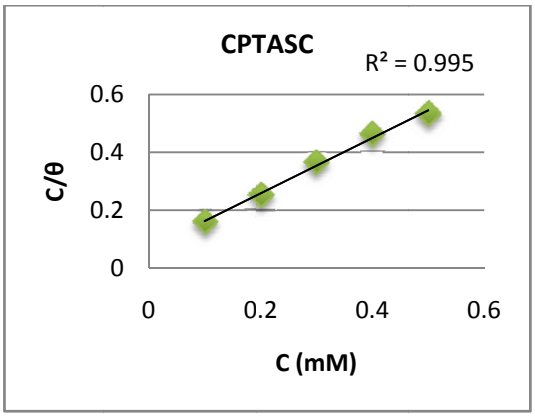

Fig. 2.83 Langmuir adsorption isotherm for CPTASC on CS in 0.5 M H_2SO_4

Table 2.24 Thermodynamic parameters for the adsorption of Schiff bases FAABA, CPFAPH, NPFASC and CPTASC on CS in 0.5 M H_2SO_4

Parameter	FAABA	CPFAPH	NPFASC	CPTASC
Isotherm	Freundlich	Freundlich	Langmuir	Langmuir
K_{ads}	942	588	10989	15151
ΔG_{ads} (kJ/mol)	-27.37	-26.18	-33.56	-34.37

Though the adsorption parameters indicate for the simultaneous physisorption and chemisorption of molecules in preventing the corrosion, the nature of isotherms and low values of the adsorption equilibrium constant suggest the possibility of the multilayer adsorption of FAABA and CPFAPH molecules. Schiff bases NPFASC and CPTASC exhibited high values of K_{ads} and ΔG_{ads} implies that monolayer of the protective molecules formed on the surface mainly through chemical interaction. Even if the rate of corrosion of CS in sulphuric acid was very high, these molecules are capable for making a good protection barrier against the dissolution of Fe atoms. Since the free energies of adsorption were negative, the adsorption of all Schiff base molecules was spontaneous in nature.

Corrosion inhibition studies of parent compounds

The corrosion inhibition efficiency of the parent aldehyde and amino compounds were studied by weight loss measurements and compared with the inhibition efficiencies of Schiff base. Table 2.25 exhibits the inhibition efficiencies of furan-2-aldehyde (FA), carboxyphenyl furan-2-aldehyde (CPFA), carboxyphenyl thiophene-2-aldehyde (CPTA), nirophenyl furan-2-aldehyde (NPFA), semicarbazide (SC), phenyl hydrazine (PH) and m-aminobenzoic acid (ABA) for the concentrations 0.1, 0.3 and 0.5 mM at 24 h.

Table 2.25 Corrosion inhibition efficiencies (η_w%) of parent compounds FA, CPFA, CPTA, NPFA, SC, PH and ABA on CS surface in 0.5 M H_2SO_4

C (mM)	FA	CPFA	CPTA	NPFA	SC	PH	ABA
0.1	5.22	26.66	34.21	49.21	0.89	28.88	21.94
0.3	8.31	29.83	44.93	57.65	10.14	35.63	49.24
0.5	8.64	47.35	58.85	62.32	7.368	43.02	54.83

On comparison of the values of Table 2.23 and 2.25 it is clear that the Schiff base FAABA displayed high corrosion inhibition efficiency than its parent aldehyde furan-2-aldehyde at all the studied concentrations, but the η_w% of the Schiff base was comparable to the η_w% of the parent amine m-aminobenzoic acid. This may be due to the complete hydrolysis of FAABA molecules into its parent compounds towards the end of 24 h and the resultant products were inhibited the corrosion less effectively. Similar results were reported by A. B. da Silva et al [27].

The inhibition efficiency of CPFAPH molecule was slightly less than or equal to the η_w% of its parent compounds CPFA and PH. The molecule was not much effective in reducing the corrosion rate of CS. Even though the Schiff bases NPFASC and CPTASC were susceptible to hydrolysis in acidic medium, they exhibited good η_w% on CS surface. This can be explained by the strong tendency of these molecules to attach on the surface of CS through the negatively charged sulphate ions. These sulphate ions first form a spontaneous layer on the positively charged metal surface and the protonated Schiff base molecules make strong interaction on the CS surface. It is unambiguous from this investigation that the adsorbed molecules on CS surface do not undergo hydrolysis considerably. The η_w% of these Schiff bases was noticeably higher than the inhibition efficiencies of their parent aldehyde and amines. The role of azomethine linkage in preventing the dissolution of metal is thus once again established by this investigation.

Electrochemical Corrosion Studies

A rapid corrosion test in the laboratory can be performed with the aid of electrochemical analysis such as impedance studies and polarization studies. Even

though these analyses were quick and accurate, the reliability in predicting the corrosion inhibition capacity of an organic molecule is sometimes questionable only with these techniques because of the instability of certain molecule in acidic media. As explained in the discussion part of weight loss studies, the low corrosion inhibition capacities of the three Schiff bases namely FAABA, CPFASC and CPFAPH at 24 h is attributed to the slow hydrolysis of the molecules in sulphuric acid medium. No other factors such as synergistic effect (which works in a medium containing halide ions) plays in the sulphuric acid medium to reduce the hydrolysis and to lower the metal dissolution appreciably.

Even though we are more concerned in the prolonged corrosion inhibition response of a molecule in acidic medium (determined by weight loss studies), to answer the following questions, the electrochemical studies such as potentiodynamic polarization analysis and electrochemical impedance spectroscopic analysis were performed on these Schiff bases in sulphuric acid medium.

a) "What will be the inhibitive nature of these Schiff bases at a period of 30 minutes?"
b) "Are the corrosion inhibition values obtained by these techniques comparable with the values of gravimetric studies?"
c) "Which is the main electrochemical site of interaction by the Schiff base molecule, anodic, cathodic or mixed?"

Detailed investigation was conducted to answer the above questions and the results are summarized in subsequent paragraphs. Electrochemical analyses

were done in a three electrode assembly. The working electrode (CS) was made in contact with the aggressive solutions in the absence and presence of various concentrations of five Schiff bases namely FAABA, CPFASC, CPFAPH, NPFASC and CPTASC.

Electrochemical impedance spectroscopic studies

All tests were performed under unstirred conditions. Constant potential (OCP) was maintained in all measurements and a frequency range of 1 KHz to 100 mHz with amplitude of 10 mV as excitation signal was employed. The percentage of inhibition from impedance measurements was calculated using charge transfer resistance values by the following expression

$$\eta_{EIS}\,\% = \frac{R_{ct} - R'_{ct}}{R_{ct}} X100$$

where R_{ct} and R'_{ct} are the charge transfer resistances of working electrode with and without inhibitor respectively.

Figures 2.84 to 2.88 represent the Nyquist and Bode plots for the Schiff bases on CS in sulphuric acid medium. Table 2.26 explores the impedance parameters such as charge transfer resistance and double layer capacitance. The corrosion inhibition efficiencies of various Schiff bases at different concentrations ranges from 0.1-0.5 mM is also listed in this table.

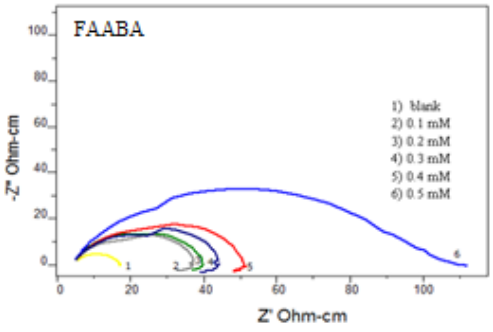

Fig. 2.84a Nyquist plot of CS in the presence and absence of FAABA in 0.5 M H_2SO_4

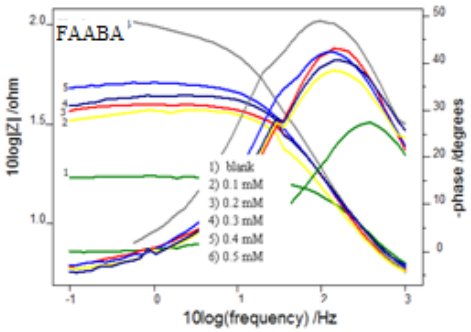

Fig. 2.84b Bode plots of CS in the presence and absence of FAABA in 0.5 M H_2SO_4

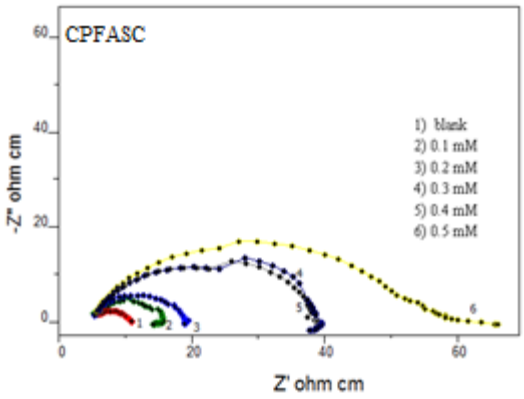

Fig. 2.85a Nyquist plots of CS in the presence and absence of CPFASC in 0.5 M H_7SO_4

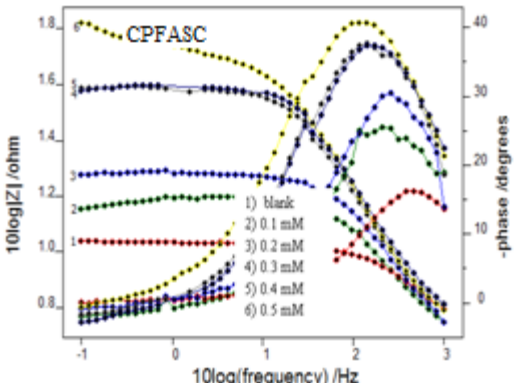

Fig. 2.85b Bode plots of CS in the presence and absence of CPFASC in 0.5 M H_2SO_4

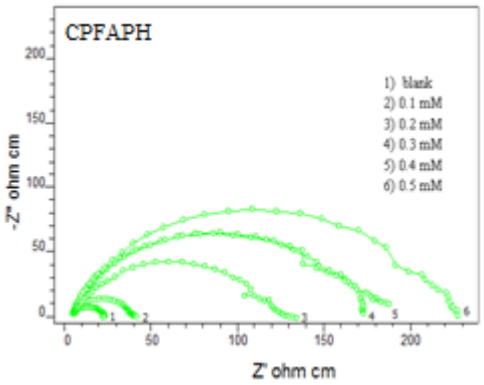

Fig. 2.86a Nyquist plots of CS in the presence and absence of CPFAPH in 0.5 M H_2SO_4

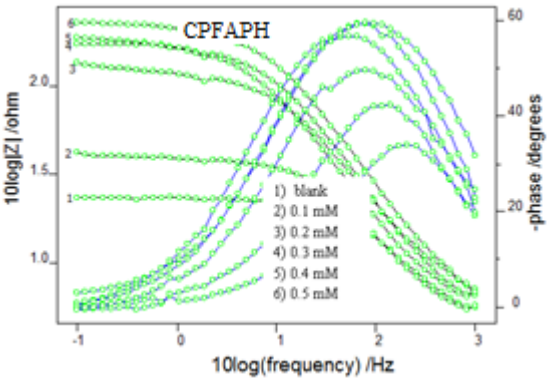

Fig. 2.86b Bode plots of CS in the presence and absence of CPFAPH in 0.5 M H_2SO_4

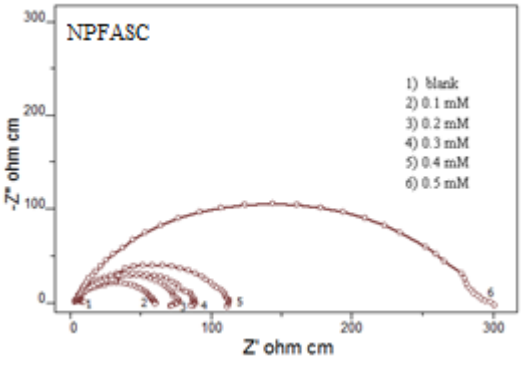

Fig. 2.87a Nyquist plots of CS in the presence and absence of NPFASC in 0.5 M H_2SO_4

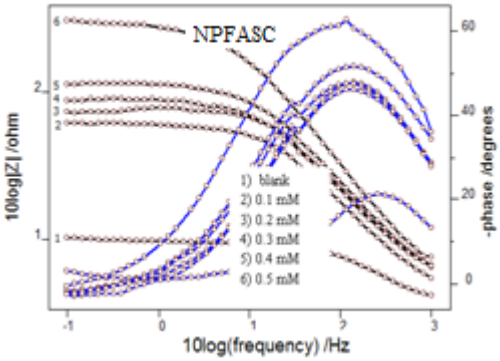

Fig. 2.87b Bode plots of CS in the presence and absence of NPFASC in 0.5 M H_2SO_4

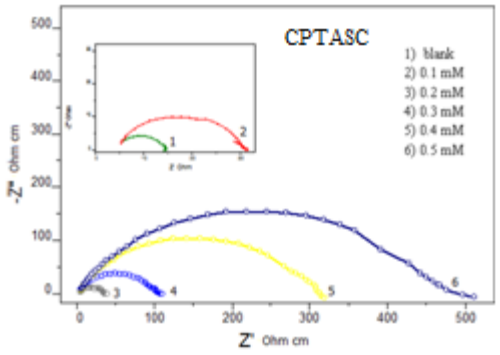

Fig. 2.88a Nyquist plots of CS in the presence and absence of CPTASC in 0.5 M H_2SO_4

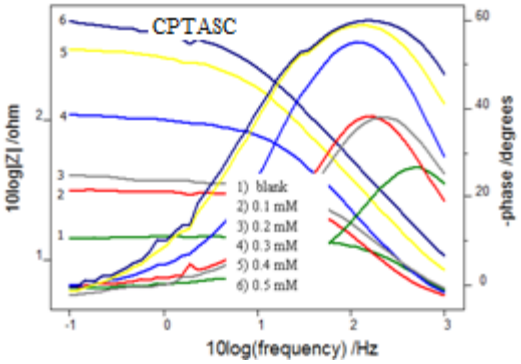

Fig. 2.88b Bode plots of CS in the presence and absence of CPTASC in 0.5 M H_2SO_4

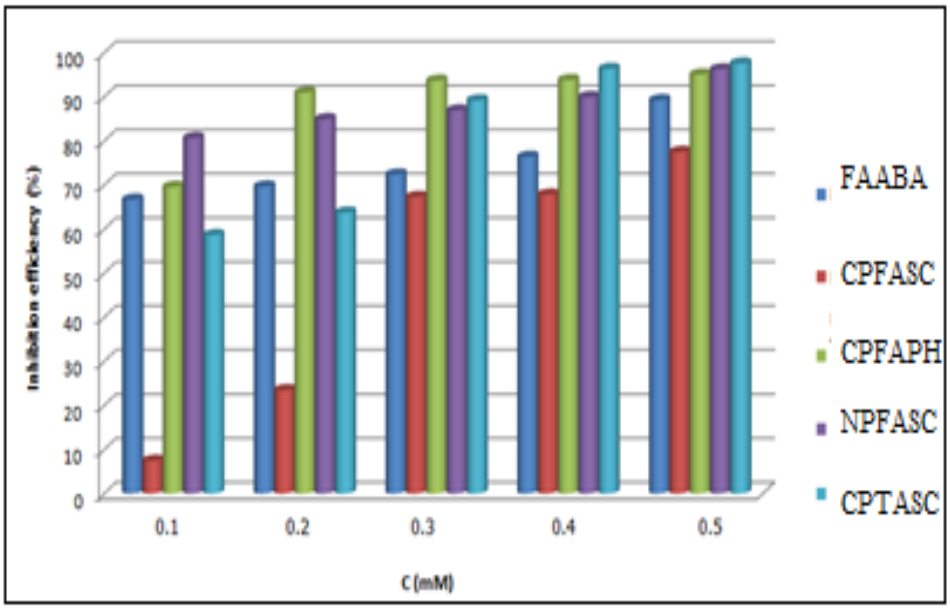

Fig. 2.89 Comparison of corrosion inhibition efficiencies (η_{EIS}%) of Schiff bases, FAABA, CPFASC, CPFAPH, NPFASC and CPTASC on CS in 0.5 M H_2SO_4

Table 2.26 Electrochemical impedance parameters of CS in the presence and absence of Schiff bases, FAABA, CPFASC, CPFAPH, NPFASC and CPTASC in 0.5 M H_2SO_4

Schiff base	C (mM)	C_{dl}	R_{ct}	η_{EIS}%
	0	133	9.72	-
FAABA	0.1	132	29.16	66.66
	0.2	122	32.03	69.65
	0.3	122	35.16	72.35
	0.4	118	41.15	76.38
	0.5	113	90.31	89.24
CPFASC	0.1	128	10.5	7.43
	0.2	118	12.7	23.46
	0.3	118	29.7	67.27
	0.4	101	30.2	67.81
	0.5	100	43.2	77.50
CPFAPH	0.1	129	31.93	69.56
	0.2	107	107.3	90.94
	0.3	167	153.1	93.65
	0.4	123	156.2	93.78
	0.5	95	196.7	95.06
NPFASC	0.1	132	50.15	80.62
	0.2	121	64.44	84.92
	0.3	103	74.28	86.91
	0.4	98	96.69	89.95
	0.5	85	257	96.22
CPTASC	0.1	132	23.49	58.62
	0.2	105	26.8	63.73
	0.3	102	89.95	89.19
	0.4	75	265.1	96.33
	0.5	58	399.3	97.57

EIS studies revealed that all the Schiff bases except CPFASC acted as very good corrosion inhibitor in the studied period of 30 minutes. It is evident from Table 2.26 and Figure 2.89 that the corrosion inhibition efficiencies appreciably enhanced with the concentration of the Schiff bases. The formation of the protective layer of these molecules on CS surface was confirmed by C_{dl} values, which were decreased with the concentration of Schiff bases. The corrosion inhibition values obtained by gravimetric studies were comparable with the EIS measurements only for NPFASC and CPTASC. Other three Schiff bases exhibited poor inhibition efficiency according to gravimetric studies. This disparity between the results of corrosion monitoring investigations can be regarded to the slow decomposition of the Schiff bases FAABA, CPFASC and CPFAPH in the acidic medium. To conclude, at the early period of treatment of CS in sulphuric acid medium, all the Schiff bases behaved as good inhibitors by forming protective layers on the surface, but as the immersion time was increased, notable decomposition to the Schiff base molecules such as FAABA, CPFASC and CPFAPH occurred and they displayed poor corrosion inhibition efficiency towards the end of studied period (24h). At the highest concentration of 0.5mM, η_{EIS}% of Schiff bases follows the order CPFASC< FAABA <CPFAPH <NPFASC <CPTASC. A maximum of 97.6% inhibition efficiency was observed for the molecule CPTASC at a concentration of 0.5 mM.

Potentiodynamic polarization studies

Electrochemical polarization studies of CS specimens in 0.5 M sulphuric acid with and without inhibitor were performed by recording anodic and cathodic

potentiodynamic polarization curves. Polarization plots were obtained in the electrode potential range -100 to +100 mV vs equilibrium potential at a sweep rate of 1mV/sec. The percentage of inhibition efficiency ($\eta_{pol\%}$) was assessed from the measured I_{corr} values using the following relation :

$$\eta_{pol}\,\% = \frac{I_{corr} - I'_{corr}}{I_{corr}}\ X100$$

where I_{corr} and I'_{corr} are the corrosion current densities of the exposed area of the working electrode in the absence and presence of inhibitor.

From the slope analysis of the linear polarization curves in the vicinity of corrosion potential of blank and different concentrations of the inhibitor, the values of polarization resistance (R_p) were obtained. From the evaluated polarization resistance, the inhibition efficiency was calculated using the relationship

$$\eta_{R_p}\,\% = \frac{R'_p - R_p}{R'_p}\ X100$$

where R'_p and R_p are the polarization resistance in the presence and absence of inhibitor respectively

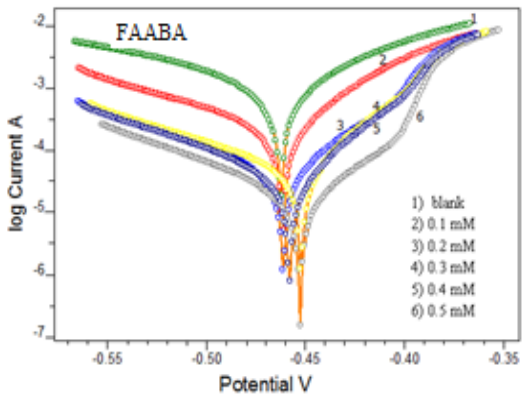

Fig. 2.90a Tafel plots of CS in the presence and absence of FAABA in 0.5 M H_2SO_4

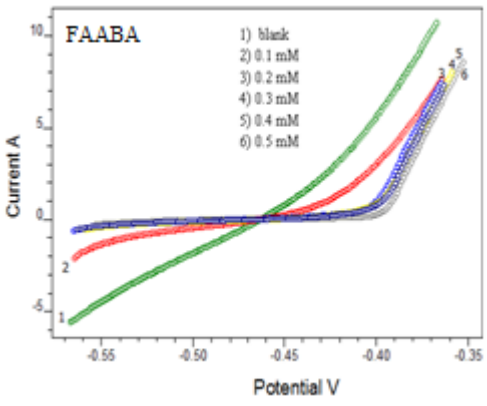

Fig. 2.90b Linear polarization curves of CS in the presence and absence of FAABA in 0.5 M H_2SO_4

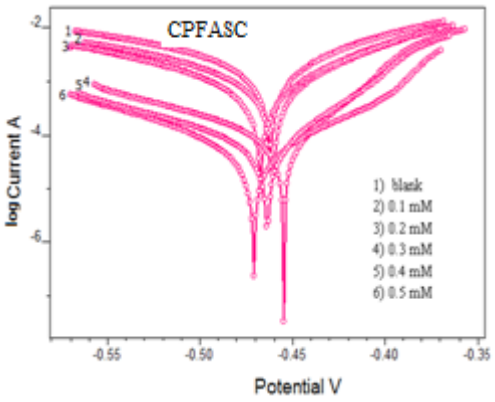

Fig. 2.91a Tafel plots of CS in the presence and absence of CPFASC in 0.5 M H_2SO_4

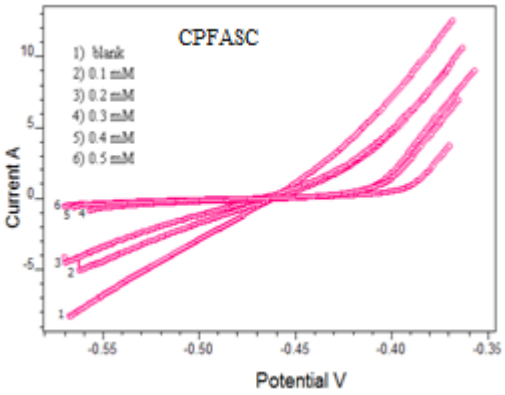

Fig. 2.91b Linear polarization curves of CS in the presence and absence of CPFASC in 0.5 M H_2SO_4

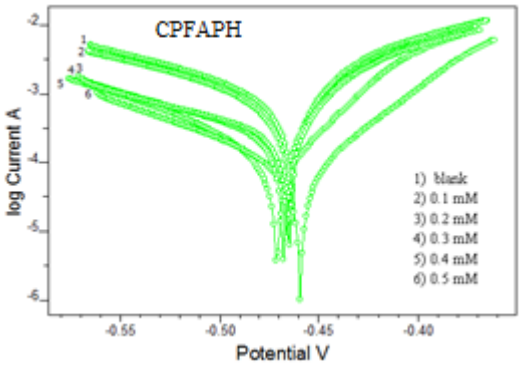

Fig. 2.92a Tafel plots of CS in the presence and absence of CPFAPH in 0.5 M H_2SO_4

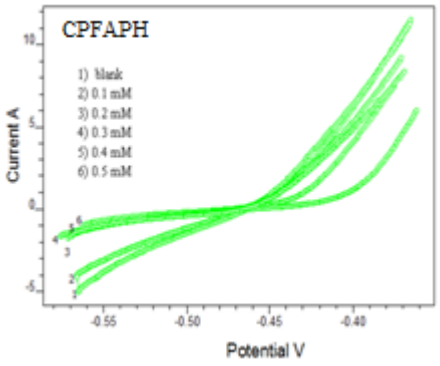

Fig. 2.92b Linear polarization curves of CS in the presence and absence of CPFAPH in 0.5 M H_2SO_4

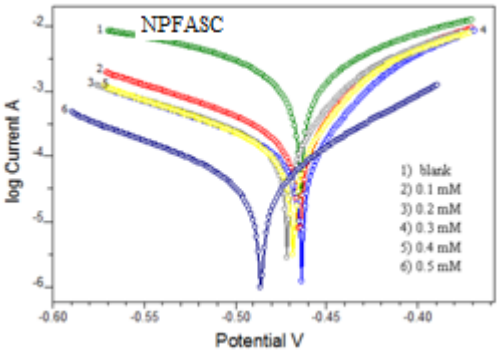

Fig. 2.93a Tafel plots of CS in the presence and absence of NPFASC in 0.5 M H_2SO_4

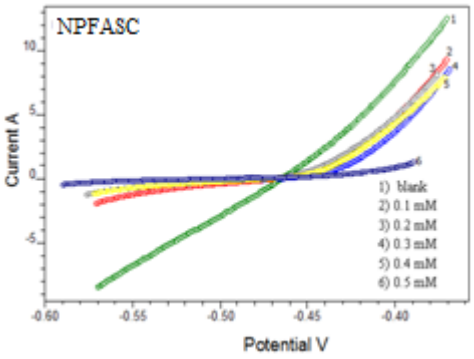

Fig. 2.93b Linear polarization curves of CS in the presence and absence of NPFASC in 0.5 M H_2SO_4

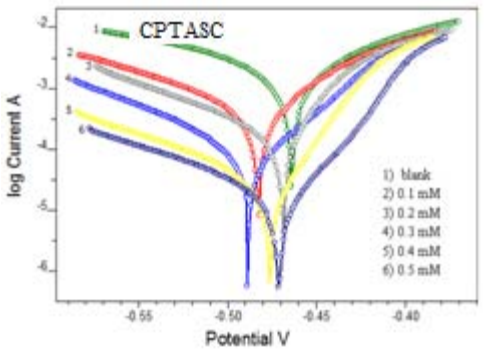

Fig. 2.94a Tafel plots of CS in the presence and absence of CPTASC in 0.5 M H_2SO_4

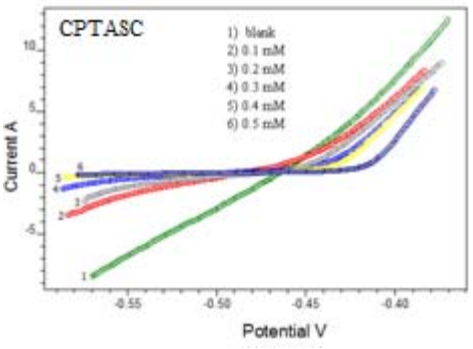

Fig. 2.94b Linear polarization curves of CS in the presence and absence of CPTASC in 0.5 M H_2SO_4

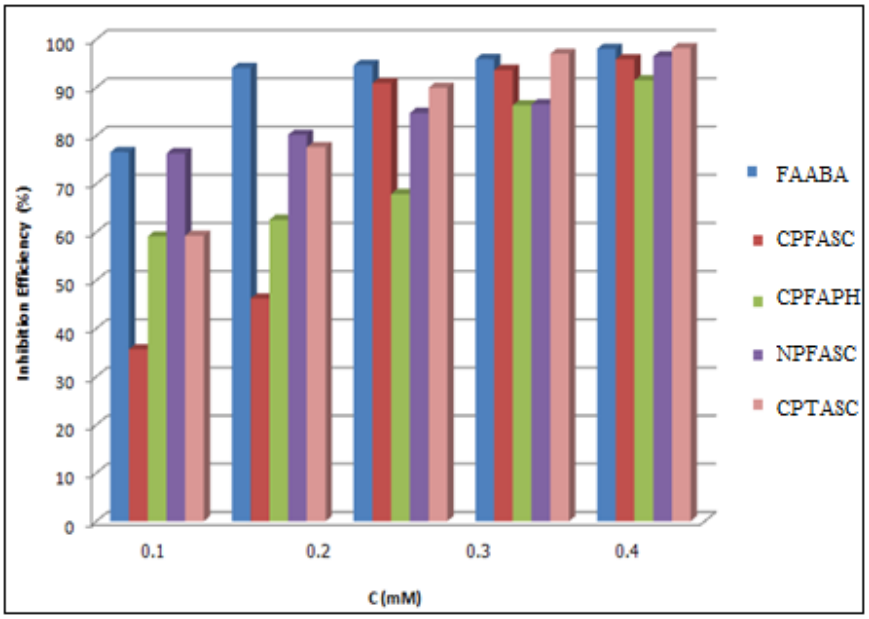

Fig. 2.95 Comparison of corrosion inhibition efficiencies (η_{pol}%) of Schiff bases, FAABA, CPFASC, CPFAPH, NPFASC and CPTASC on CS in 0.5 M H_2SO_4

Table 2.27 Potentiodynamic polarization parameters in the presence and absence of Schiff bases, FAABA, CPFASC, CPFAPH, NPFASC and CPTASC in 0.5 M H_2SO_4

		Tafel Data					Linear polarization data	
Schiff Base	C (mM)	$-E_{corr}$ (mV/SCE)	I_{corr} ($\mu A/cm^2$)	$-b_c$ (mV/dec)	b_a (mv/dec)	$\eta_{pol\%}$	R_p (ohm)	$\eta_{Rp\%}$
	0	482	1041	126	85	-	14.09	-
FAABA	0.1	461	233.8	113	59	77.54	60.14	76.57
	0.2	464	40.72	102	34	96.09	236.0	94.029
	0.3	446	36.62	95	34	96.48	262.9	94.64
	0.4	450	31.51	93	35	96.97	342.3	95.88
	0.5	450	10.83	88	21	98.96	709.0	98.01
CPFASC	0.1	458	752.9	113	74	27.68	21.9	35.66
	0.2	465	611.6	110	73	41.25	26.19	46.20
	0.3	446	72.21	107	34	93.06	154.5	90.88
	0.4	456	53.07	107	40	94.90	220.8	93.62
	0.5	466	39.71	88	62	96.19	339.9	95.85
CPFAPH	0.1	476	440.0	117	93	57.73	34.44	59.09
	0.2	492	371.5	137	82	64.31	37.6	62.53
	0.3	490	338.2	123	75	67.51	43.85	67.87
	0.4	468	126.8	93	43	87.82	102.8	86.29
	0.5	455	74.29	95	46	92.86	164.9	91.46
NPFASC	0.1	477	261.3	105	61	74.90	59.52	76.33
	0.2	488	209.5	112	62	79.86	71.14	80.19
	0.3	484	171.2	104	59	83.55	92.1	84.70
	0.4	474	133.2	103	58	87.20	104.5	86.52
	0.5	486	36.02	94	61	96.54	394.5	96.43
CPTASC	0.1	485	436.8	104	70	58.04	34.58	59.25
	0.2	488	73.81	96	65	73.96	62.97	77.62
	0.3	479	271.1	84	40	92.91	139.9	89.93
	0.4	473	28.97	98	30	97.22	466.1	96.98
	0.5	458	13.69	100	25	98.68	773.1	98.18

Tafel polarization and linear polarization curves of various Schiff bases are represented in Figures 2.90-2.94 and data such as anodic slope, cathodic slope, corrosion potential and corrosion current density for the five Schiff bases derived from furan-2-aldehyde and thiophene-2-aldehyde are displayed in the Table 2.27. The corrosion inhibition efficiencies are also listed and compared in the above table and Figure 2.95.

From the polarization studies it is evident that all Schiff bases behaved as potential corrosion inhibitors. All the Schiff bases reduced the corrosion current density of CS specimens which was in contact with sulphuric acid. Significant corrosion inhibition efficiency (>90%) was shown by all Schiff bases at a concentration of 0.5 mM. Even though the first three Schiff bases FAABA, CPFASC and CPFAPH showed very poor inhibitive response at 24 h as per weight loss studies, their initial corrosion inhibition power according to the polarization studies were beyond the expectation. For instance, the Schiff base FAABA displayed 98% of inhibition efficiency at 0.5 mM as per polarization studies, while it was merely 51% according to weight loss studies. Hetero atoms, aromatic rings and azomethine linkage present in the molecule would cause to enhance the corrosion inhibition of these Schiff base when compared to the Schiff bases derived from 3-acetylpyridine in sulphuric acid. On close examination of the Tafel slopes, it is understandable that the four Schiff bases namely FAABA, CPFASC, CPFAPH and CPTASC affect the anodic and cathodic sites of corrosion and can be called as mixed corrosion inhibitor. But the Schiff base NPFASC only affect the cathodic slope considerably and hence this molecule can

be regarded as a cathodic inhibitor. Corrosion potential (E_{corr}) of CS specimens did not change considerably in all investigations in the presence of various Schiff bases.

Synergistic Effect Studies

From the gravimetric corrosion inhibition studies for 24 h it was proved that the inhibition efficiency of the Schiff bases such as FAABA, CPFASC and CPFAPH were poor. But the rapid corrosion analysis such as electrochemical investigations exposed the higher inhibitive response of these molecules on CS surface in sulphuric acid medium for 30 minutes. To improve the corrosion inhibition efficacy of these molecules for a period 24 h, 0.2 mM KI solution (1ml) was added to the corrosive solutions containing the Schiff bases at various concentrations and the gravimetric studies were performed. The results of gravimetric studies are summarized and compared with the results of corrosion studies without adding iodide ions (Table 2.28).

On the addition of KI to the corroding solutions, the three Schiff bases exhibited much enhanced corrosion inhibition. FAABA displayed excellent corrosion inhibition efficiencies (>90%) for all studied concentrations. A maximum of 98% of η_w showed by the CPFASC molecule at 0.4 mM, which was very higher than the η_w% of corroding solution containing only Schiff base (45%). At a concentration of 0.4 mM, the CPFAPH exhibited η_w% of 27, while on the addition of KI a drastic change in the inhibition efficiency was noticed. The very poor inhibition efficiencies of the Schiff bases were thus radically increased on the addition of KI synergistically. The primarily adsorbed iodide ions on the CS surface strongly hold the Schiff base molecules to prevent the metal

dissolution in acidic medium without any decomposition or hydrolysis for the studied period of corrosion testing (24 h). The mechanism of inhibition was further confirmed by plotting most suitable adsorption isotherms with the help of correlation coefficient. The three Schiff bases followed Langmuir adsorption isotherms (Table 2.29 and Figures 2.96 to 2.98).

Table 2.28 Corrosion inhibition efficiency (η_w%) of Schiff bases, FAABA, CPFASC and CPFAPH on CS in the presence and absence of KI in 0.5 M H_2SO_4

System	C (mM)	Corrosion Rate (mmy^{-1})		η_w%	η_w%
		Schiff base	Schiff base+ KI	Schiff base	Schiff base+ KI
Blank	0	23.5	-	-	-
Blank +KI (0.2 mM)	0	-	19.4	-	20.4
FAABA	0.1	19.64	1.55	16.44	93.39
	0.2	18.66	0.37	20.59	98.41
	0.3	13.81	0.31	41.25	98.70
	0.4	12.91	0.35	45.07	98.52
CPFASC	0.1	10.23	3.85	56.51	83.61
	0.2	11.23	2.86	52.27	87.83
	0.3	13.91	2.84	40.88	87.92
	0.4	13.02	0.51	44.66	97.85
CPFAPH	0.1	21.18	15.25	9.99	35.11
	0.2	20.01	11.68	14.96	50.28
	0.3	18.02	7.97	23.40	66.08
	0.4	17.13	5.17	27.20	78.00

The adsorption equilibrium constant and free energy of adsorption were deducted from the isotherms. These three compounds exhibited higher values of adsorption parameters compared to the corrodent containing only Schiff base. On addition of KI, the FAABA molecule adsorbed on the metal surface through chemisorption. Even though other two Schiff base interact with chemical as well as physical forces, their free energy of adsorption clearly established the existence of strong force of attraction between the metal surface and the inhibiting molecules.

Negative values of ΔG_{ads} confirmed the spontaneity of the interaction of Schiff bases through iodide ion on the metal surface.

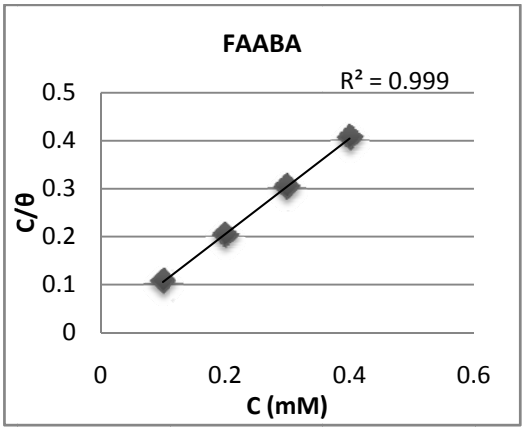

Fig. 2.96 Langmuir adsorption isotherm for FAABA+ KI on CS in 0.5 M H_2SO_4

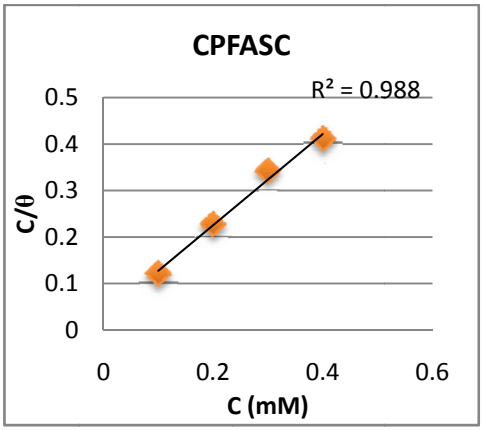

Fig. 2.97 Langmuir adsorption isotherm for CPFASC+ KI on CS in 0.5 M H_2SO_4

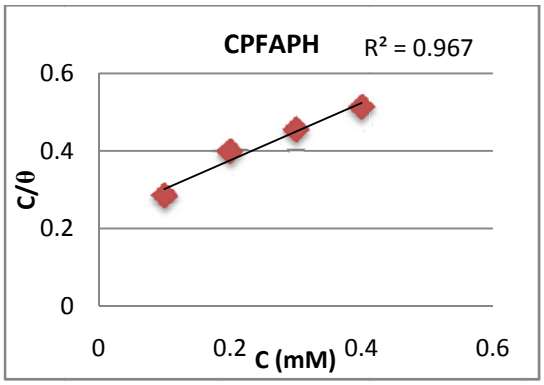

Fig. 2.98 Langmuir adsorption isotherm for CPFAPH+ KI on CS in 0.5 M H_2SO_4

Table 2.29 Thermodynamic parameters for the adsorption of Schiff bases, FAABA, CPFASC and CPFAPH on CS in the presence of KI in 0.5 M H_2SO_4

System	Isotherm	K_{ads}	$-\Delta G_{ads}$ kJ mol^{-1}	Type of interaction
FAABA + KI	Langmuir	200000	40.87	Chemisorption
CPFASC +KI	Langmuir	34483	36.44	Physisorption and Chemisorption
CPFAPH+ KI	Langmuir	1351	28.28	Physisorption and Chemisorption

Synergism parameter

It is evident from Table 2.27 that the addition of KI drastically increased the $\eta_W\%$ values for all Schiff bases. It is also clear that $\eta_W\%$ for KI in combination with inhibitor is higher than the sum of $\eta_W\%$ for single KI and single inhibitor, which is synergism in nature. Aramaki and Hackerman [90] calculated the synergism parameter S_θ using the following equation.

$$S_\theta = \frac{1-\theta_{1+2}}{1-\theta'_{1+2}}$$

where $\theta_{1+2} = (\theta_1 + \theta_2) - (\theta_1\,\theta_2)$; θ_1= surface coverage by anion (iodide ion); θ_2= surface coverage by cation (protonated Schiff base); θ'_{1+2} = measured surface coverage by both anion and cation. S_θ approaches unity when there are no interactions between the inhibitor compounds, while $S_\theta > 1$ points to a synergistic effect; in the case of $S_\theta < 1$, the antagonistic interaction prevails. The values of the synergism parameter for the various concentrations of three Schiff bases studied by gravimetric analysis are presented in Table 2.30. Variation of synergism parameter with the concentration of the Schiff base is portrayed in the Figure 2.99. From the figure and table it is obvious that the molecule FAABA has displayed a very high synergism parameter, which indicates that these molecules adsorb on the surface of CS via chemical interaction. The synergistic effect played by FAABA has shown its maximum value at 0.2 mM. Beyond this concentration S_θ decreased slightly. CPFASC also exhibited high value of S_θ. The synergism parameter of the three compounds decreases in the order FAABA> CPFASC >CPFAPH.

Table 2.30 Synergism parameter (S_θ) for the Schiff bases, FAABA, CPFASC and CPFAPH at different concentrations in 0.5 M H_2SO_4

C (mM)	FAABA	CPFASC	CPFAPH
0.1	10.06	2.11	1.10
0.2	39.75	3.12	1.36
0.3	35.97	3.89	1.79
0.4	29.54	20.48	2.63

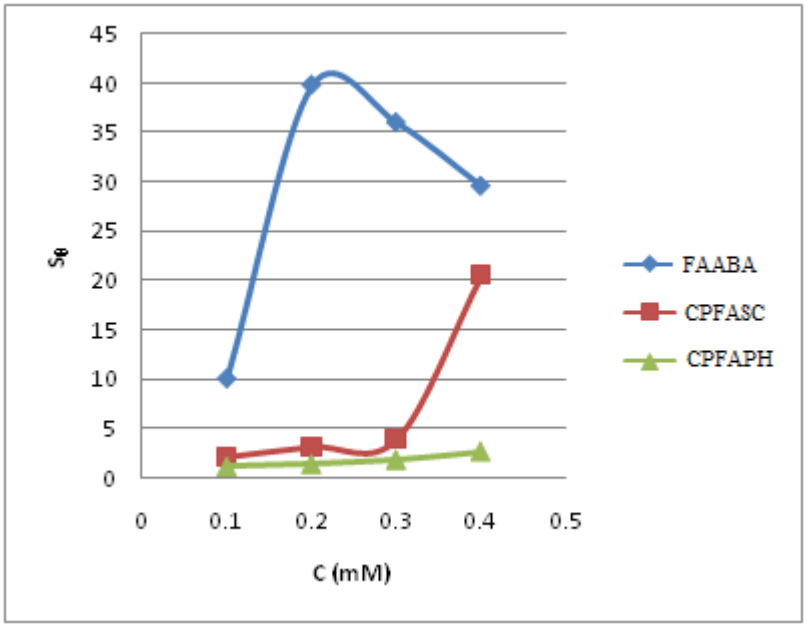

Fig. 2.99 Variation of synergism parameter (S_θ) with concentration of Schiff bases FAABA, CPFASC and CPFAPH

SUMMARY

Carbon steel corrosion inhibition efficiencies (in 1.0 M HCl and 0.5 M H_2SO_4) of newly synthesized heterocyclic Schiff bases such as 3-acetylpyridine semicarbazone (APSC), 3-acetylpyridine thiosemicarbazone (APTSC), 3-acetylpyridine phenylhydrazone (APPH), furan-2-aldehyde-3-aminobenzoic acid (FAABA), carboxyphenyl furan-2-aldehyde semicarbazone (CPFASC), carboxyphenyl furan-2-aldehyde phenylhydrazone (CPFAPH), nitrophenyl furan-2-aldehyde semicarbazone (NPFASC) and carboxyphenyl thiophene-2-aldehyde semicarbazone (CPTASC) were evaluated using gravimetric corrosion inhibition studies and electrochemical corrosion monitoring methods such as electrochemical impedance spectroscopy (EIS) and potentiodynamic polarization studies. Majority of the Schiff bases behaved as good corrosion inhibitors on carbon steel in acidic media. The mechanism of corrosion inhibition of the heterocyclic Schiff bases was verified by adsorption studies and confirmed by surface morphological analysis.

The three Schiff bases which are derived from 3-acetylpyridine showed excellent corrosion inhibition efficiencies on CS surface in 1.0 M HCl. In general, corrosion inhibition efficiencies of the Schiff bases followed the order APSC < APTSC < APPH. The higher inhibitive nature of APPH was due to the presence of aromatic ring system in the molecule. The three Schiff bases followed Langmuir adsorption isotherm on CS surface. Effect of temperature on the corrosion rate was studied by performing the corrosion studies of CS in 1.0 M HCl in the presence and absence of Schiff bases APSC, APTSC and APPH.

Surface morphological studies revealed that these molecules make a protective barrier on CS surface and thus prevent the metallic dissolution appreciably. Results obtained from the ac impedance studies and polarization analyses were comparable with the gravimetric studies. Polarization studies revealed that the three Schiff bases acted as mixed type inhibitors, although they showed greater affinity towards cathodic sites.

In sulphuric acid medium, the corrosion inhibition behaviour of Schiff base APTSC was good, but APSC displayed poor inhibition response. The Schiff base APPH, which showed excellent corrosion inhibition efficiency in HCl medium, behaved as a corrosion antagonist in H_2SO_4. This was verified by gravimetric corrosion studies for a period of 24 h and an attempt was made to improve the inhibitive capacity of this Schiff base, by adding very small quantity of KI (synergistic effect) and the obtained results were highly remarkable. Freundlich and El-Awady adsorption isotherms were followed by APSC and APTSC molecules respectively on CS surface in sulphuric acid medium. EIS and polarization studies were also conducted to check the corrosion inhibition response of these molecules for a period of 30 minutes. Synergistic study revealed that the molecule APPH was attached on the CS surface through iodide ions by a strong chemical attraction without any hydrolytic decomposition, which was further verified by surface morphological analysis using scanning electron micrographs.

Schiff bases which are mainly derived from furan-2-aldehyde and thiophene-2-aldehyde such as FAABA, CPFASC, CPFAPH, NPFASC and

CPTASC showed appreciable corrosion inhibition efficiency on CS in 1.0 M HCl. A maximum of 90% of η_w was achieved by FAABA at a concentration of 0.5 mM. The corrosion inhibition response of all compounds was explained on the basis of their optimized molecular structures. Langmuir adsorption isotherm was obeyed by FAABA, CPFAPH and CPTASC, while the Schiff bases CPFASC and NPFASC followed Freundlich and Temkin adsorption isotherms respectively. Results of electrochemical corrosion studies and weight loss studies were comparable for these Schiff bases in HCl medium. Potentiodynamic polarization studies established that the Schiff bases FAABA, CPFASC and NPFASC behaved as pure mixed type inhibitors on carbon steel, while CPFAPH and CPTASC acted as cathodic inhibitors.

The Schiff base CPTASC was highly effective in preventing the corrosion of carbon steel in sulphuric acid, but other heterocyclic molecules derived from furan-2-aldehyde or thiophene-2-aldehyde exhibited moderate or poor corrosion inhibition efficiency. FAABA and CPFAPH obeyed Freundlich adsorption isotherm while, NPFASC and CPTASC followed Langmuir isotherm on CS. It was also noticed that CPFASC did not follow any adsorption isotherm, since the inhibition efficiency of this molecule was followed an inverse relationship with concentration. To improve the corrosion inhibition efficiency of these molecules, synergistic studies were performed in the presence of 0.2 mM KI solution. The drastic change in the inhibition efficiency was noted for these molecules, on the addition of potassium iodide. Synergistic parameters were also evaluated from these studies. Polarization studies showed the Schiff bases FAABA, CPFASC,

CPFAPH and CPTASC affected the anodic and cathodic sites of corrosion (mixed type inhibitor), while NPFASC only affected the cathodic site of corrosion considerably and can label as cathodic inhibitor.

REFERENCES

1. *The Financial Express*-e-news paper Oct 10 (2012)
2. E. Mary, W. de Gruyter, "*Concise Encyclopedia Chemistry"*revised edn. (1994) 834
3. L. David, Lipták, G. Béla, "*Environmental Engineers' Handbook"*, CRC Press (1997) 973
4. F. M. Arline, "*Textile Techniques in Metal: For Jewelers, Textile Artists & Sculptors"*, Lark Books (2003) 32
5. S. R. Rao, "*Resource Recovery And Recycling From Metallurgical Wastes"*, Elsevier, (2006) 179
6. I. L. Rozenfeld, L. V. Frolova, V. M. Brusnikina, *Sov. Sci. Rev.*, *Section B, Chem. Rev.*, 8 (1987) 115
7. C. C. Nathan, *"Corrosion Inhibitors"*, NACE, Houston: Texas (1981)
8. C.G. Munger, *"Corrosion Prevention By Protective Coatings"*, NACE (1999)
9. G. Gunasekaran, N. Palanisamy, B. V. A. Rao, V. S. Muraleedharan, *Electro. Chim. Acta*, 42 (1997) 1427
10. A. Arora, S. K. Pandey, "*SPE International Conference And Exhibition On Oilfield Corrosion"*, U.K (2012)
11. P. Munn, *Corrs. Sci.*, 35 (1993) 1495
12. W. J. Lorenz, F. Mansfield, *Corros. Sci.*, 21 (1981) 647
13. A. A. Aksutt, W. J. Lorenz, F. Mansfield, *Corros. Sci.*, 22 (1982) 611

14. M. Hosseini, S. F. L. Mertens, M. Ghorbani, M. R. Arshadi, *Mater. Chem. Phy.*, 28 (2003) 800

15. N. Saxena, S. Kumar, M. K. Sharma, S. P. Mathur, *Pol. J. Chem. Tech.*, 15(1) (2013)

16. Toliwal, S. D. Jadav, K. Pavagadhi, Tejas, *Indian J. Chem. Tech.*, 18(4) (2011) 190

17. H. Keleş, M. Keleş, *Res. Chem. Intermed.*, (2012) DOI 10.1007/s11164-012-0955-5

18. D. Gopi, K. M. Govindaraju, L. Kavitha, *J. Appl. Electrochem.*, 40 (2010) 1349

19. S. M. A. Hosseini, A. Azimi, *Mater. Corros.*, 59 (1) (2008) 41

20. A. J. A. Nasser, M. A. Sathiq, *Int. J. Engg. Sci. Tech.*, 2 (11) (2010) 6417

21. S. Jauhari, S. Vallabhbhai, B. Mistry, *Corrosion*, Houston, Texas (2011)

22. A. S. Fouda, M. Abdallah, M. Medhat, *Prot. Metals Phy. Chem. Surf.*, 48 (4) (2012) 477

23. K. M. Govindaraju, D. Gopi, L. Kavitha, *J. Appl. Electrochem.*, 39 (12) (2009) 2345

24. R. K. Upadhyay, S. Anthony, S. P. Mathur, *Russ. J. Electrochem.*, 43 (2007) 238

25. I. A. Aiad, N. A. Negam, *J. Surfactants Deterg.*, 12 (4) (2009) 313

26. S. Issaadi, T. Douadi, A. Zouaoui, S. Chafaa, M. A. Khan, G. Bouet, *Corros. Sci.*, 53 (4) 2011

27. A. B. da Silva, E. D. Elia, J. A. Gomes, *Corros. Sci.*, 52 (3) (2010) 788

28. A. Yurt, A. Balaban, S. U. Kandemir, G. Bereket, B. Erk, *Mater. Chem. Phys.*, 85 (2004) 420
29. X. Li, S. Deng, H. Fu, T. Li, *Electrochim. Acta*, 54 (2009) 4089
30. E. Kamis, *Corrosion,* 46 (1990) 478
31. S. S. Abd El-Rehim, A. Magdy, M. Ibrahim, F. Khaled, *J. Appl. Electrochem.*, 29 (1999) 599
32. E. McCafferty, H. Leidheiser Jr., "*Corrosion Control By Coating"*, Science Press, Princeton (1979)
33. M. Bouklah, N. Benchat, B. Hammouti, A. Aouniti, S. Kertit, *Mater. Lett.*, 60 (2006) 1901
34. J. O'M. Bockris, A. K. N. Reddy, "*Modern Electrochemistry-2*", Plenum Press, New York (1970)
35. E. Gileadi, "*Electrode Kinetics For Chemists, Chemical Engineers And Material Scientists*", VCH publishers, New York (1993)
36. D. A. Jones, "*Principles and Prevention of Corrosion*", Macmillam publishing, New York (1992)
37. R. Baboian, "*Electrochemical Techniques for Corrosion*", National association of corrosion engineers, Houston, TX (1977)
38. U. Bertocci, F. Mansfeld, "*Electrochemical Corrosion Testing*", ASTM STP 727, ASTM international, West Conshohocken, PA (1979)
39. H. H. Uhlig, R. W. Revie, "*Corrosion And Corrosion Control*", John Wiely & Sons, New York (1985)

40. L. L. Shreir, R. A. Jarman, G. T. Burstein, "*Corrosion, Metal/Environmental Reactions"* Butherworth-Heinemann, Oxford (1994)

41. T. Badea, M. Popa, M. Nicola, "*Ştiinţa şi Ingineria, Coroziunii", Ed. Acad. Române, Bucureşti",* (2002) 134

42. N. Perez, *"Electrochemistry and Corrosion Science"*, Kluwer Academic Publishers, Boston (2004) 83

43. M. Dekker, *"Electrochemical Techniques in Corrosion, Science and Engineering"*, New York (2003)

44. R. Baboian, *"Corrosion Tests and Standards: Application and Interpretation"*, ASTM stock NO: MNL-20, 2nd edn. (1998)

45. C. Wagner, W. Z. Traud, *Electrochem.,* 44 (1938) 391

46. T. Badea, M. Nicola, I. D. Vaireanu, I. Maior, A. Cojocaru, *"Electrochimie si Coroziune, Matrixrom, Bucuresti"*,(2005) 150

47. M. G. Fontana, N. D. Greene, *"Corrosion Engineering"*, McGraw-Hill, New York (1978)

48. J. Newman, *"Electrochemical Systems"*, Prentice-Hall (1973)

49. M. Stern, R.M. Roth, *J. Electrochem. Soc.*, 104 (1957) 390

50. M. Stern, A.L. Geary, *J. Electrochem. Soc.*, 105 (1958) 638

51. A. Raman, P. Labine "*Reviews on Corrosion Inhibitor Science and Technology",* NACE, Houston, TX , 1 (1986)

52. D. D. MacDonald, *"Transient Techniques in Electrochemistry"*, Plenum press. New York, (1977)

53. Q. Qu, Z. Hao, S. Jiang, L. Li, W. Bai, *Mater. Corros.*, 59 (2008) 883

54. F. Bentiss, M. Traisnel, M. Lagrenee, *Corros. Sci.*, 42 (2000) 127

55. D. P. Schweinsberg, G. A. George, A. K. Nanayakkara, D. A. Steinert, *Corros. Sci*., 30 (1988) 33

56. H. Shokry, M. Yuasa, I. Sekine, R.M. Issa, H.Y El-baradie, G. K. Gomma, *Corros. Sci*., 40 (1998) 2173

57. A. K. Singh, M. A. Quraishi, *J. Appl. Electrochem*., 40 (2010) 1293

58. E. Cano, J.L. Polo, A. La Iglesia, J.M. Bastidas, *Adsorption*, 10 (2004) 219

59. F. Bentiss, M. Lebrini, M. Lagrenée, *Corros. Sci*., 47 (2005) 2915

60. A. Fouda, A. Hussein, *J. Kor. Chem. Soc.*, 56 (2) 2012, doi.org/10.5012/jkcs.2012.56.2.264

61. H. H. Hassan, E. Abdelghani, M. A. Amin, *Electrochim. Acta*, 52 (2007) 6359

62. M. S. *Abdel-Aal, M.S. Morad, Br. Corros. J*., 36 (2001) 253

63. P. Bommersbach, C. A. Dumont, J.P. Millet, B. Normand, *Electrochim. Acta*, 51 (2005) 1076

64. M. H. Hussin, M. J. Kassim, *Int. J. Electrochem. Sci.*, 6 (2011)1396

65. A. S. Priya, V.S. Muralidharam, A. Subramannia, *Corrosion*, 64 (2008) 541

66. M. El Azhar, B. Mernari, M. Traisnel, F. Bentiss, M. Lagrenée. *Corros. Sci.*, 43 (2001) 2229

67. A.K. Satapathy, G. Gunasekaran, S. C. Sahoo, Kumar Amit, P. V. Rodrigues, *Corros. Sci*., 51 (2009) 2848

68. O. Lahodry-Sarc, F. Kapor, *Mater. Corros.*, 53 (2002) 266

69. A. K. Singh, S. K. Shukla, M. Singh, M.A. Quraishi, *Mater. Chem. Phy*., 129 (2011) 68

70. F. Mansfeld, *Corrosion*, 36 (1981) 301

71. M. MaCafferty , N. Hackerman, *J. Electrochim. Soc.*, 119 (1972) 146

72. X. Li, S. Deng, H. Fu, *Corros. Sci.*, 51 (2009) 1344

73. E. S. Ferreira, C. Giacomelli, F.C Giacomelli, A. Spinelli, *Mater. Chem. Phys*., 83 (2004) 129

74. S. Cheng, S. Chen, T. Liu, X. Chang, Y. Yin, *Mater. Lett*., 61 (2007) 3279

75. Y. Feng, K. S. Siow, W. K. Teo, A. K. Hsieh, *Corros. Sci.*, 41 (1999) 829

76. P.C .Okafor, Y. Zheng, *Corros. Sci*., 51 (2009) 850

77. E. E. Ebenso, H. Alemu, S. A. Umoren, I. B. Obot, *Int. J. Electrochem. Sci*., 3 (2008) 1325

78. S. A. Umoren, U. M. Eduok, E. E. Oguzie, *Portug. Electrochim. Acta*, 26 (2008) 533

79. Z. A. Iofa, V. V. Batrakov, Cho-Ngok-Ba Ba, *Electrochim. Acta*, 9 (1964) 645

80. F. El-Taib, A. S. Fouda M. S. Radwan, *Mater. Chem. Phys.*, 125 (2011) 26

81. S. John, A. Joseph, *Mater. Chem. Phys.,* 133 (2012) 1083

82. A. Béchamp, *Annales de chimie et de physique,* 42 (1854) 186

83. T. Hurlen, H. Lian, O. S. Odegard, T. Valand, *Electrochim. Acta,* 29 (1984) 579

84. J. O. M. Bockris, D. Drazic, *Electrochim. Acta*, 7 (1962) 293

85. H. Ashassi-Sorkhabi, S. A. Nabavi-Amri, *Acta Chim. Slov.,* 47 (2000) 512

86. I. B. Obot, N. O. Obi-Egbedi, *Corros. Sci.*, 52 (2010) 198

87. B. Omar, O. Mokhtar, *Arab. J. Chem.*, (2010) doi:10.1016 /j. arabjc .2010. 07.016

88. G. N. Mu, T. P. Zhao, M. Liu, T. Gu, *Corrosion*, 52 (1996) 853

89. N.O. Obi-Egbedi, I.B. Obot, *Arab. J. Chem.*, 6 (2013) 211

90. K. Aramaki, M. Hackerman, *J. Electrochem. Soc*., 116 (1969) 568